journal of the international meteor organization

WGN

45:6
december 2017

IMC 2018 final announcement
October Camelopardalids recorded in 2017
Analysis of video Kappa Cygnids
May–June video meteors
October CAMS BeNeLux video meteors
Historical report of a possible Anthelion fireball

ISSN 1016-3115

WGN Vol. 45, No. 6, December 2017, pp. 115 – 165

Administrative

Conferences

Meteor science

Preliminary results

History

Front cover photo

Fireball of visual magnitude −6 to −8 photographed on 2017 September 9 at $18^{h}22^{m}$ UT from De Kelders, Cape Province, South Africa. Canon EOS 7D, Sigma 10–20mm lens at $f/4$ was used, with 30 s exposure at ISO 1600. Photo courtesy: Jonathan Shock.

Writing for WGN This Journal welcomes papers submitted for publication. All papers are reviewed for scientific content, and edited for English and style. Instructions for authors can be found in WGN **45:1**, 1–5, and at `http://www.imo.net/docs/writingforwgn.pdf` .

Legal address International Meteor Organization, Jozef Mattheessensstraat 60, 2540 Hove, Belgium.

From the Treasurer — IMO Membership/WGN Subscription Renewal for 2018

Marc Gyssens

Renewal rates

Most members/subscribers whose membership/subscription has expired should have received a reminder email. Via this way, we invite them again to renew for 2018.

The fees are as tabulated below. We are happy that we can offer WGN at the same cost as last year. We also continue to offer an electronic-only subscription at a reduced rate.

IMO Membership/WGN Subscription 2018				
Electronic + paper with surface mail delivery:		€26		US$ 35
Electronic + paper with airmail delivery (outside Europe only):		€49		US$ 65
Electronic only:		€21		US$ 25
Supporting membership:	add	€26	add	US$ 35

It is also possible to renew for two or more years in a row.

When you renew, give a few minutes of thought to becoming a **supporting member** by paying at least 26 EUR/35 USD extra. Smaller gifts are of course also appreciated. As you may know, there is an IMO Support Fund. With this Support Fund, we offer support to meteor-related projects. Our ability to provide this service to the meteor community depends primarily on the gifts we receive from supporting members!

Another way to help meteor workers with limited funds is to offer them a gift subscription.

We already thank all our members that will renew for their continued trust in our Organization!

New membership benefits

The IMO Council is seeking to expand the benefits of memberships.

In this regard, it was decided that the IMO's *Handbook for Meteor Observers* and *Meteor Shower Workbook* will be made available for free to IMO members in digital form. In this way, IMO members have at their disposal these two invaluable tools to prepare an observing session and to interpret its results. To access these publications, go to the IMO website and click on the menu item "Free Meteor Books" under the tab "Resources".

Another decision is that IMO members who renew their membership at an International Meteor Conference (IMC) get a reduction of 5 EUR for a renewal (or for becoming a new member) for the next year. While this measure has been taken primarily to encourage IMC participants who are not yet an IMO member to become one, established IMO members also get a small advantage each time they attend an IMC. Mind that the next IMC will take place in Pezinok-Modra near Bratislava in Slovakia from August 30 to September 2, and that more info about this event can be found elsewhere in this issue!

We intend to expand membership benefits even further in the near future.

Payment instructions

If you are not yet familiar with the new IMO website, you first must log in into your account if you want to renew. For this purpose, click the log-in button in the upper right-hand corner. As login, use the email address on which you received my reminder email. In case you forgot your password, you can use the "forgot password" link to reset it. Once logged in, you will see your profile picture (or the space provided for it). If you read on the green button below it that your membership has expired, click it, and the rest will be self-explanatory.[1] This procedure is described in more detail and with screenshots of the different screens you see during the process in the October 2017 issue of WGN.

The outcome of this process is that you will see the total amount due and your payment options. If you choose to pay using PayPal (or using a credit card via PayPal), you can complete the payment on our website.

If you experience any difficulties, do not hesitate to contact me at `treasurer@imo.net`.

One final request: every year, a lot of members renew late. As a consequence, back issues that already appeared have to be sent out to these members. Please support our volunteers in their bimonthly effort to have WGN shipped to you by renewing promptly! Thank you for your understanding and cooperation!

[1]Alternatively, you can also click on "Extend your membership" in the pull-down menu to the right of your name in the upper right-hand corner, with the same result.

Letter — Periodic nature of κ-Cygnids – Congratulations on 10 years of the SonotaCo network

Masahiro Koseki[1]

We can confirm the 7 year period of κ-Cygnids activity by continual observations of the SonotaCo network. The author proposed a 2014 campaign for κ-Cygnids on the basis of 2007 κ-Cygnids observations by the SonotaCo network (Koseki, 2014a). The members of the SonotaCo network have been continuing observations patiently from 2007 to now and present their results to everybody openhandedly. Their voluntary efforts provide 10 years observations of κ-Cygnids and make clear its nature. We describe κ-Cygnids only here, but you can access SonotaCo data (SonotaCo, 2017) fully and survey other streams further. The long timeframe and open data give us very important opportunities to uncover hidden mysteries in meteor science.

Received 2017 October 15

1 Introduction

Japanese meteor enthusiasts tried to use surveillance cameras (CCTV) in the 2000's and they intended firstly to detect a meteorite fall and selected a wide field lens. Soon they noticed a bright and short focus lens can catch more meteors than a longer focus one. They have continued to use such lenses, for example: Watec WAT-100N, $f = 6$ mm $F/0.8$. Japanese observers have used UFOCapture developed by SonotaCo and his other useful computer software. The SonotaCo network published meteor data on the Web for 2007–2016 (SonotaCo, 2017). The calculations and surveys are offered to be easily carried out by individual observers/ researchers, though CAMS data are analyzed collectively. This author himself is not a member of the SonotaCo network but can access full data in SonotaCo archives. He would like to celebrate the SonotaCo network's 10 years and show the changes of κ-Cygnids in 10 years as the most symbolic results.

2 Results

The SonotaCo network has recorded 230 996 orbits in total during 2007–2016 and has gotten 576 KCGs in these 10 years based on SonotaCo's own shower definition (Table 1).

Table 1 – Number of meteors registered as KCG by SonotaCo network from 2007 to 2016.

Year	2007	2008	2009	2010	2011	2012	2013	2014	2015	2016	Total
KCG	204	13	18	34	16	44	54	140	21	32	576

Figures 2a-j show the radiant distribution around $(\lambda - \lambda_\odot, \beta) = (151°, 73°)$ between $\lambda_\odot = 115 \sim 165$ degrees and the unique activity area (radiant) is recognized easily. We confirm KCG went into outburst in 2007 with the most intense activity during these 10 years followed by the 2014 outburst in Figures 2a-j also.

The definition of KCG is widely different among researchers and it is necessary to prevent the profile from leading to misunderstanding of KCG. We use the entire number of radiants in the Figure 2a-j area instead of only those identified as KCG in SonotaCo data and Figure 1 shows the 5 degrees moving mean of them. The profiles in the figure, therefore, represent the combined number of KCG and

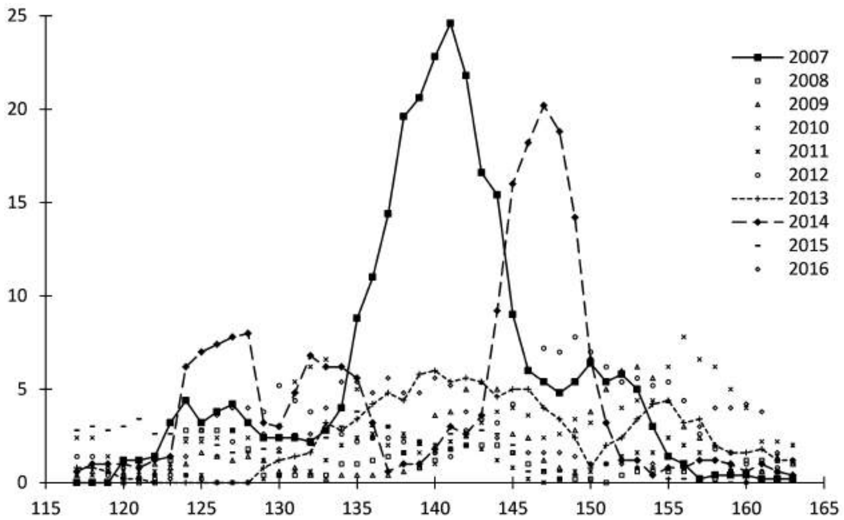

Figure 1 – The profile of the number of radiants in the Figure 2a-j area between 2007 and 2016. x-axis is the solar longitude and y-axis is the 5 degrees moving mean of the number of radiants.

[1] Nippon Meteor Society (NMS), 4-3-5 Annaka, Annaka-shi, Gunma-ken, 379-0116, Japan.
Email: geh04301@nifty.ne.jp

IMO bibcode WGN-456-koseki-kcg NASA-ADS bibcode 2017JIMO...45L.116K

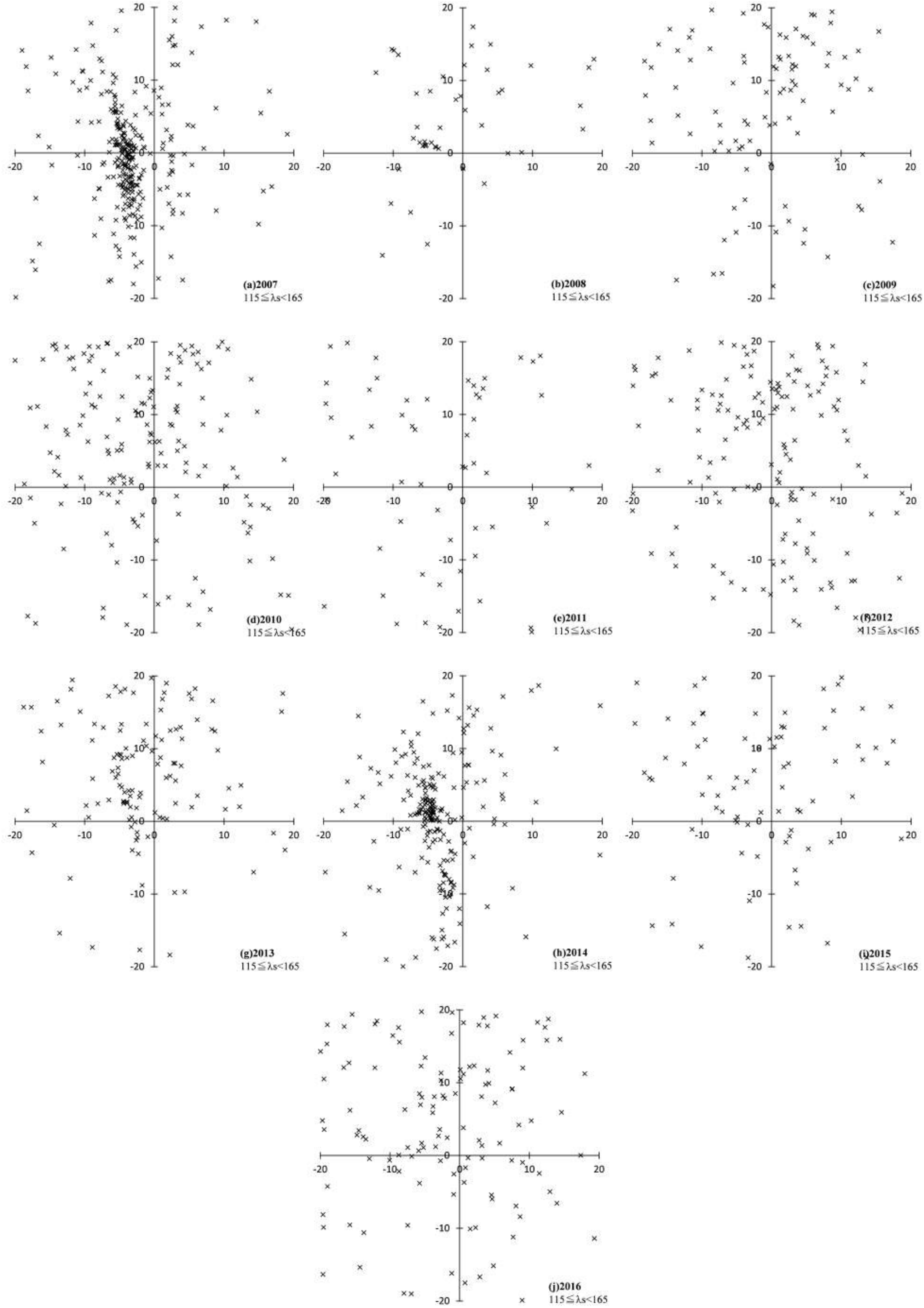

Figure 2 – Radiant distribution around $(\lambda - \lambda_{\odot}, \beta) = (151^{\circ}, 73^{\circ})$ between $\lambda_{\odot} = 115^{\circ} - 165^{\circ}$. λ and β are the ecliptic coordinates and $\lambda_{\odot}$ is the solar longitude (λs in plots). $(\lambda - \lambda_{\odot}, \beta)$ coordinates reduce the radiant shift.

other activities. We can see extra high meteor activity in 2007 but an irregular one in 2014. Untimely weather obstructed Japanese observers from Perseids and κ-Cygnids in 2014 unfortunately and if not, we might have had another rich display of KCG in 2014 judging from the 2014 profile around the maximum.

Koseki (2014a,b) analyzed SonotaCo data with old photographic records and called for a 2014 KCG campaign. Roggemans et al. (2015) reported the intense activity of KCG by video observations but Rendtel and Arlt (2015) denied the periodic nature of KCG through IMO visual data. KCG is a difficult target for visual observers, because of the complexity of activities of sporadics and other showers, and moreover, the meteor rates are very low for a single naked eye observer even in the outburst. Video observations patiently continue efforts all night long and their meteor rates are accumulated ones. Estimated hourly rates of KCG at the maximum from video observations are 3 and 0.5 for the outburst and normal years respectively, if we assume the video rates are the 8 hours accumulated number. Sporadic and other activities cover up real KCG rates.

3 Conclusion

The voluntary work of SonotaCo network members builds up continual records of meteor activities. We appreciate their generous handling of the results that makes it possible to survey the changes in shower activities. κ-Cygnids is the most impressive case but we can add one smaller example: η-Virginids (EVI) show clear changes year by year (Table 2). Though large amounts and precise data are very useful, the continual and open data are more valuable.

Table 2 – Number of meteors registered as EVI (η-Virginids) by SonotaCo network from 2007 to 2016.

Year	2007	2008	2009	2010	2011	2012	2013	2014	2015	2016	Total
EVI	4	7	54	15	12	4	27	20	5	14	162

References

Koseki M. (2014a). “Call for observations of κ-Cygnids in 2014”. *WGN, Journal of the IMO*, **42:3**, 89.

Koseki M. (2014b). “Various meteor scenes II: Cygnid-Draconid Complex (κ-Cygnids)”. *WGN, Journal of the IMO*, **42:5**, 181–197.

Rendtel J. and Arlt R. (2015). “Kappa-Cygnids: search for periodic activity”. In *Proceedings of the IMC, Mistelbach, 2015*. pages 70–72.

Roggemans P., Johannink C., and Breukers M. (2015). “Status of the CAMS-BeNeLux network”. In *Proceedings of the IMC, Mistelbach, 2015*. pages 41–50.

SonotaCo (2017). “SonotaCo Network Simultaneously Observed Meteor Data Sets”. `http://sonotaco.jp/doc/SNM/` .

Conferences

Thirty-Seventh International Meteor Conference, Pezinok-Modra, Slovakia, August 30–September 2, 2018

Pavol Zigo, Leonard Kornoš, Juraj Tóth and Tomáš Paulech

Introduction

As we already announced in the June 2017 issue of WGN, the 37th *International Meteor Conference* (IMC) will be held in Pezinok-Modra, Slovakia, from August 30 till September 2, 2018. Pezinok is the birthplace of Slovak astronomer Dr. Ján Štohl (1932–1993) and Modra is the location of the Astronomical and Geophysical Observatory (AGO). After 10 years, the IMC returns to Slovakia again. The last IMC in Slovakia was held in Šachtička in 2008. The two previous IMCs were in Stará Lesná in 1998 and in Smolenice in 1992, both in conjunction with *Meteoroids* conferences.

Local Organization

Our Local Organzing Committee (LOC) mainly consists of employees of the Astronomical and Geophysical Observatory (AGO) in Modra. This institution is a part of the Faculty of Mathematics and Physics of the Comenius University in Bratislava, and was officially established in 1992. A great deal of effort is focused on meteor research. Also, we will celebrate the 20th anniversary of the famous Leonid meteor shower all-sky photograph of 1998, which is schematically depicted in the logo of the IMC 2018.

Conference dates

While the IMC 2017 in Petnica, Serbia, was organized at the traditional time around the third weekend of September, the IMC 2018 will take place slighly earlier, from August 30 till September 2, 2018. The reason for this shift is the nearby XXXth IAU General Assembly in Vienna, Austria, from August 20 till 31. Clearly, this will be a great opportunity to attract IAU attendees to come to IMC. We expect this coupling may both enrich scientific program significantly, and save time and minimize travel expenses for some of the IMC participants. Moreover, the weather is usually nicer around the end of August.

Location

The conference will be held at the Hotel Rozalka in the suburb of Pezinok (ca. 20 km from the capital city of Bratislava, easily accessible from there within less than 30 minutes). On the hotel premises, neighboring a complex of horse-riding arenas, there is a congress residence with conference hall, lobby bar, and roofed terrace. Poster panels will be arranged in the conference hall. You can find the resort at $48\overset{\circ}{.}297858$ N and $17\overset{\circ}{.}254766$ E.

Figure 1 – Left: Location of Slovakia in Central Europe. *Right*: Conference location relative to Vienna, Bratislava, and Budapest. The conference hotel is marked by the red pin.

Accommodation and venue

Hotel Rozalka provides accommodation in three separate residences for 130 guests in double bedrooms, family rooms, or apartments with terrace. There is a limited number of single rooms. Every room is equipped with cable TV with flat screen, internet connection, telephone, bathroom with toilet, shower cabinet, and toilet facilities.

[1]Astronomical and Geophysical Observatory Modra, Faculty of Mathematics, Physics and Informatics, Comenius University in Bratislava, Slovakia, imc2018@imo.net

Figure 2 – Aerial view of Hotel Rozalka and its surroundings.

The hotel and its surroundings is covered by free WiFi. The indoor restaurant where all meals will be served has a capacity of around 80 guests, plus a summer terrace with view on the riding parcours. Special food requirements, horse riding, or other sport activities can be arranged in advance with the help of the reception.

Although a no-accommodation option is provided on the registration form, we strongly recommend participants to choose the full-board accommodation at the Rozalka Hotel. Nevertheless, if for whichever reason you prefer to have alternative accommodation, the LOC will of course be available for more information and recommendations in function of your concrete needs. Please bear in mind, however, that if you choose the no-accommodation option, you are responsible for arranging transportation between your hotel and the conference location—the LOC cannot provide facilities for this!

Program and social events

The scientific program consisting of talks and poster sessions will be specified shortly after the end of the registration period. We would like to invite some presenters to give review talks, which can serve for beginners on the one hand and for professionals or advanced amateurs on the other hand. We also expect short contributions concerning various types of meteor observations as well as data analyses. As usual, the overall goal of the conference will be to encourage mutual collaboration among amateurs and between amateur and professional meteor astronomers.

All presentations, both talks and posters, will be included in the IMC 2018 Proceedings, which are published after the conference. Instructions on how to prepare a contribution are given on the IMC web pages. While there are no formal page limits, proceedings contributions are supposed to be rather concise. Therefore, we encourage presenters to consider writing—besides their paper for the IMC 2018 Proceedings—a more extended paper for WGN where no size restrictions apply whatsoever.

At the IMCs of Egmond, the Netherlands, in 2016, and Petnica, Serbia, in 2017, there was a contest for the best poster and the best meteor photograph. We have decided to continue this recent tradition at the IMC 2018! More information will be provided at the IMC web pages and via newsletters in due time.

We are also exploring the possibility of one or more pre-IMC workshops on Wednesday, August 29. More information about this will be posted in due time on the IMC 2018 web pages. The financial aspect of such workshops will be dealt with separately from the registration fee for the actual IMC.

Apart from evening activities and informal contacts among the participants, the social events include a Saturday afternoon excursion, as usual. For this year, we have selected for this purpose two interesting places close to the conference venue. The first sight is the Červený kameň (Red Stone) Castle, situated in the Little Carpathian Mountains, only 17 km from Pezinok. We will take a guided tour of the castle built in the 13th century. It has a huge underground part and an impressive fortification system. Next, our excursion will continue to Astronomical and Geophysical Observatory (AGO) in Modra, where we can take a short tour through the facility followed by small refreshments.

Figure 3 – Accommodation of Hotel Rozalka. *Top left*: Example of a double room. *Top right*: Lobby bar, the ideal place to socialize! *Bottom*: Restaurant.

Registration and payment

The standard conference registration fee has been set to 170 EUR, which we hope will be acceptable for all interested to attend. This fee includes full board (accommodation in a double bedroom, breakfast, lunch, and dinner) from Thursday evening August 30 (dinner included) till Sunday noon September 2 (lunch included), all lecture and poster sessions, coffee breaks, and the Saturday afternoon excursion. A limited number of apartments and family rooms is also available for the price of 170 EUR per participant. The price for accommodation in a single bedroom is 240 EUR (also limited availability).

The no-accommodation fee is 110 EUR and includes the same as the standard fee, except for accommodation and breakfast. We strongly recommend full-board accommodation at Rozalka Hotel to be full part of the socializing. We repeat that, while the LOC can provide guidance in finding alternative accommodation, you are responsible for transportation between this accommodation and the conference venue!

T-shirts of different sizes and printed proceedings can be purchased separately upon registering, but electronic proceedings will be made available to all participants free of charge.

Registration is expected to begin towards the January 2018. Detailed information concerning registration, as well as the registration form, and conference program will be available via the IMC 2018 web pages, which will be linked on the IMO website. Please check regularly!

Figure 4 – The Saturday afternoon excursion will bring participants to the nearby Red Stone Castle (*left*) and the Astronomical and Geophysical Observatory (AGO) in Modra (*right*).

Figure 5 – Main conference hall, with possible extension up to 200 seats. Posters can be arranged in the back of the room.

The early registration deadline is set at May 31, 2018. After this date, an additional late registration fee of 20 EUR will be charged. The final registration deadline is June 30, 2018. We would like to emphasize that registration may be closed earlier if the maximum capacity of 130 participants is reached.

Finally, notice that if your travel plans require you to stay extra nights before or after the conference at Hotel Rozalka, you must book them directly with them.

Traveling to Pezinok

Pezinok is easily accessible from Bratislava by train, bus, or car within 30 minutes.

Bratislava, the country's capital, is served by its own Bratislava International Airport (BTS) having 22 regular destinations mainly in Europe. If this Airport happens to be less convenient to reach from where you live, you may want to consider Vienna (VIE) or Budapest Ferihegy (BUD) International Airports as alternatives: From Vienna, there are several possibilities to use low-cost airport shuttle busses operating on a daily basis or the train

Figure 6 – Map of Bratislava and Pezinok-Modra surroundings. Major roads and railways are shown.

from Vienna Hauptbahnhof to Bratislava hlavná stanica (or Main Railway Station), an approximately 1-hour journey. From Budapest, the best way to travel is to use an international train from Keleti Railway Station to Bratislava Main Railway Station, an approximately 3-hour journey.

The map in Figure 6 comes from the site `https://en.mapy.cz/`, where you can easily plan your trip by train (Bratislava hlavná stanica to Pezinok), bus (Bratislava AS to Pezinok), or car. More details on how to use this site will be provided in due time on the IMC 2018 web pages.

There is public transportation within Pezinok, but we recommend to take a taxi from Pezinok train/bus station to Hotel Rozalka for 3–5 Euros.

If you travel by car, the best option is to use highway D1 and take exit Pezinok-Senec, some 20 km north-east from Bratislava. Then, follow local road No. 503 which leads directly to Pezinok. The LOC will provide assistance and individual travel recommendations if needed.

Contact information

Further information about this upcoming International Meteor Conference will be published in WGN following this announcement as well as in dedicated newsletters, and posted shortly at the IMC 2018 web pages `http://imc2018.imo.net/` and the IMO website `http://www.imo.net/`. You may contact the LOC any time at `imc2018@imo.net`.

We hope you will be able to attend the IMC 2018 and are already looking forward to welcoming you in Slovakia, in Pezinok-Modra!

Figure 7 – LOC member Juraj Tóth with Detlef Koschny at the IMC 2017 in Petnica, Serbia. Both are showing off the IMC 2018 t-shirts!

Acknowledgement

The preparatory work of the LOC for the IMC 2018 was supported by Grant No. APVV-16-0148.

Meteor science

October Camelopardalids activity recorded by CAMS

Carl Johannink[1]

During routine CAMS observations on 2017 October 5, CAMS BeNeLux collected 15 meteors belonging to a minor stream called the October Camelopardalids (IAU#281, OCT). Radiant positions and orbital elements are in good agreement with results reported by Jenniskens et al. (2005) and Jenniskens (2016).

Received 2017 November 22

1 Introduction

The weather in the first week of October 2017 was very unsettled for CAMS BeNeLux (Jenniskens et al., 2011), so it was no surprise that our network could only collect 380 orbits during the few clear spells. Fortunately, October 5/6 was the best night for observing during the week. During this night 18 of 21 stations had longer clear periods. They collected 99 orbits in this night alone.

2 History

In the course of the last century, observers noticed meteor activity from a region near the northern celestial pole in 1902, 1942 and 1976. On 2005 October 5 several video-observers in Finland (Moilanen, Yrjölä, Lyytinen) and Germany (Molau) captured several bright meteors from a radiant near the border of the constellations Draco and Camelopardalis. Moilanen captured 19 meteors in the period 17^h06^m–22^h41^m UT. Twelve of them shared the same radiant. Most of these meteors appeared between 17 and 20 hours UT (Jenniskens et al., 2005). Mean radiant of these twelve meteors was at RA $= 164\overset{\circ}{.}1 \pm 2\overset{\circ}{.}0$ and Dec $= 78\overset{\circ}{.}9 \pm 0\overset{\circ}{.}5$. Mean geocentric velocity was $V_g = 46.9 \pm 2.6$ km/s. Mean orbital elements are summarized in Table 1. According to Jenniskens et al. (2005) this stream is debris from a yet unknown long period comet, because of uncertainty in the semi major axes a Halley type comet cannot be excluded.

In 2016 Lyytinen forecasted higher activity for this stream on October 5 at 14^h45^m UT (Lyytinen, 2017) and indeed, CAMS California captured 9 meteors between 08^h45^m and 13^h15^m UT that could be matched to this stream. CAMS UAE also detected three candidates between 14^h48^m and 19^h15^m UT. Finally, CAMS BeNeLux added four more candidates until 22^h00^m UT. Orbital element for these meteors are also listed in Table 1.

For 2017, Lyytinen forecasted enhanced activity on October 5 at 20^h47^m UT, although possibly at a lower rate than 2016 due to a greater distance between the dust trail and the earth this year (Lyytinen, 2017).

3 Processing the 2017 data

While processing the data of October 5/6, a cluster of radiants became visible near RA = 170 degrees and Dec = 74 degrees. A total of 15 meteors showed orbital elements in good agreement with the now called October Camelopardalids (IAU#281, OCT). Six of these OCT's appeared between 18 and 19 hours UT. The other nine members appeared between 19 and 24 hours UT.

Figure 1 shows radiant positions of all captured simultaneous meteors from October 5/6. The OCTs are colored red in this plot. They form a striking compact radiant. D-criterium is < 0.05 for 13 out of these 15 OCTs. OCTs with the highest and lowest declination in this plot have D_d $0.08 - 0.09$, just below the limit of Drummond's D-criterium (Drummond, 1981).

Figure 2 shows a plot of the orbital elements inclination against longitude of the perihelion. Again a striking compact picture. The OCTs with $D_d > 0.05$ are the ones with lowest and highest value of longitude of the perihelion.

Table 1 shows mean orbital elements of OCTs in (Jenniskens et al., 2005) and (Jenniskens, 2016) and our data in 2017.

4 Conclusion

Until 2016 we found nearly no members of this stream in the CAMS BeNeLux data. In 2016 and 2017 this stream is clearly visible in our data. In 2017 the highest activity seems to be between 18 and 19 hours UT, more than one hour earlier than predicted. However, we should keep in mind that in early October our network cannot start collecting data before 17^h30^m UT (eastern parts of the Netherlands). Higher activity before 18^h UT cannot be excluded.

Acknowledgements

Thanks to Reinder Bouma for his critical comments on this article. We thank all CAMS stations for their quick processing of all data.

References

Drummond J. D. (1981). "A test of comet and meteor shower associations". *Icarus*, **45**, 545–553.

Jenniskens P. (2016). "October 5 - outburst of October Camelopardalids". `https://www.seti.org/`

[1]Email: `c.johannink@t-online.de`

IMO bibcode WGN-456-johannink-oct
NASA-ADS bibcode 2017JIMO...45..125J

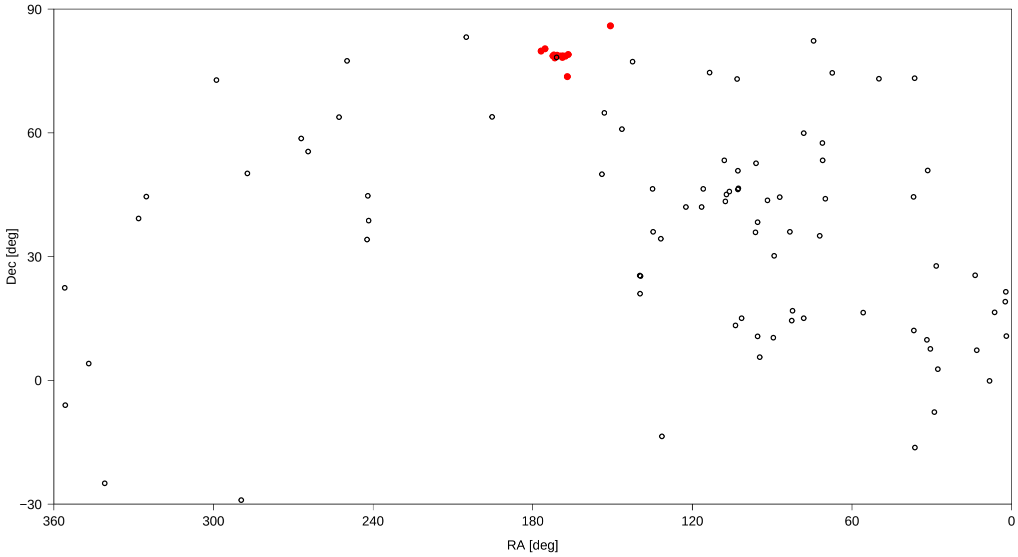

Figure 1 – Radiant plot for 2017 October 5; red full circles represent #281 OCT.

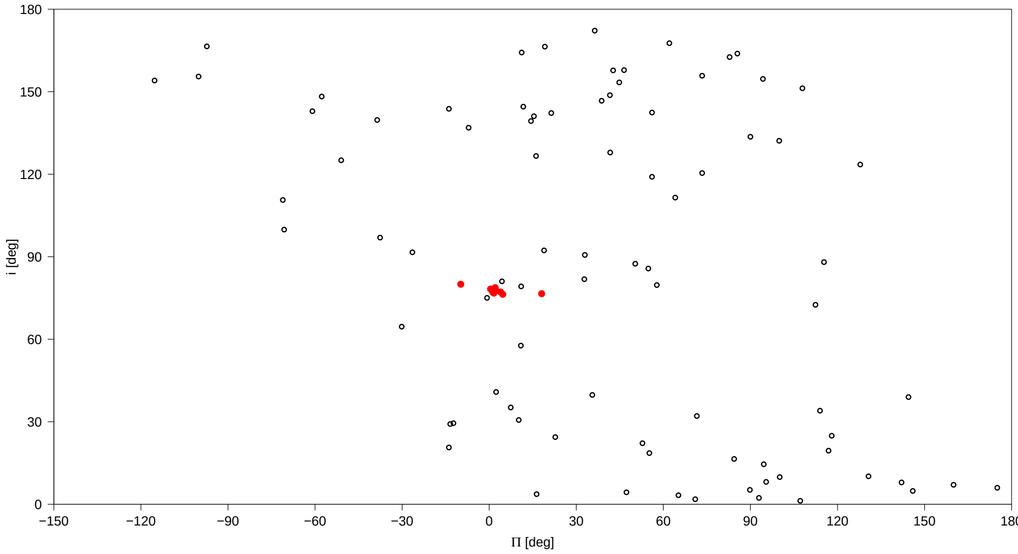

Figure 2 – Plot of inclination (i) against longitude of the perihelion (Π) for 2017 October 5; red full circles represent #281 OCT.

`seti-institute/news/october-5-outburst-october-camelopardalids`.

Jenniskens P., Gural P. S., Dynneson L., Grigsby B. J., Newmane K. E., Borden M., Koop M., and Holman D. (2011). "CAMS: Cameras for Allsky Meteor Surveillance to establish minor meteor showers". *Icarus*, **216**, 40–61.

Jenniskens P., Moilanen J., Lyytinen E., Yrjölä I., and Brower J. (2005). "The 2005 October 5 outburst of October Camelopardalids". *WGN, Journal of the IMO*, **33:5**, 125–128.

Lyytinen E. (2017). "October Camelopardalis outburst model comparisons in the years 2005, 2016, 2017". *eMeteorNews*, **4**, 135–136.

Handling Editor: Javor Kac

Table 1 – Orbital elements of IAU#281, OCT.

	Jenniskens et al. (2005)	Jenniskens (2016)	CAMS BeNeLux 2017
q [AE]	0.993 ± 0.001	0.990 ± 0.005	0.9912 ± 0.006
e	—	0.93 ± 0.08	0.948 ± 0.05
i [deg]	78.3 ± 0.5	77.1 ± 1.0	77.6 ± 2.3
ω [deg]	170.5 ± 1.0	168.2 ± 2.5	169.4 ± 4.1
Ω [deg]	192.59 ± 0.04	192.41 ± 0.15	192.35 ± 0.25

Kappa Cygnids (KCG) by TV observation results

Yasuo Shiba[1]

The kappa Cygnids (KCG) and its nearby region were researched by using Japanese automatic TV observation network (SonotaCo network) results for 2007–2016. KCG in 2007 and 2014 were observed with an enhancement of eight times as many meteors than ordinary years at solar longitude 145 degrees. Also the 2013 KCG were enhanced with three times the number of meteors recorded than ordinary years at solar longitude 135 degrees. In years of observed enhanced KCG (2007, 2013, 2014) luminous magnitudes were brighter than in ordinary years. The 2007 and 2014 KCG radiant distributions were similar but shifted 5 degrees to the north in 2013. The 2013 KCG orbital elements were systematically different from 2007 and 2014. If a continuous meteoroid distribution in the solar system causes the enhanced KCG, it is suggested that a distorted 'swarm' has been constructed. The annual KCG radiant distribution and distributions of every orbital element have some peaks which indicate a complex meteor shower. Luminous trajectory altitudes in years of observed enhanced KCG were higher than the annual KCG height. August Draconids (AUD) is an annual meteor shower, many meteors of which are decided to also belong to KCG by using the D′ criterion, but each meteor shower is independent because they have different characteristics. AUD radiants on the celestial sphere drift to the west and form an arc lasting till the end of September. I recommend to create a standard to decide for two meteor showers whether they are truly two meteor showers or not.

Received 2017 September 18

1 Introduction

The kappa Cygnid meteor shower (KCG) is a minor meteor shower observed from the end of July to the end of August when the major meteor shower Perseids is simultaneously observable. Numbers of KCG meteors can be seen as ZHR=3 (Rendtel, 2016) at its maximum, only one-fifteenth of the Perseid meteor shower. The KCG diffuse radiant distribution close to some minor meteor showers on the celestial sphere makes it difficult to research by visual observations. However, slow moving fireballs with explosions attracted many meteor observers' interest.

The possible parent body of KCG is thought to be asteroid 153311 (2001 MG_1) (Moorhead et al., 2015). The August Draconids' parent body is thought to be asteroid 361861 (2008 ED_{69}) (Jenniskens & Vaubaillon, 2008).

Recent KCG observation results describe enhanced displays in 2007 and 2014 (Green, 2007; Trigo-Rodriguez et al., 2009; Moorhead et al., 2015; Rendtel & Molau, 2015; Rendtel & Arlt, 2016). Historical observation results also recognized enhanced meteor activity with a seven year periodicity (Koseki, 2014; Moorhead et al., 2015), thought to be caused by the 5:3 resonance with Jupiter (7.116 years). Photographic meteor records from 1950 to 1993 in the IAU MDC are shown in Figure 1 (Lindblad, 1995). Seven year intervals are labeled on the Figure 1 horizontal axis: we can recognize bright meteors belonging to the KCG appearing in a cycle of seven years or a little more. The number of alpha Lyrid meteors classified by Lindblad (1995) is added to the KCG number in Figure 1 because these meteor shower radiants and orbit distributions are continuous and thought to evolve in a common dynamical environment in the solar system even if these radiant

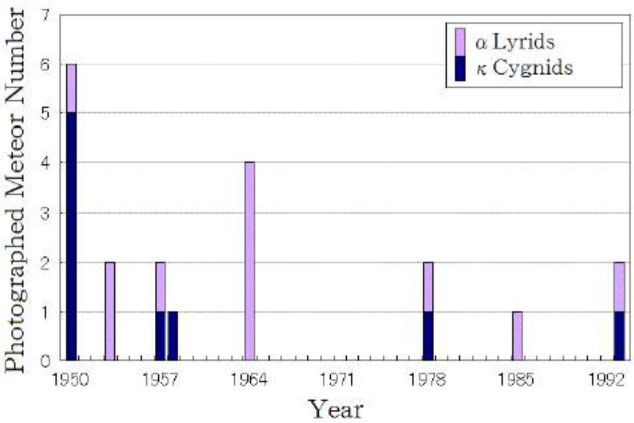

Figure 1 – Photographic KCG (Lindblad, 1995).

positions and orbits do not agree. From 41 years of visual observation results, that is middle size meteoroid observations, a periodic seven year enhanced meteor display was not found clearly (Rendtel & Arlt, 2016). For smallest size meteoroids radio observation results show a 10 times enhanced meteor rate in 2014, however only a twice enhanced rate recorded in 2007 (Moorhead et al., 2015). These results indicate the existence of a seven year periodic activity enhancement although not always supported by detailed results. Photographic observations till the 1990s presented few but accurate bright meteor orbit data. These observations did not present a quantity for statistical analysis. Visual observations as the classical observation by many observers had recorded statistical quantities of data over a long duration. However reliable evaluation of visual data is difficult because Perseids and other meteor showers appear simultaneously with KCG and some additional minor meteor showers exist near the KCG radiant region. Visual data are generally made from observations at single locations, thus observers cannot decide so easily that individual meteors belong to any meteor shower.

TV meteor observations by using low light TV cameras became popular from the 2000s. TV observation

[1]SonotaCo Network, Japan.

IMO bibcode WGN-456-shiba-kcg
NASA-ADS bibcode 2017JIMO...45..127S

Table 1 – Research area for KCG.

	range[deg]
Solar longitude [deg:J2000.0]	127∼160
Right Ascension [deg:J2000.0]	260∼305
Declination [deg:J2000.0]	+30∼+75

Table 2 – Standard orbital elements of KCG, AUD and IOD.

	a[AU]	q[AU]	e	p[yr]	peri	node	i
KCG	4.09	0.968	0.763	8.28	205.7	140.8	34.9
AUD	3.08	1.004	0.674	5.4	185.1	146.5	33.3
IOD	3.27	1.004	0.693	5.92	172.8	154.7	32.8

data are generally less accurate than photographic observations but a great amount of data for statistical study can be taken. Early TV observation results were from single camera sites (Triglav-Čekada, 2006; Molau & Rendtel, 2009). Recent TV observations are generated by multi station networks. The SonotaCo Network (SonotaCo, 2009) started from 2007 in Japan; the Croatian network (Šegon et al., 2015) and EDMOND (Kornoš et al., 2013) started in Europe. CAMS (Jenniskens et al., 2011) started in America (California) from which preliminary but comprehensive results are published (Jenniskens & Nénon, 2016; Jenniskens et al. 2016a,b,c). I describe results of the kappa Cygnids (KCG) and its adjoining meteor showers in this paper based on ten years published data from the SonotaCo network.

2 Data reduction

The data source is the 'SonotaCo Network' (`http://sonotaco.jp/`) meteor reduction csv file daily upload site, 'CSV HUB', data from 2007 to 2014. The extracted radiant points region is described in Table 1 as solar longitude and celestial coordinates. The radiant distribution for each year is shown in Figures 2 to 5. Figures 2, 3 and 4, show respectively radiant right ascension, radiant declination and geocentric velocity against solar longitude. Figure 5 shows radiant declination against right ascension. The years 2007 and 2014 when enhanced KCG were observed are shown as integrated data in panels (k) of Figures 2 to 5. Years 2008, 2009, 2010, 2011, 2012, 2015 and 2016 when remarkable KCG were unobserved (i.e., normal years) are shown as integrated data in panels (m). Enhanced KCG were observed in 2007 and 2014 at the same level of activity. In 2013 KCG was weak but a certain activity recognized (Figures 2 to 5 (g)). In Figure 5(m), the sparse radiant region forms an arc on the west side (right side of figure, i.e. west of about 270°) of the main concentration of KCG radiants. The radiant concentration recognizable in Figure 5(k) was defined in this paper as the kappa Cygnids (#12 KCG) with reference to the IAU meteor shower list (Porubčan & Jopek, 2017). This continuous radiant distribution contains the alpha Lyrids (Lindblad, 1995; Jones et al., 2006) area. The concentration of sparse radiants seen in Figure 5(m) was defined as the August Draconid meteor shower (#197 AUD). These two individual radiant distributions include dilution by bad weather conditions but no inner interruption. The AUD radiant distribution is too wide to define whether meteors belong to a shower by using the D′ criterion for each meteor. So an additional meteor shower the iota Draconids (#703 IOD) was defined in the final stage of the AUD active duration. I judged meteors individually as belonging to any of these three showers based on the distribution in Figures 2 to 5. Average orbital elements were calculated from defined individual meteor shower members (Table 2).

The following equations are a linear approximation to KCG radiant drift, where R.A. is radiant right ascension, Decl is declination, V_g is geocentric velocity and $\lambda_\odot$ is solar longitude (eq:2000.0).

$$\begin{aligned} \text{R.A.} &= 0.59(\lambda_\odot - 140.8) + 286.5 \ \ \text{[deg]} \\ \text{Decl} &= 0.87(\lambda_\odot - 140.8) + 49.4 \ \ \text{[deg]} \\ V_g &= 0.20(\lambda_\odot - 140.8) + 23.3 \ \ \text{[km/s]} \end{aligned}$$

AUD radiant drift is described in Section 3.

I judged which meteor showers all meteors of the Table 1 area belonged to using the D′ criterion equation (Drummond, 1981). So if the D′ value based on the Table 2 standard orbit is

$$D' < 0.105$$

then the meteor belongs to the shower. Now the D′ criterion calculated for KCG and AUD standard orbits relative to each other is

$$D' = 0.094$$

suggesting KCG and AUD are a united meteor shower. Because of that orbital similarity, many meteors were judged belonging to double meteor showers KCG and AUD. The calculated D′ value with the KCG standard orbit is labeled D'_k and with the AUD standard orbit is labeled D'_a. When individual meteors belong to both meteor showers, i.e.:

$$D'_k < 0.105 \quad \text{and} \quad D'_a < 0.105$$

then if:

$$D'_k < 2 * D'_a$$

they are judged KCG, whereas if:

$$D'_k > 2 * D'_a$$

they are judged AUD. The reason for the factor of 2 in D′ taken with AUD compared with KCG is that radiant concentrations are better explained for 2007 and 2014 KCG observed results. A part of IOD to the west of AUD meteors also was judged KCG. In this case, twice the strict D′ parameter was also applied to IOD compared with KCG. While the AMD (#470) meteor shower described in Jenniskens & Nénon (2016) exists between AUD and IOD, the AMD was not investigated because I think most of AMD must be included in AUD or IOD. IOD and AMD are incorporated to AUD in this paper because there is no interruption between the AUD

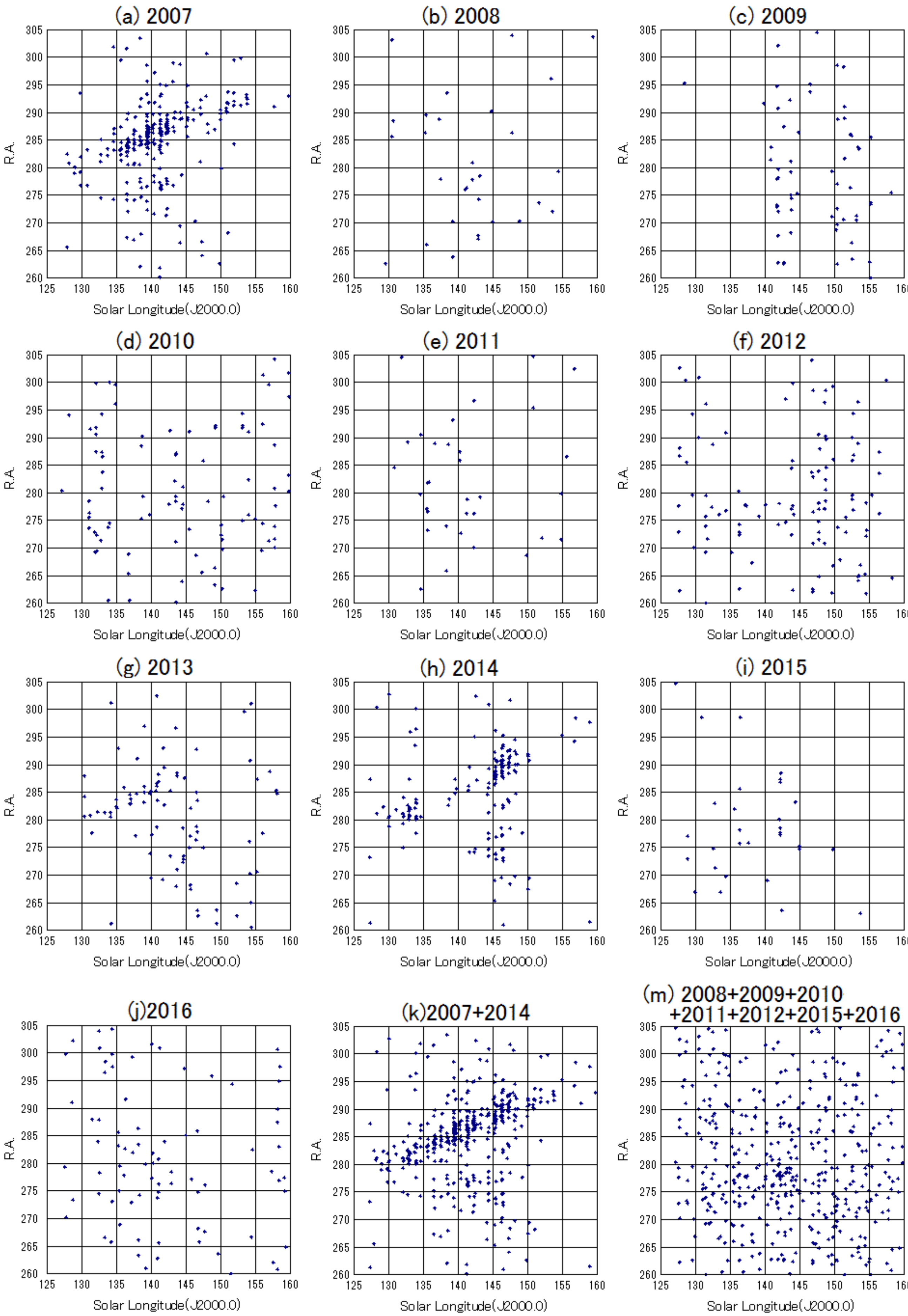

Figure 2 – Radiant region around KCG (Solar longitude – R.A.).

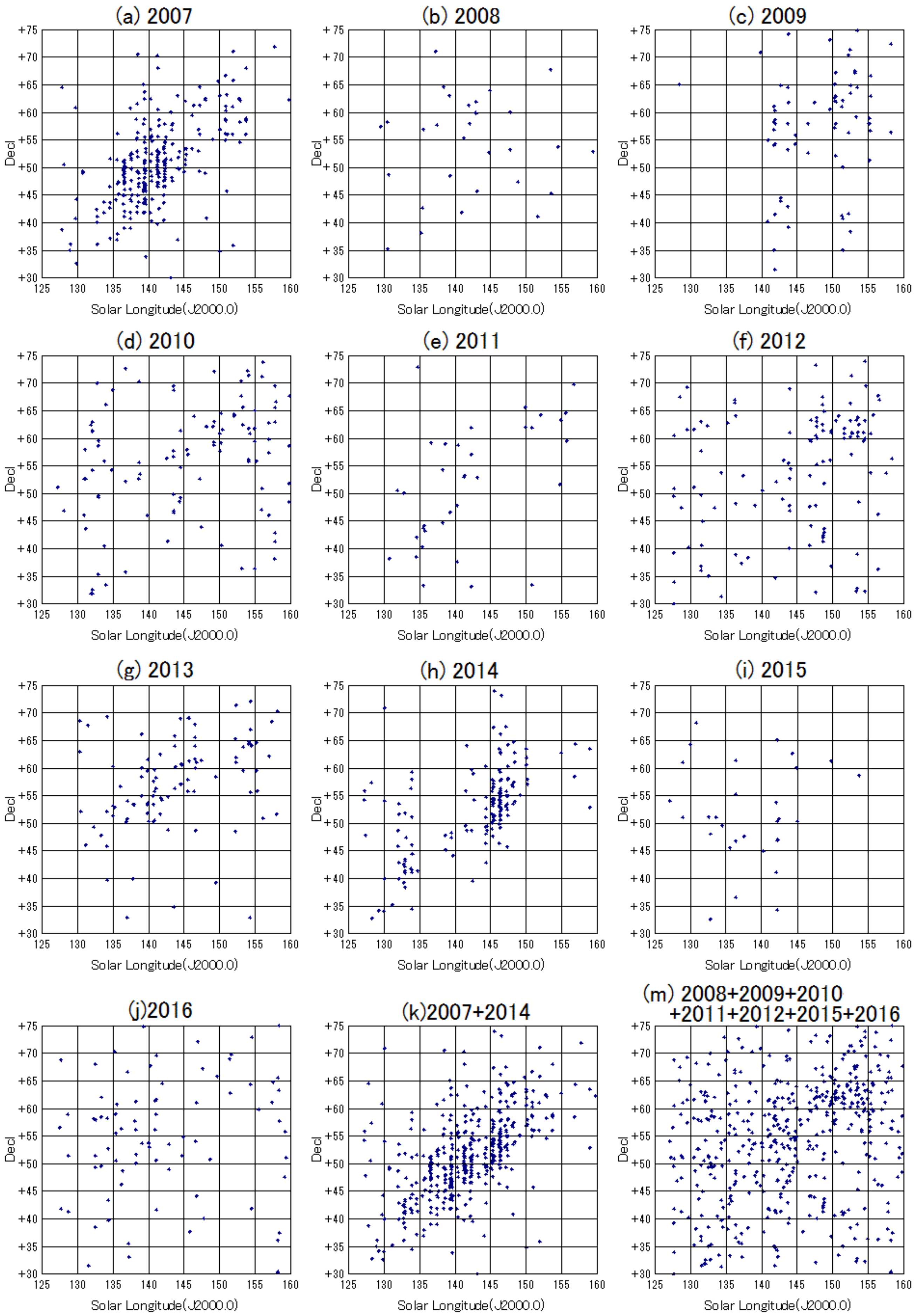

Figure 3 – Radiant region around KCG (Solar longitude – Decl.).

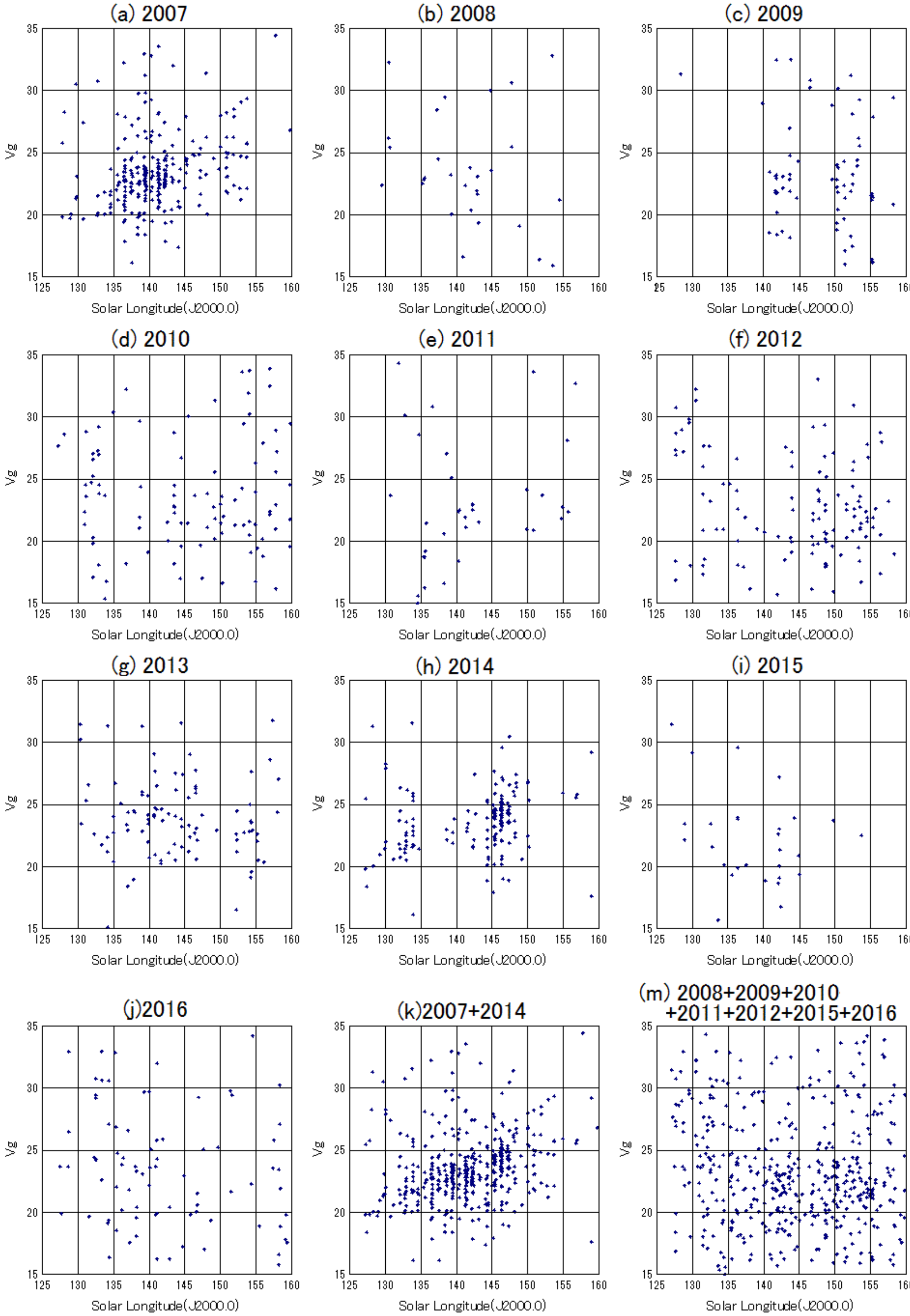

Figure 4 – Geocentric velocity around KCG radiant region (Solar longitude – V_g).

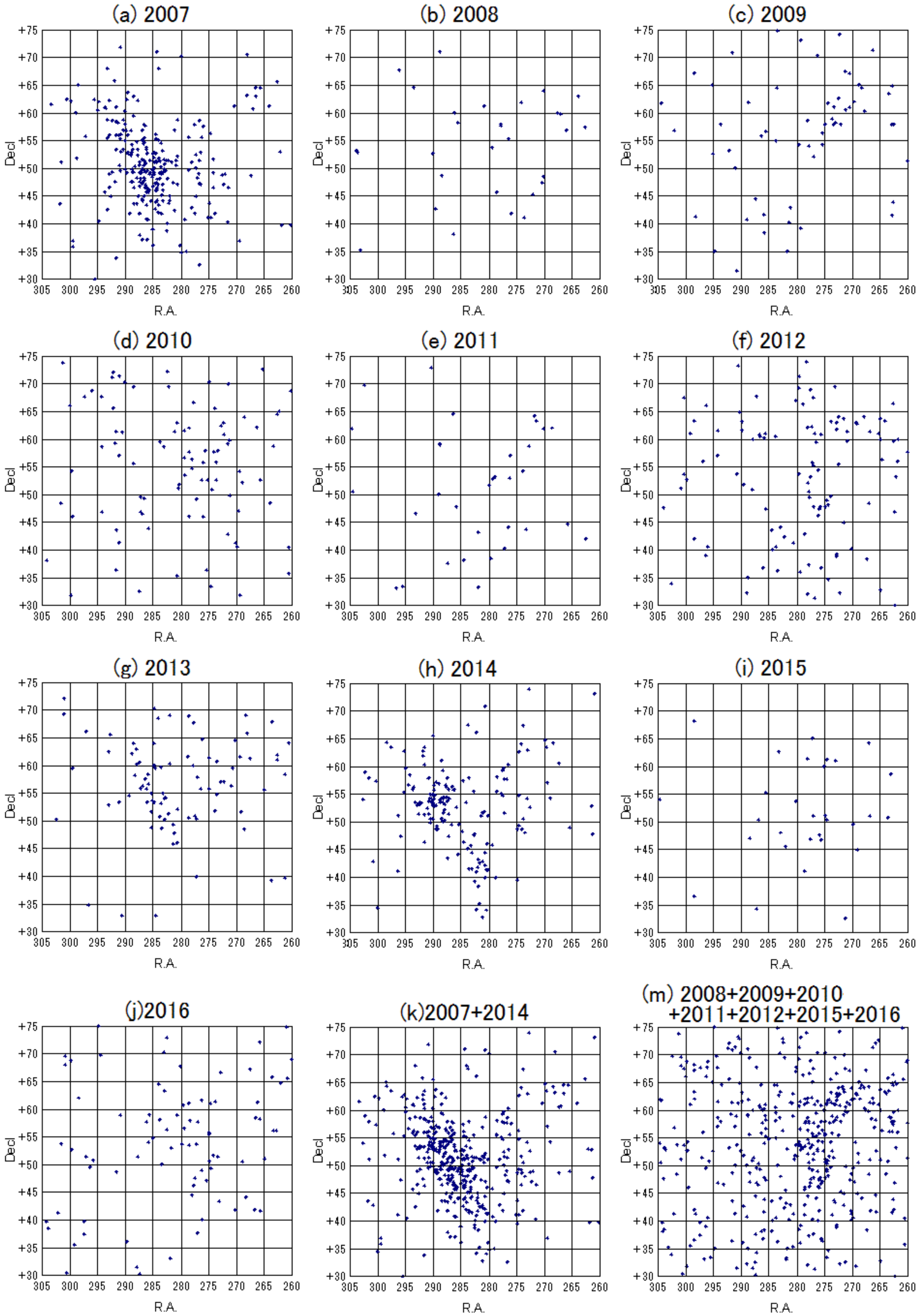

Figure 5 – Radiant distribution around KCG (R.A. – Decl.).

Table 3 – Meteor showers used to decide sporadic meteors.

IAU No.	Code	Shower Name
001	CAP	alpha Capricornids
005	SDA	Southern delta Aquariids
007	PER	Perseids
026	NDA	Northern delta Aquariids
033	NIA	Northern iota Aquariids
191	ERI	eta Eridanids
183	PAU	Piscis Austrinids
184	GDR	July gamma Draconids
187	PCA	psi Cassiopeiids
188	XRI	Daytime xi Orionids
206	AUR	Aurigids
208	SPE	September epsilon Perseids
533	JXA	July xi Arietids
587	FNC	59 Cygnids
523	AGC	August gamma Cepheids
701	BCE	beta Cepheids

and IOD radiant distributions (Figure 5m) so that they are understood as one meteor shower.

Sporadic meteors are decided by excluding shower meteors in Table 3 from all meteors. Table 3 includes all established meteor showers at IAU MDC (Porubčan & Jopek, 2017) active in the KCG season. Three showers 587 FNC, 523 AGC and 701 BCE are on the MDC 'Working list' (as opposed to established showers) at 2017 June. The deciding method for these showers was automatic judgment by UFOOrbit Ver2. Four meteor showers 184 GDR, 587 FNC, 523 AGC and 701 BCE in Table 3 are described in Section 3.6.

3 Results

3.1 KCG activity year by year

The D′ criterion described in Section 2 was applied to meteors recorded from 2007 to 2016 within 127–160° in $\lambda_\odot$(J2000.0), deciding shower membership of KCG and AUD. Table 4 are the results, where Sp(near) under 'Mean luminous magnitude' is mean magnitude of sporadic meteors whose radiants are in the research area and duration. Sp(far) is mean magnitude of sporadic meteors with $V_g = 22 - 27$ km/s whose radiant is outside the research area but which appeared in the simultaneous season. The ratio of KCG and AUD meteor numbers to sporadics is shown in Figure 6. Yearly variations in mean magnitude of KCG, AUD and sporadic meteors are shown in Figure 7.

Figure 6 indicates that the percentage of KCG in 2007 and 2014 is eight times enhanced compared with other years. For 2013 KCG, a two times enhanced rate is indicated. The AUD indicate a constant rate every year. Although the 2014 AUD look enhanced in Figure 6, it was estimated to include contamination of KCG meteors: it is difficult to separate both meteor showers reliably. In 2007, 2013 and 2014 KCG mean luminous magnitude (Figure 7) is brighter than in other years where KCG enhanced rates are not observed. The 2011 KCG and 2015 AUD had brighter recorded mean magnitude but sporadic meteors were simultaneously brighter. It can be estimated that in these years, many faint meteors could not be observed under bad sky conditions.

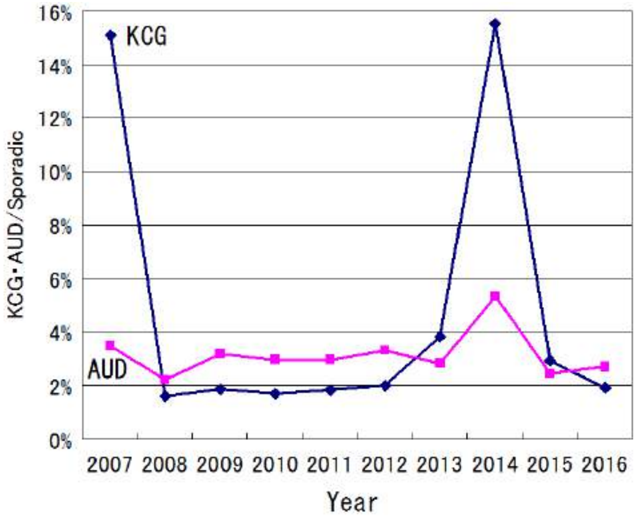

Figure 6 – Yearly changes of meteor rate (KCG and AUD).

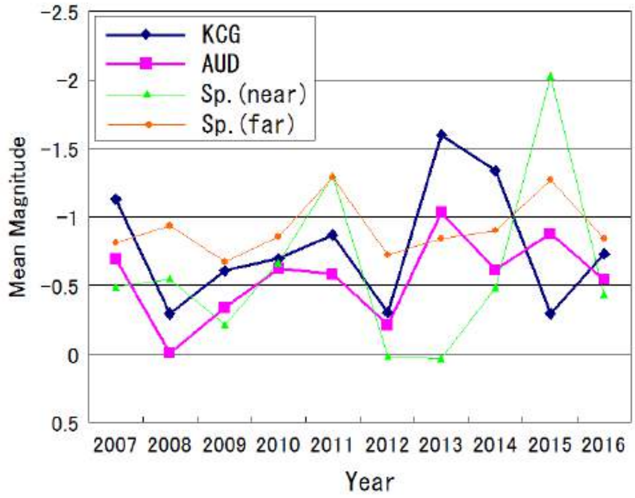

Figure 7 – Yearly changes of mean magnitude.

3.2 Activity curve

Meteor shower percentages compared to sporadic meteors for 5° bins in $\lambda_\odot$ were calculated (Figure 8). The years 2007 and 2014 with similarly enhanced observed

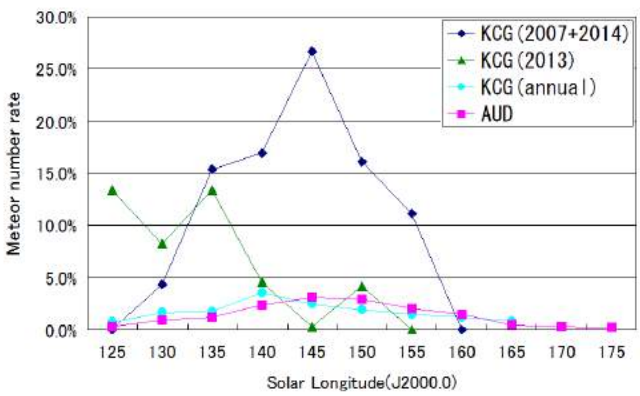

Figure 8 – Activity rate versus Solar longitude.

Table 4 – Numbers of meteors and mean magnitude. Sp = Sporadic.

Year	Meteor number					Meteor number percent		Mean luminous magnitude			
	All	Shower	Sp	KCG	AUD	KCG/Sp	AUD/Sp	KCG	AUD	Sp(near)	Sp(far)
2007	4424	2756	1407	212	26	15.07%	3.48%	−1.13	−0.70	−0.50	−0.81
2008	2167	1334	802	13	18	1.62%	2.24%	−0.30	−0.01	−0.55	−0.94
2009	2117	836	1219	23	39	1.89%	3.20%	−0.61	−0.34	−0.22	−0.67
2010	4198	1824	2268	39	67	1.72%	2.95%	−0.70	−0.63	−0.67	−0.85
2011	2477	1566	869	16	26	1.84%	2.99%	−0.87	−0.59	−1.31	−1.29
2012	4490	2010	2355	47	78	2.00%	3.31%	−0.30	−0.21	+0.02	−0.72
2013	3476	2008	1376	53	39	3.85%	2.83%	−1.60	−1.03	+0.03	−0.85
2014	1844	893	787	122	42	15.50%	5.34%	−1.34	−0.61	−0.48	−0.90
2015	1665	1017	615	18	15	2.93%	2.44%	−0.29	−0.88	−2.03	−1.27
2016	4216	2484	1655	32	45	1.93%	2.72%	−0.73	−0.54	−0.44	−0.85

Table 5 – Altitude from sea level at beginning and ending of luminous trajectory.

	Beginning[km]	Ending[km]	$\overline{V_g}$[km/s]	$\overline{\text{mag}}$	γ	n	BEG	END
KCG (2007 & 2014)	93.8 − 0.32mag	82.0 + 1.38mag	23.25	−1.2	2.1	334	93.8	82.0
KCG (2013)	92.1 − 0.71mag	81.8 + 1.36mag	23.85	−1.6	2.0	53	91.8	81.5
KCG (annual)	91.4 − 0.60mag	79.5 + 1.75mag	22.15	−0.5	2.1	189	91.8	79.9
AUD	90.6 − 0.69mag	78.7 + 2.16mag	21.05	−0.5	2.3	418	91.8	79.8
Sp(near)	91.8 − 0.54mag	80.6 + 2.56mag	24.22	−0.5	3.3	209	91.3	80.1
Sp(far)	90.2 − 0.03mag	79.6 + 2.65mag	23.21	−0.4	3.9	659	90.2	79.6

KCG rates were considered together. Years labeled 'annual' are the average of seven years when spectacular KCG were not observed (2008, 2009, 2010, 2011, 2012, 2015 and 2016). AUD is all ten years averaged.

Enhanced KCG years 2007 and 2014 had activity peak at $\lambda_\odot \approx 145°$ (Figure 8). The three times percentage enhanced KCG recorded at the 2013 peak was earlier by about 10° in $\lambda_\odot$ than the annual peak, while at $\lambda_\odot \approx 125°$ in 2013 only two KCG meteors were observed because the estimated weather condition was worse. The AUD peak is about a week later than the KCG (annual) peak.

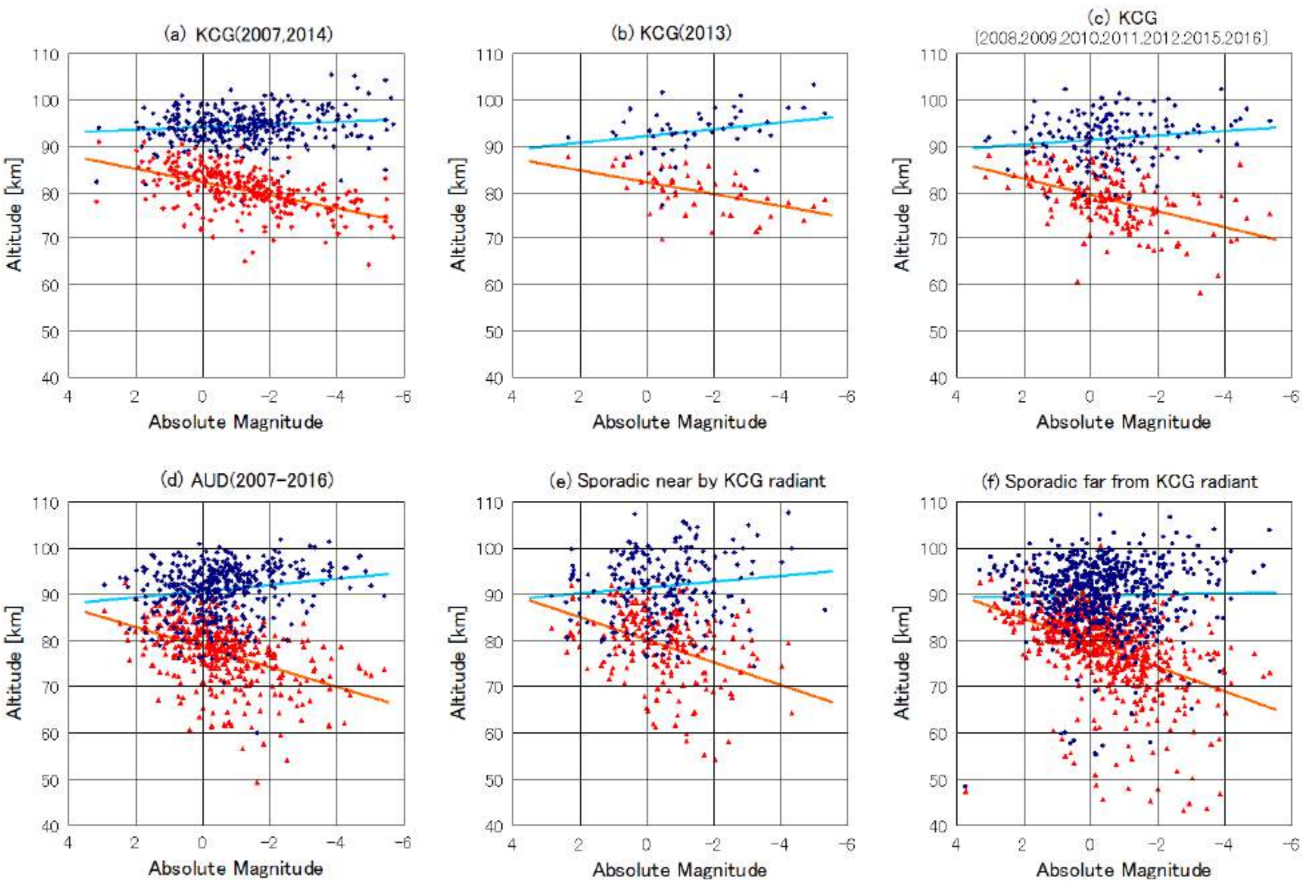

Figure 9 – Altitude from sea level at beginning and ending of luminous trajectory.

Table 6 – Radiant drift of KCG and AUD.

$\lambda_\odot$	KCG (2007+2014)			KCG (2013)			KCG (annual)			AUD (Observation)			Predict (2008 ED$_{69}$)			Predict (2002 GJ$_8$)		
	α	δ	V_g	α	δ	V_g	α	δ	V_g	α	δ	V_g	α	δ	V_g	α	δ	V_g
J2000.0	deg	deg	km/s	deg	deg	km/s	deg	deg	km/s	deg	deg	km/s	deg	deg	km/s	deg	deg	km/s
125	275.4	36.6	20.0				277.7	35.4	21.1	272.6	50.1	21.0	267.3	53.3	21.5	261.1	51.0	18.8
130	280.7	39.4	21.6	281.0	50.7	23.0	280.3	43.0	21.9	271.7	50.7	20.5	266.8	56.8	22.0	259.6	54.0	19.1
135	283.0	45.2	22.2	284.2	49.6	23.2	281.2	45.9	21.9	266.6	53.4	20.4	265.1	59.7	22.5	256.9	56.4	19.4
140	285.9	49.0	23.0	284.2	54.8	24.4	281.1	50.6	22.5	271.2	54.3	20.8	262.1	62.0	22.9	253.2	58.1	19.6
145	288.6	53.0	24.0	284.0	57.8	25.2	281.1	49.8	22.2	268.6	58.6	21.7	257.7	63.6	23.2	248.7	58.9	19.7
150	289.9	57.3	25.2							262.9	61.6	22.1	252.3	64.3	23.3	243.6	58.9	19.7
155	290.2	60.0	25.9							254.7	59.8	21.2	246.3	64.1	23.3	238.5	57.9	19.7
160										255.4	56.2	20.1	240.5	62.9	23.2	233.9	56.1	19.6
165										250.3	55.5	20.1	235.6	60.7	23.0	230.0	53.4	19.4
170										245.6	54.5	20.4	231.7	57.7	22.7	227.0	49.9	19.2
175										244.3	51.7	19.9	228.9	54.0	22.3	224.8	45.8	19.0

3.3 Luminous height

The beginning and ending altitudes of the luminous trajectory were fitted as linear approximations to absolute magnitude (Table 5). The meaning of KCG (annual) is the same as in Figure 8; Sp(near) and Sp(far) are the same as Table 4. AUD, Sp(near) and Sp(far) are averages from 2007 to 2016. In the 'Beginning' and 'Ending' columns, 'mag' is absolute luminous magnitude. $\overline{V_g}$ is mean geocentric velocity, $\overline{\text{mag}}$ is mean luminous magnitude, γ is population index, and n is number of meteors in the sample. Beginning and ending height distributions are in Figure 9 with the individual linear approximations also shown. Note that beginning and ending heights H_b and H_e vary according to V_g. Linear approximations of average H_b and H_e to V_g, for sporadic meteors in the same (KCG) season, are shown in Figure 10. In the velocity range V_g=20 to 27 km/s, sporadic meteors, that are similar velocity to KCG, were averaged in 1 km/s bins. The two rightmost column values 'BEG' and 'END' are standardized values that corrected this influence of velocity to the KCG (2007, 2014) average velocity (23.33 km/s) and to zero magnitude.

H_b and H_e for KCG (2007 & 2014) are the greatest, in particular significantly different from KCG (annual) (Figure 9). When sporadic meteor heights are compared with each other, those nearby the KCG radiant have higher altitude than meteors far from the radiant.

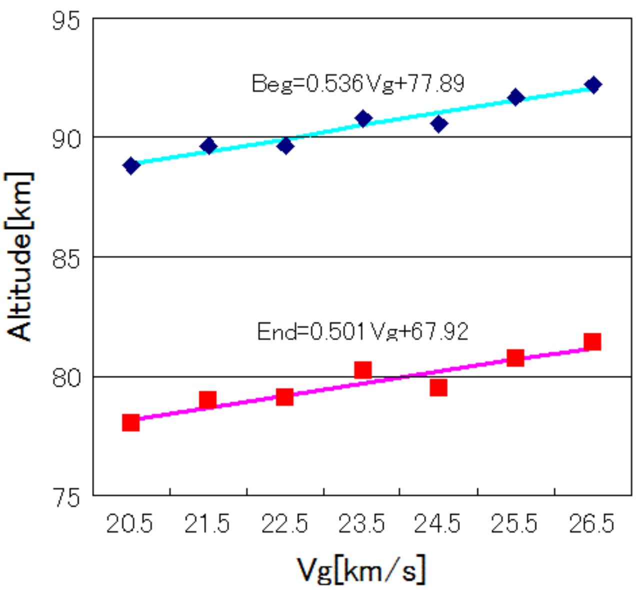

Figure 10 – Velocity dependence of beginning and ending altitude for sporadic meteors.

3.4 Radiant drift

Radiant drifts of KCG and AUD are shown in Table 6. Right ascension and declination of radiant are averaged for 5° bins in $\lambda_\odot$. Two labels 'Predict' for asteroid 361861 (2008 ED$_{69}$) and (2002 GJ$_8$) (NASA JPL, 2017) are based on ejected particle prediction by using Hasegawa (1990). The data are also shown in Figure 11. Note that 2002 GJ$_8$ ejection was predicted based on its orbit after 2015 June at which time it had approached Jupiter.

The KCG radiant drifts north-north-east, varying to north at the terminal stage. The KCG (2013) radiant position is about 5° north of KCG (2007 & 2014). The AUD radiant drift is unusual, moving west when drawn in an arc. Observational results are more similar to the prediction from 361861 (2008 ED$_{69}$) than from

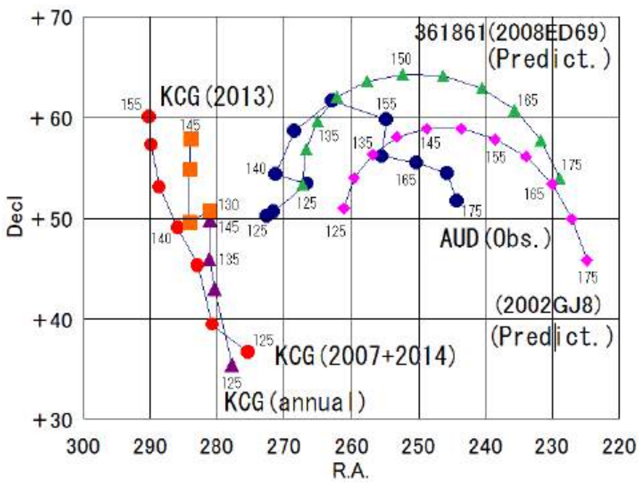

Figure 11 – Radiant drift of KCG and AUD. Numbers beside points are $\lambda_\odot$ (J2000.0).

Table 7 – Minor showers nearby KCG.

IAU	IAU MDC			This work (average)											
Code	$\lambda_\odot$	R.A.	Decl.	D′	N	$\lambda_\odot$	R.A.	Decl.	V_g	a	q	e	peri	node	i
GDR	124.0	280.1	+50.3	0.053	54	125.2	280.6	+50.6	28.3		0.977	1.011	202.3	125.2	41.2
FNC	137	314.2	+47.5	0.105	44	135.3	312.9	+46.6	35.7	23.5	0.851	0.964	227.6	135.3	54.6
C/1940 O1 (Whipple-Paraskevopoulos)										*56.5*	*1.082*	*0.981*	*235.7*	*135.1*	*54.7*
AGC	156.0	354.2	+76.6	0.053	44	154.5	356.9	+75.9	45.0	27.2	1.005	0.963	188.3	154.5	76.6
BCE	153.0	325.4	+75.8	0.053	15	154.4	315.9	+75.9	38.7	24.3	1.006	0.959	187.2	154.4	63.4
TLA	133	332.2	+44.8	Could not judge existence or absence											
ODR	110.0	259.3	+55.8	Not detected											
ETP	135.4	334.6	+32.7												
ZED	115.7	251.6	+66.5												
ZDR	122	261.7	+67.8												

(2002 GJ_8) although details do not match. The observed AUD geocentric velocity is at the middle of the two asteroids' predictions (Table 6).

3.5 Orbital elements

Distributions of some orbital elements are shown in Figure 12: orbital period p, perihelion longitude λ and inclination i. At the top of the p panels, periods having integer ratio with Jupiter are indicated. From the left in Figure 12 are KCG (2007, 2014), KCG (2013), KCG (annual) and AUD. A peak for KCG (2007, 2014) exists in 7.0–8.6 yr but not clearly. The KCG (2013) peak period is shorter, 6.8–7.6 yr. These are longer than 5:3 resonance with Jupiter (7.116 yr). Perihelion longitude of KCG (2013) is 10° smaller than KCG (2007, 2014) and inclination 5° larger. All orbital elements of KCG (annual) have two or more peaks. The three AUD plots indicate only one peak. The AUD peak in p is around 5.6 yr, longer than the period (4.97 yr) of the possible parent body 361861 (2008 ED_{69}).

Perihelion distance q (top), argument of perihelion ω (middle) and inclination i (bottom) are shown in Figure 13 as functions of solar longitude (eq:2000.0). Perihelion distance and argument of perihelion of KCG (2013) and KCG (annual) indicate intermediate features between KCG (2007, 2014) and AUD. Distributions of all orbital elements of KCG (2013) were shifted to ~10° smaller $\lambda_\odot$ than KCG (2007, 2014). All KCG (annual) distributions were very diffuse. The AUD q distribution (mean=1.001) is more similar to 2002 GJ_8 (q=1.031) than 361861 (2008 ED_{69}: q=0.760).

3.6 Nearby meteor showers

I studied minor meteor showers adjoining the KCG radiant position and season. Nine showers described at IAU MDC (Porubčan & Jopek, 2017) at 2017 February were researched. For judgement of existence of individual meteor showers, radiant concentrations were researched on plotted figures for $\lambda_\odot$–R.A., $\lambda_\odot$–Declination, $\lambda_\odot$–V_g and R.A.–Declination. The results in Table 7 include four meteor showers existing and four absent.

The left side columns 'IAU MDC' of Table 7 are from Porubčan & Jopek (2017). The right side of Table 7 is researched results in this work, where D′ is the

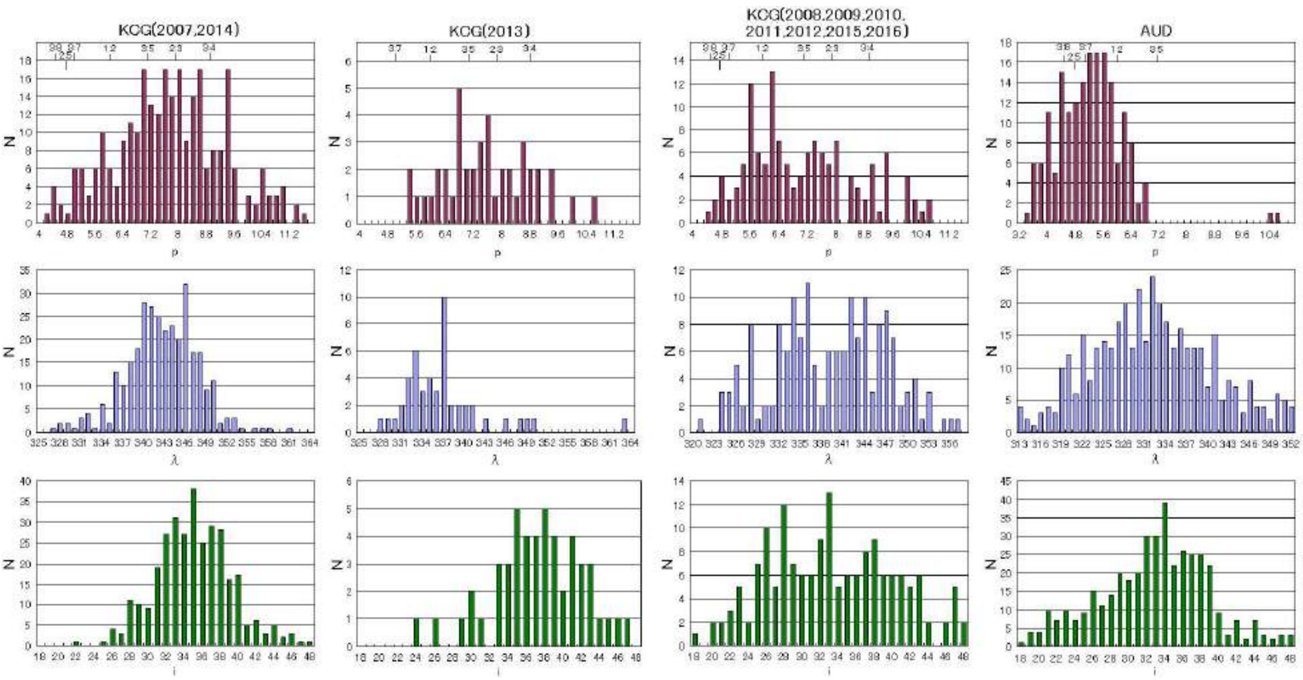

Figure 12 – Orbital period, perihelion longitude and inclination distributions.

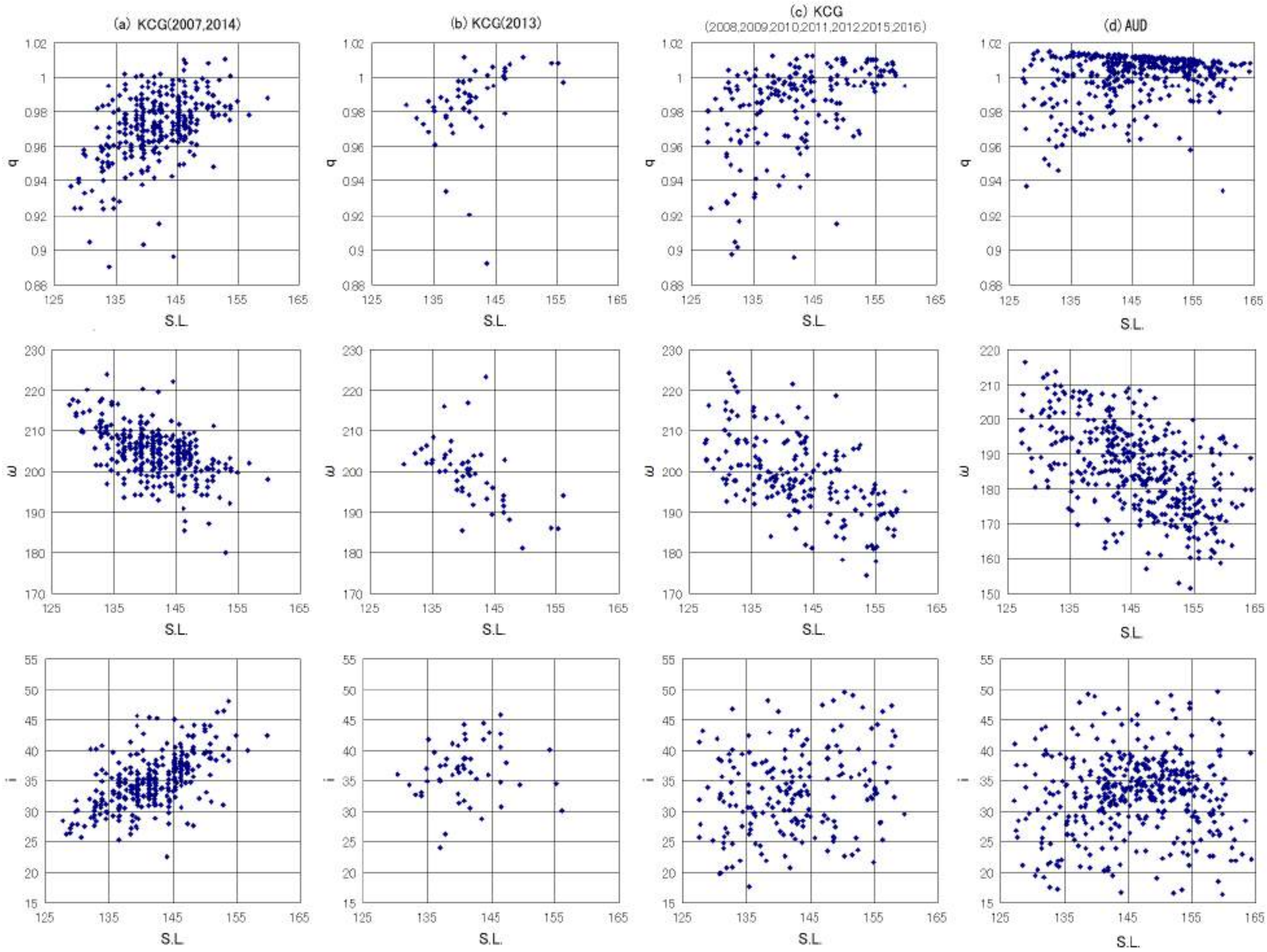

Figure 13 – Orbital element variations with solar longitude.

D′ criterion value used for deciding shower membership, N is number of meteors belonging to shower in ten years, $\lambda_\odot$ solar longitude, 'R.A.' and 'Decl.' radiant right ascension and declination, V_g geocentric velocity, a semimajor axis, q perihelion distance, e eccentricity, 'peri' argument of perihelion, 'node' ascending node, i inclination.

GDR (July gamma Draconids **#184**)

Radiant position is very close to KCG and appears in initial part of KCG season. Short observable duration of 120–133° in $\lambda_\odot$ indicates narrow peak. D′ criterion used half the traditional value because GDR have a concentrated radiant in a short observable duration. Radiant drift is:

$$\begin{aligned} \text{R.A.} &= -0.07(\lambda_\odot - 125.2) + 280.6 \\ \text{Decl} &= 0.02(\lambda_\odot - 125.2) + 50.6 \\ V_g &= -0.15(\lambda_\odot - 125.2) + 28.3 \quad \text{[km/s]} \end{aligned}$$

Average magnitude is −1.0, and population index is 2.5. Linear approximations to beginning height (H_b) and ending height (H_e) are below, where 'mag' is magnitude.

$$\begin{aligned} H_b &= 96.6 - 0.64\text{mag} \quad \text{[km]} \\ H_e &= 84.2 + 2.9\text{mag} \quad \text{[km]} \end{aligned}$$

H_b is similar to KCG (2007, 2014) and H_e is somewhat lower than comparable velocity sporadic meteors. GDR will be easy to identify by TV observation but difficult to separate from the nearby KCG radiant by visual observations.

FNC (59 Cygnids **#587**)

FNC meteors appear from further east than KCG and show more rapid geocentric velocity (Figure 14). The time interval when they appear is 128–148° in $\lambda_\odot$ (J2000.0). Plotted radiants in Figure 14 are from 130 to 145° in $\lambda_\odot$. The traditional value of the D′ criterion was used because of the diffused radiants. Radiant drift is:

$$\begin{aligned} \text{R.A.} &= 0.02(\lambda_\odot - 135.3) + 312.9 \\ \text{Decl} &= 0.17(\lambda_\odot - 135.3) + 46.6 \\ V_g &= -0.20(\lambda_\odot - 135.3) + 35.7 \quad \text{[km/s]} \end{aligned}$$

Average magnitude is −1.4, and population index is 2.8. Linear approximations to beginning height and ending height are below, where 'mag' is magnitude.

$$\begin{aligned} H_b &= 97.8 - 1.08\text{mag} \quad \text{[km]} \\ H_e &= 87.8 + 1.24\text{mag} \quad \text{[km]} \end{aligned}$$

H_b is same as KCG (2007, 2014) and H_e is rather high. Identifying this meteor shower is easy by TV observations because of the differences of radiant point and

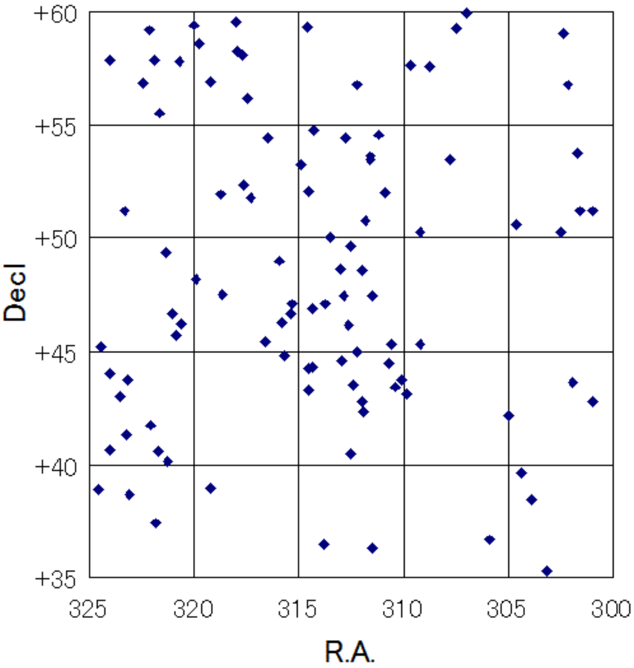

Figure 14 – Radiant area of FNC.

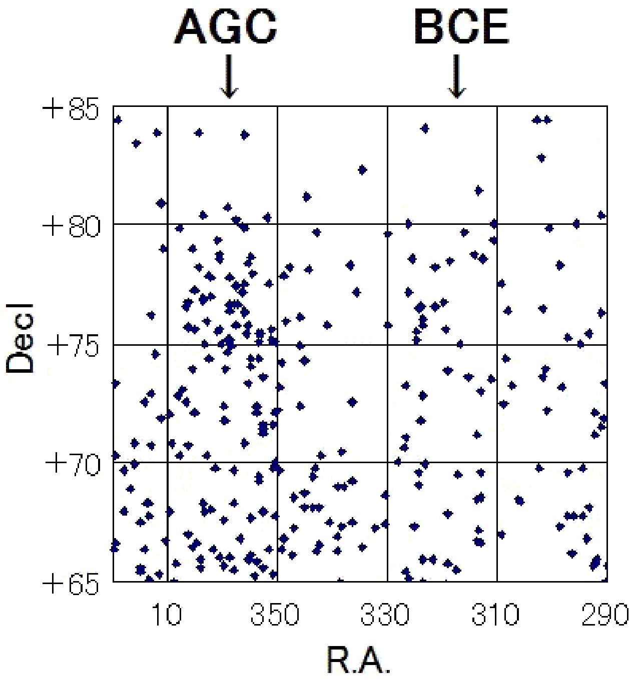

Figure 15 – Radiant area of AGC and BCE.

velocity although it overlaps with KCG season. Identifying with KCG will be difficult by visual observations. Orbital elements resemble C/1940 O1 (Whipple-Paraskevopoulos) (NASA JPL, 2017).

AGC (August gamma Cepheids **#523**)

Active duration is 149–161° in $\lambda_\odot$. Radiant distribution is diffuse. Radiant position is nearby BCE, but there is an empty area between the two radiant distributions (Figure 15). Half the traditional value of the D′ criterion was taken despite the diffuse radiant distribution, because if the traditional value (0.105) is chosen then many meteors are decided as belonging to both

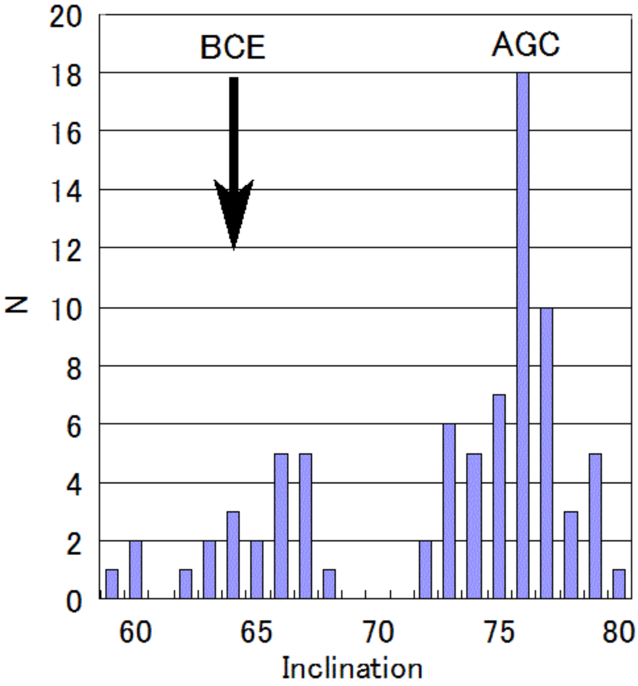

Figure 16 – Inclination distribution of AGC and BCE.

meteor showers. Radiant drift linear approximations are:

$$\begin{aligned}
\text{R.A.} &= 0.71(\lambda_\odot - 154.5) + 356.9\\
\text{Decl} &= 0.38(\lambda_\odot - 154.5) + 75.9\\
V_g &= 0.06(\lambda_\odot - 154.5) + 45.0 \quad [\text{km/s}]
\end{aligned}$$

Orbital elements are similar to AUD in perihelion distance, node and argument of perihelion. Mean magnitude is −1.3, population index is 2.8. Linear approximations to beginning height and ending height are below, where ‘mag’ is magnitude.

$$\begin{aligned}
H_b &= 104.3 + 0.70\text{mag} \quad [\text{km}]\\
H_e &= 93.2 + 3.09\text{mag} \quad [\text{km}]
\end{aligned}$$

BCE (beta Cepheids **#701**)

Weak meteor shower identified (Figure 15), however this meteor shower was described as absent (Jenniskens et al., 2016c) in SonotaCo data. It appeared for a short duration between 151–160° in $\lambda_\odot$. Radiant drift was not clear. D′ criterion was taken as half of traditional value, same as AGC. Mean magnitude −1.8 was bright. Orbital elements have characteristics similar to AGC except inclination 10° smaller. There may be relevance between both meteor showers however inclination clearly isolates the two meteor showers as separate (Figure 16). Figure 16 is shown for the ranges $\lambda_\odot$ 150–160°, R.A. 305–10° and declination +73 to +80°.

4 Discussion

Meteor shower identification techniques are adopted in two ways in this study. One is meteor orbit calculation software UFOOrbit V2 where evaluation is based on radiant position and meteor velocity. A ‘csv’ file defining predetermined meteor showers includes meteor shower duration in solar longitude, radiant position with its drift, geocentric velocity, radiant position error and velocity error. Moreover, UFOOrbit V2 is able to expand duration, radiant position error and velocity individual error. Its specifications conform to TV meteor observations that tend to have larger velocity error than photographic observations. In this study, the V_g error allowed ±6.5 km/s for KCG, that velocity correlating with a wide radiant declination range, and ±3.9 km/s for AUD. Calculated orbital elements tend to indicate larger error on velocity dominated elements. Thus semi-major axis and argument of perihelion have larger error but inclination and perihelion distance have smaller error. The other way of meteor shower identification is the D′ criterion (Drummond, 1981), an orbital similarity evaluation method adopted to classify meteors as belonging to KCG or AUD (with IOD). These two methods could not always conclude the same results. 78% of the D′ criterion results for KCG (2014) were also decided by UFOOrbit as KCG but 22% belong to AUD or sporadic. UFOOrbit decision and D′ criterion agreement for 2013 KCG meteors was only 8%, and for KCG (annual) was 15%. Too many meteors were misclassified by either method. One reason is orbital similarity between KCG and AUD whose D′ criterion relative to each other is 0.094 so that they could be judged as a single meteor shower. I aimed that significantly enhanced shower radiant concentrations observed in 2007 and 2014 can be explained as KCG. Therefore, twice as high a threshold was used for KCG than AUD to decide which shower individual meteors belong to. However misjudged meteors still may exist that can be seen on Figure 6. I aimed for accurate meteor shower classification in this study but I could not succeed in removing doubtful meteor shower decisions completely. To solve this problem, many further orbital data with low errors need to be obtained.

There are statistical errors in meteor trajectory heights. For some meteors, not all the trajectory with its beginning and end points could be recorded, for reasons of limited viewing angle lenses used or interference of clouds and buildings. However many SonotaCo network observers use short focal length lenses generally, so that most beginning or end points will be in the lens field of view. Therefore many meteors were estimated for which the whole luminous trajectory can be calculated. Other reasons exist for errors in calculated beginning and end heights, including sensitivity differences between different specification cameras or lenses, and differences in distances from observation sites to the meteor. Automatic meteor reduction software UFOAnalyzer cannot recognize too faint a part of a meteor trail that is near the beginning and end. In all these cases, beginning and end point heights tend to become closer to each other because of the error. Comparison between equivalent durations of SonotaCo Network observation results will involve very few statistical errors because of similar observation equipment used. On the other hand, in comparison between different times, statistical height errors would originate from a few differences of observation equipment. But error is estimated as not so large because many observers continuously use equipment for a long time. Errors in luminous height comparison between different meteor showers can be neglected because samples are sufficiently many in this study.

Generally, TV meteor observation results generate larger error than photographic observations. However peaks in orbital element distributions become blurred whereas shifts in the peak are very small. Details were described in Shiba (2016).

The existence of the seven year KCG activity cycle had been pointed out by some researchers (Koseki, 2014; Moorhead et al., 2015). In this study, the seven year interval at 2007 and 2014 with eight times enhanced KCG could be confirmed. This result matches past photographic observation results (Lindblad, 1995) proving the distribution of large size meteoroids. On the other hand, visual observation results surprisingly could not find the seven year cycle (Rendtel & Arlt, 2016) corresponding to the medium size meteoroid distribution. Radio observation results for the smallest meteoroids particle distribution show a ten times enhanced rate of KCG in 2014 but only 20% of that recorded in 2007 (Moorhead et al., 2015). TV meteor observation research can span between photographic and visual size meteoroids. If these inconsistent results are accurate, the source of the KCG enhancement consisted of a strange meteoroid size distribution. Future work will elucidate whether such a meteoroid distribution exists, or any observation error existed in any of the data sets.

Historical photographic observation results (Lindblad, 1995) and also 2007 and 2014 enhanced KCG observation results can be explained consistently by the 5:3 resonance (7.116 yr) with Jupiter's period (11.862 yr). However longer orbital period KCG meteors than 7.116 yr (Figure 12) were rather many in this study. In general, there are some considerable reasons that the meteor orbital period is observed to be short due to the observation error, but there are few reasons that shift to longer orbital period. Next, more accurate orbits from all KCG are selected (Figure 17). Figure 17-a is all KCG (2007+2014) orbits. Figure 17-b selects meteors that cross an angle $> 25°$ and having luminous duration > 0.5 seconds. The more accurate period distribution (Figure 17-b) shows a 0.2 yr decrease in average period, closer to the 5:3 resonance but still not enough to match. Unknown reasons may exist causing orbital period overestimates in this calculation.

If the seven year periodic KCG enhancement has orbital period same as the 5:3 resonance with Jupiter, it could be caused by encounter with a 'swarm' (Asher & Izumi, 1998). The 2013 KCG caused by the periphery of the swarm was not only fewer meteors appearing than 2007 and 2014 but also systematic differences observed in radiant position, orbital elements and earlier finishing of activity.

If enhanced 2007, 2014 and 2013 KCG are caused by only a single continuous swarm, it suggests that a distorted swarm exists. The reason for distortion may be Jupiter's gravity acting in the opposite direction before and after the KCG ascending node (triangle in Figure 18). Note that the 2013 KCG weather at the start of the

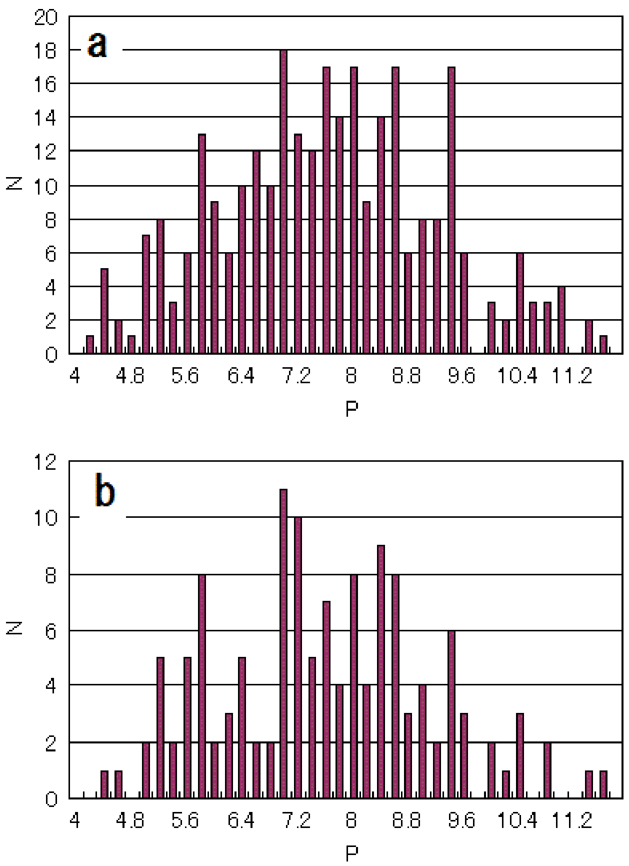

Figure 17 – KCG orbital periods, showing effect of error: lower plot includes more accurate orbits only.

season was bad and very few orbital data were taken. The data source for 2013 KCG in Figure 8 at $\lambda_{\odot}$=125° was only KCG=2 and sporadic=15. A future 2020 observation chance is expected.

When the D′ criterion is applied to the AUD orbit, the most similar asteroid orbit is judged as 2002 GJ_8 but not 361861 (2008 ED_{69}). It seems that the AUD parent body is 2002 GJ_8. However, 2002 GJ_8 approached Jupiter to a distance of 0.052 AU in 2015 June and the orbit changed dramatically (NEODyS-2, 2017). The previous orbit is so different from recent AUD, especially with only 5°1 inclination (IAU MPEC 2002-G63). 2002 GJ_8 as observed before 2015 is never the AUD parent body. It may be the first case that a meteor shower's parent body is not the object with the most similar orbit. Still, the orbitally unstable asteroid 2002 GJ_8 may be a Cygnids complex member, and with the possibility to create future meteor showers similar to AUD.

Four Halley type or long period comet type meteor showers were identified near the KCG radiant. The AGC and BCE relation in these showers is interesting. Only the inclination difference is 10° but all other orbital elements exactly agree with each other (Table 7). I described them above as independent showers because clear voids exist between both meteor shower orbits. However I am interested whether the gap will fill in or not with future observation results. If further radiants fill in the gap, these two showers must be considered as a single meteor shower.

Standard evaluation criteria for identifying meteor showers are needed for accurately understanding complex radiant areas such as the 'Cygnids complex'. When two meteor showers exist on nearby orbits, I propose that a criterion to decide the existence of two independent meteor showers is to agree with least one of the two requirements below:
(1) There is reason to presume that the two showers have individual parent bodies.
(2) A gap clearly exists in at least one of activity duration, radiant distribution, velocity and orbit.
Some historical examples are next. The Andromedid radiant position and active duration changed considerably through its observation history. Observed meteor showers clearly indicate a gap in broad radiant area or long active duration. However all showers were thought to have a common parent body (3D/Biela). Thus, these are described as the same meteor shower, namely the Andromedids (Kronk, 1988). Eta Aquarids and Orionids are thought to have a common parent body (1P/Halley) but had been recognized as different meteor showers because radiant distribution and active duration are not continuous when meteoroids collide with the Earth at ascending node and at descending node. The Taurid meteor shower is generally classified as two meteor showers 'Southern Taurids (STA)' and 'Northern Taurids (NTA)'. These radiant positions are close to each other and have simultaneous active duration but there is an orbital distribution gap in the ecliptic plane. The above two requirements agree with some traditional manners of meteor shower classification. Note that in requirement (2), 'gap' does not mean 'decreases'. When a decrease is observed, it means that we observed a shower's interior structure. If an observed population is sparse, we may find a fake gap. We must get many accurate individual meteor orbit data to allow accurate meteor shower classifying.

Based on the above requirements, I described alpha Lyrids (Lindblad, 1995) as an initial part of KCG in this paper. (#464)KLY and (#413)MUL orbits were described in Jenniskens & Nénon (2016) from only 2014 observation data, so that these match belonging to KCG. Therefore, these meteor shower orbit distributions are very broad, especially inclination is spread by 10° or more, but these showers are thought to comprise one cluster that is constrained in a resonance by Jupiter, termed a 'swarm' (Asher & Izumi, 1998). On the other hand, annual KCG have a similar orbit but that is thought to evolve through other processes. KCG (annual) is labeled 'KCG' in this paper because its orbit was similar with KCG (2007 & 2014). However it is possible that sufficient future observation will reveal as a new complex meteor showers with new shower names.

AUD sparse radiants move westward while tracing out an arc-shaped trajectory over a long active period. Its strange radiant drift can be explained as dispersed particles from parent body 2002 GJ_8. (#470)AMD and (#703)IOD were explained as independent meteor showers because these did not continue from AUD (Jenniskens et al., 2016a). I took two selection standards for deciding AUD membership in this paper. I could

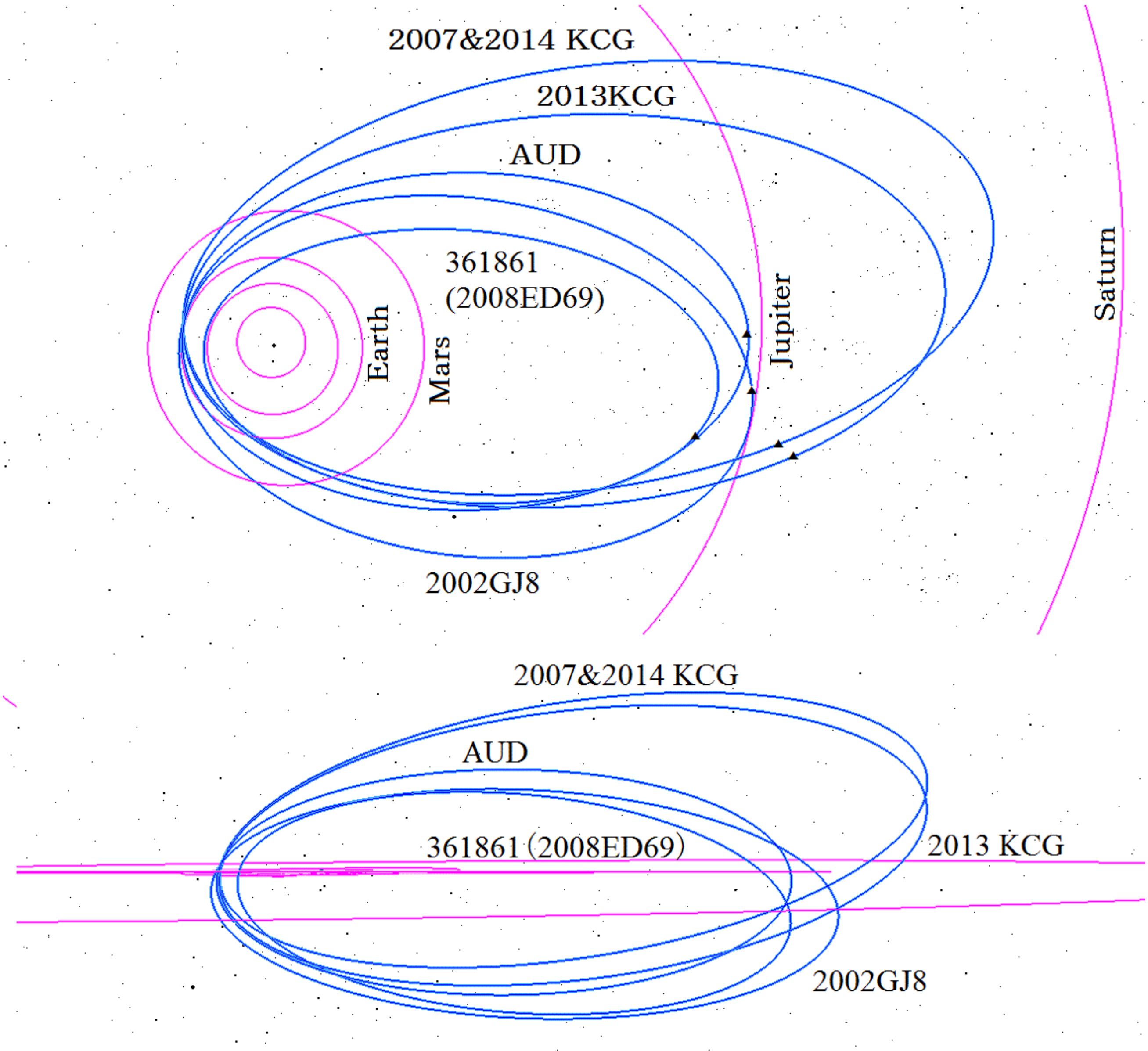

Figure 18 – Orbits of KCG, AUD and two asteroids, viewed from above ecliptic and from side. Triangles mark ascending nodes.

not find a gap in their radiant drift or orbital element distributions so that every orbital element distribution was considered to have a single maximum. Therefore, although the active period is so long and the radiant distribution is wide, I cannot find a reason to distinguish AMD and IOD from AUD. We also need to consider the relationship with KCG and AUD of showers in the vicinity: (#279)ZED, (#73)ZDR and (#220)NDR.

I discuss the possibility below that KCG and AUD are from one common parent body. KCG meteoroids never approach Jupiter because KCG exists in a quasi-stable resonance orbit. However the inclination distribution is broad which might be the result of many years orbital evolution. On the other hand, AUD meteoroids are on unstable orbits because they often encounter Jupiter. Most meteoroids cannot stay in their orbits for many years. Each meteor shower's component meteoroids are different, with KCG magnitude brighter than AUD and KCG trajectory height generally higher than AUD. At first, it cannot be possible that KCG evolved from AUD. If it happened, AUD meteoroids flow into three resonance positions on the KCG orbit and three swarms must be produced. But a KCG swarm exists at only one resonance point. The opposite possibility cannot be denied completely that AUD evolved from KCG. If KCG contains a great quantity of meteoroids in orbits unobservable from the Earth, the AUD meteor shower may be produced, though the existence of unknown processes must be proved to evolve from KCG to characteristic AUD orbital element distributions. As a conclusion of a realistic scenario, one parent body in a resonance position produced KCG and one parent body not in a resonance point produced AUD. Thus, KCG and AUD contain many similar orbit meteoroids that are difficult to classify but these are independent meteor showers.

Many meteor showers can be detected by automatic TV and radio observations recently. Enhanced detection sensitivity will give us many accurate meteor data that include many nearby radiants or orbits of meteor showers. Automatic decisions on meteor showers by CAMS (Jenniskens & Nénon, 2016) have a good compatibility with automatic TV observation, so that we expect such progress. New criteria are needed to identify whether two meteor showers are distinct or a synthesized single meteor shower. 'D criterion' thresholds were decided that are consistent with traditional meteor shower identification (i.e., Southworth & Hawkins, 1963). Incidentally, Jenniskens & Nénon (2016) apply 'high-threshold D criterion' for identifying meteor showers, not a traditional value. Their method is a superior way for concentrated radiants and short active duration showers such as 'GDR'. However this way tends to fail for broad radiants and long active duration meteor showers. Thus, new, harsher criteria are needed for concentrated radiants and short active duration showers. For diffuse radiant showers like AUD, it is necessary to apply loose judgment criteria corresponding to the component showing the widest distribution among the components of the orbital elements. But it is a difficult task to obtain reliable separation with nearby meteor showers like KCG.

Enhanced KCG encounter years also showed brighter mean magnitude KCG than normal years. Normal years KCG have two or more peaks in each orbital element distribution so that the annual KCG is considered a complex meteor shower. These features are similar to the Southern Taurids having 'swarm components' in resonance and 'annual components' (Shiba, 2016). This fact may be a general feature of resonant meteor shower swarm generation and evolution. KCG (annual) have not only complex features, but features intermediate with AUD and KCG (2007, 2014). Additionally, it is possible that we may observe an evolutionary stage of sporadic meteoroids from KCG and AUD around this area because these sporadic meteors' luminous height was higher than far radiant sporadic meteors. In this area, there may exist a substantial evolutionary stage of meteoroids corresponding to the sporadic meteors originating from KCG and AUD.

5 Conclusion

Kappa Cygnids (KCG) and neighboring meteor showers were studied by data from the automatic low light TV meteor observation network in Japan (SonotaCo Network).

In 2007 and 2014 KCG eight times enhanced meteor numbers were detected compared with KCG in annual years. This result was confirmed with a seven year active period (Figure 6) explained by previous researchers (Koseki, 2014; Moorhead et al., 2015). This period indicates the existence of a 'swarm' (Asher & Izumi, 1998) in 5:3 orbital resonance with Jupiter (7.116 yr). The calculated peak of the orbital period distribution around 8 yr (Figure 12) was thought to include error or bias for another reason. Enhanced KCG observed years 2007 and 2014 showed brighter than annual KCG magnitudes (Figure 7) and also luminous heights were greater (Table 5). These suggest that the meteoroid component in enhancement years differs from annual KCG. Annual KCG orbital element distributions show two or more peaks and therefore annual KCG as a complex meteor shower (Figure 12). This relation is similar to Southern Taurid (STA) swarm components and annual components (Shiba, 2016). In 2013, a previous year of enhanced KCG meteor numbers, a three times meteor rate was observed, originating clearly from radiants more concentrated (Figure 5g) than in annual years (Figure 8). Brighter mean magnitude and high trajectories were observed in 2007 and 2014 individually. However 2013 KCG radiants are distributed 5° further north (Figure 5g) with early end to activity compared with 2007 and 2014 (Figures 2, 3), and furthermore orbital element distributions systematically different (Figure 13). If 2007, 2013 and 2014 KCG are caused by one continuous swarm encounter, an asymmetric distorted swarm exists.

August Draconids (AUD) are a weak meteor shower with diffuse radiants to the west of KCG (Figure 5m). The beginning of AUD is almost at the same time as KCG but lasts till late September. AUD is thought to originate from asteroid 361861 (2008 ED_{69}) with prediction of ejected meteoroids indicating similar drift but shifted position (Figure 11). Since the AUD orbit intersects the Earth orbit at its perihelion, the radiant point moves westward drawing the locus of a circular arc during the long active period. AUD was considered as a complex meteor shower or two or more meteor showers due to long active duration with strange radiant drift. However, orbital distribution features indicate that AUD is only one meteor shower (Figure 12).

KCG and AUD orbits are so close as to be judged one meteor shower by the D' criterion. But differences of radiant distributions, periodic activity and physical structure can identify both meteor showers.

Some neighboring showers exist in the KCG and AUD radiant region (Table 7). These are identified as belonging to long period comet type or Halley type orbits and not relating to KCG or AUD. However separating these meteor showers and identifying with KCG and AUD by visual observation is difficult.

Acknowledgments

This work depends on over ten years observation data from the SonotaCo Network. I thank many network observers for offering data over a long duration and more especially Mr. Kanamori who was managing the network with software he produced. Local meteor workshop members in western Japan 'Juso-juku' always advised me: Mr. T. Sagayama telling me of various literature, and Mr. M. Ueda calculating meteor radiant predictions for this work. I thank Juso-juku members especially Mr. Sagayama and Mr. Ueda.

References

Asher D. J. and Izumi K. (1998). "Meteor observations in Japan: new implications for a Taurid meteoroid swarm". *Mon. Not. Roy. Astron. Soc.*, **297**, 23–27.

Drummond J. D. (1981). "A test of comet and meteor shower associations". *Icarus*, **45**, 545–553.

Green D. W. E. (2007). "Kappa Cygnids 2007". Central Bureau Electronic Telegram No. 1055.

Hasegawa I. (1990). "Predictions of the meteor radiant point associated with a comet". *Publ. Astron. Soc. Japan*, **42**, 175–186.

IAU Minor Planet Center (2002). "2002 GF8". Minor Planet Electronic Circular 2002-G63.

Jenniskens P., Gural P. S., Dynneson L., Grigsby B. J., Newman K. E., Borden M., Koop M., and Holman D. (2011). "CAMS: Cameras for Allsky Meteor Surveillance to establish minor meteor showers". *Icarus*, **216**, 40–61.

Jenniskens P. and Nénon Q. (2016). "CAMS verification of single-linked high-threshold D-criterion detected meteor showers". *Icarus*, **266**, 371–383.

Jenniskens P., Nénon Q., Albers J., Gural P. S., Haberman B., Holman D., Morales R., Grigsby B. J., Samuels D., and Johannink C. (2016a). "The established meteor showers as observed by CAMS". *Icarus*, **266**, 331–354.

Jenniskens P., Nénon Q., Gural P. S., Albers J., Haberman B., Johnson B., Holman D., Morales R., Grigsby B. J., Samuels D., and Johannink C. (2016b). "CAMS confirmation of previously reported meteor showers". *Icarus*, **266**, 355–370.

Jenniskens P., Nénon Q., Gural P. S., Albers J., Haberman B., Johnson B., Morales R., Grigsby B. J., Samuels D., and Johannink C. (2016c). "CAMS newly detected meteor showers and the sporadic background". *Icarus*, **266**, 384–409.

Jenniskens P. and Vaubaillon J. (2008). "Minor planet 2008 ED69 and the Kappa Cygnid meteor shower". *Astron. J.*, **136**, 725–730.

Jones D. C., Williams I. P., and Porubčan V. (2006). "The Kappa Cygnid meteoroid complex". *Mon. Not. Roy. Astron. Soc.*, **371**, 684–694.

Kornoš L., Koukal J., Piffl R., and Tóth J. (2013). "Database of meteoroid orbits from several European video networks". In Gyssens M. and Roggemans P., editors, *Proceedings of the International Meteor Conference, La Palma, Canary Islands, Spain, 20–23 September, 2012*. IMO, pages 21–25.

Koseki M. (2014). "Various meteor scenes II: Cygnid-Draconid Complex (κ-Cygnids)". *WGN, Journal of the IMO*, **42:5**, 181–197.

Kronk G. W. (1988). *Meteor Showers: A Descriptive Catalog*. Enslow, NJ.

Lindblad B. A. (1995). "The orbit of the kappa Cygnid and related meteor streams". *Earth, Moon, and Planets*, **68**, 397–404.

Molau S. and Rendtel J. (2009). "A comprehensive list of meteor showers obtained from 10 years of observations with the IMO Video Meteor Network". *WGN, Journal of the IMO*, **37:4**, 98–121.

Moorhead A. V., Brown P. G., Spurný P., Cooke W. J., and Shrbený L. (2015). "The 2014 KCG meteor outburst: clues to a parent body". *Astron. J.*, **150**, 122 (13 pages).

NASA JPL (2017). "Small-body database browser". `https://ssd.jpl.nasa.gov/sbdb.cgi` .

NEODyS-2 (2017). "Near Earth Objects - Dynamic Site: 2002 GJ8". `http://newton.dm.unipi.it/neodys2/index.php ?pc=1.1.8&n=2002GJ8` .

Porubčan V. and Jopek T. J. (2017). "IAU Meteor Data Center". `https://www.ta3.sk/IAUC22DB/MDC2007` .

Rendtel J. (2016). "2017 Meteor Shower Calendar". `http://www.imo.net/files/meteor-shower/cal2017.pdf` . IMO.

Rendtel J. and Arlt R. (2016). "Kappa Cygnid rate variations over 41 years". *WGN, Journal of the IMO*, **44:3**, 62–66.

Rendtel J. and Molau S. (2015). "Enhanced kappa-Cygnid activity 2014". *WGN, Journal of the IMO*, **43:2**, 43–46.

Šegon D., Andreić Ž., Korlević K., and Vida D. (2015). "Croatian Meteor Network: ongoing work 2014–2015". In Rault J.-L. and Roggemans P., editors, *Proceedings of the International Meteor Conference, Mistelbach, Austria, 27–30 August 2015*. IMO, pages 51–57.

Shiba Y. (2016). "Taurid swarm exists only in southern branch (STA)". *WGN, Journal of the IMO*, **44:3**, 78–91.

SonotaCo (2009). "A meteor shower catalog based on video observations in 2007–2008". *WGN, Journal of the IMO*, **37:2**, 55–62.

Southworth R. B. and Hawkins G. S. (1963). "Statistics of meteor streams". *Smithson. Contrib. Astrophys.*, **7**, 261–285.

Triglav-Čekada M. (2006). "The radiant ephemerides of κ-Cygnids from IMO video database". In Bastiaens L., Verbert J., Wislez J.-M., and Verbeeck C., editors, *Proceedings of the International Meteor Conference, Oostmalle, Belgium, 15–18 September 2005*. IMO, pages 74–84.

Trigo-Rodriguez J. M., Madiedo J. M., Williams I. P., and Castro-Tirado A. J. (2009). "The outburst of the κ Cygnids in 2007: clues about the catastrophic break up of a comet to produce an Earth-crossing meteoroid stream". *Mon. Not. Roy. Astron. Soc.*, **392**, 367–375.

Handling Editor: David Asher

Preliminary results

Results of the IMO Video Meteor Network — May 2017, and flux density calculation

Sirko Molau[1], *Stefano Crivello*[2], *Rui Goncalves*[3], *Carlos Saraiva*[4], *Enrico Stomeo*[5], *and Javor Kac*[6]

The IMO Video Meteor Network cameras recorded over 16 000 meteors in more than 7 300 hours of observing time during 2017 May. The flux density profile of the 2017 η-Aquariids is presented and compared to the average of 2011–2016. Population index profile of the Lyrids is calculated, using video data from the period 2011–2017. The flux density calculation procedure is improved.

Received 2017 November 23

1 Introduction

The weather in May showed two different faces. Whereas in the first half we see large gaps in the observing statistics with as few as 60 observing hours on May 11/12, the weather improved significantly in the second half of May with over 300 hours during many nights. In total, the 77 active video cameras accumulated more than 7 300 hours of effective observing time (Table 1 and Figure 1), which matches well the results during the previous three years. However, with the average meteor rate being slightly lower (2.2 meteors per hour), the total meteor count consequently fell a few percent below that seen previously.

2 η-Aquariids

In early May, the η-Aquariids reach their broad maximum. Since the shower can only be observed briefly and at a low radiant altitude at European observing sites, it is difficult to obtain a complete activity profile for this shower from IMO Network data. Figure 2 compares the flux density of 2017 with the average for the years 2011 to 2016 (excluding 2013, when the activity was significantly enhanced – see Molau et al. (2013)). At the solar longitudes 44° and 45° (covering dates from May 4–6) the 2017 activity was somewhat higher, but otherwise it matched the long-term average well. The peak flux density of almost 50 meteoroids per 1 000 km^2 per hour during these nights, which corresponds to a ZHR of about 100, is remarkable.

To get a reliable population index of the η-Aquariids, we have to combine a relatively large number of shower meteors into a single data point. Figure 3 presents the

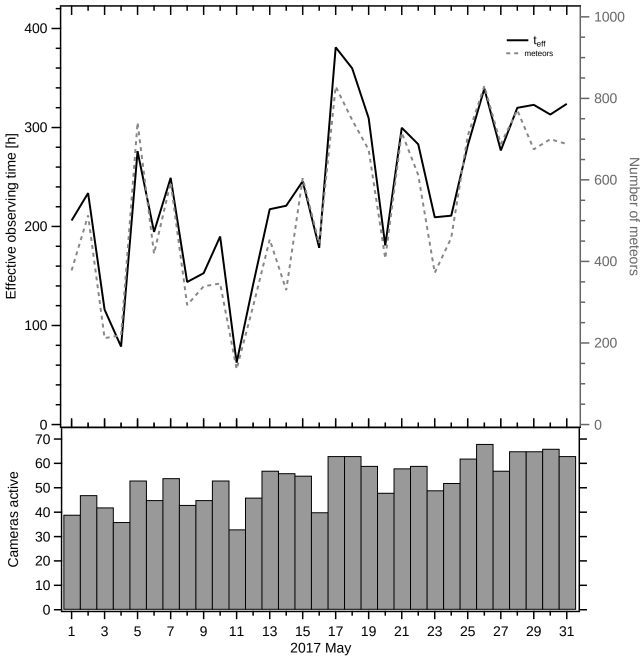

Figure 1 – Monthly summary for the effective observing time (solid black line), number of meteors (dashed gray line) and number of cameras active (bars) in 2017 May.

r-profiles of the sporadic meteors and η-Aquariids, derived from data of the years 2011 to 2017 (again without 2013). Whereas the sporadic r-value scatters around 2.65, we find a clearly smaller population index near 2.0 for the η-Aquariids. We see an outlier at 46° solar longi-

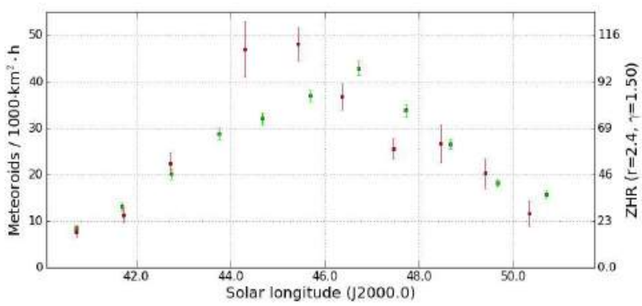

Figure 2 – Comparison of the η-Aquariid flux density 2017 (darker/red) with the average flux density profile in the years 2011–2016 (lighter/green, without 2013), derived from video data of the IMO Network.

[1]Abenstalstr. 13b, 84072 Seysdorf, Germany. Email: `sirko@molau.de`
[2]Via Bobbio 9a/18, 16137 Genova, Italy. Email: `stefano.crivello@libero.it`
[3]Urbanizacao da Boavista, Lote 46, Linhaceira, 2305-114 Asseiceira, Tomar, Portugal. Email: `rui.goncalves@ipt.pt`
[4]Rua Aquilino Ribeiro, 23 - 1 Dto. 2790028 Carnaxide, Portugal. Email: `carlos.saraiva@netcabo.pt`
[5]via Umbria 21/d, 30037 Scorze (VE), Italy. Email: `stom@iol.it`
[6]Na Ajdov hrib 24, 2310 Slovenska Bistrica, Slovenia. Email: `javor.kac@orion-drustvo.si`

IMO bibcode WGN-456-molau-vidmay
NASA-ADS bibcode 2017JIMO...45..144M

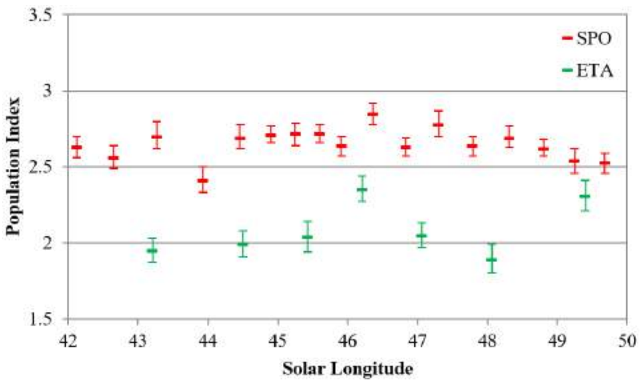

Figure 3 – Population index profile of the η-Aquariids (lighter/green) and sporadic meteors (darker/red), derived from video observations between 2011 and 2017 (without 2013).

tude, but on average the population index is smaller by more than 0.5, i.e. the percentage of bright η-Aquariids is clearly higher than the percentage of bright sporadic meteors.

2.1 η-Lyrids

The η-Lyrids follow directly after the peak of the η-Aquariids. Their activity is one order of magnitude lower, but they can be better observed from Europe. Figure 4 compares the flux density derived in 2017 with the higher resolution profile for 2011–2016. The new values fit perfectly to the earlier profile.

The population index of the η-Lyrids resembles that of the η-Aquariids. Once again, the sporadic population index is about 2.6 and the r-value of the η-Lyrids somewhat below 2.0. An outlier at the begin of the activity interval (solar longitude of $48^\circ\!.5$) may be explained by increased "sporadic dilution" at the edges of the activity interval.

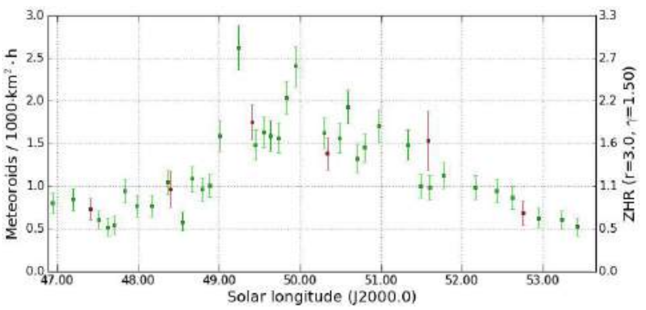

Figure 4 – Comparison of the η-Lyrid flux density 2017 (darker/red) with the average flux density profile during the years 2011–2016 (lighter/green), derived from video data of the IMO Network.

3 Flux density calculation revisited

For the η-Aquariids in particular, it is vital to avoid inaccuracies or systematic errors in the flux density calculation, since under such extreme conditions (low radiant altitude at which the shower can be observed from most sites hosting the IMO Network cameras) they may quickly lead to significant deviations in the result. A discussion with Till Credner, an astronomy teacher

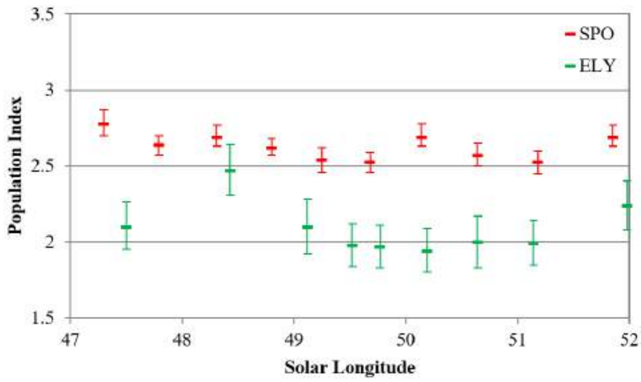

Figure 5 – Population index profile of the η-Lyrids (lighter/green) and sporadic meteors (darker/red), derived from video observations between 2011 and 2017.

from Baden Württemberg, revealed such an inaccuracy in the current flux density calculation procedure, and this shall be discussed in more detail now.

To calculate the flux density, we divide the number of meteors by the effective observing time and collection area of the camera. The latter one is precisely calculated for each camera, whereby some parameters are determined on a pixel-by-pixel basis and others are constant in the full field of view.

Among the pixel-dependent parameters we have:

- the collection area per pixel, i.e. the monitored atmospheric layer,
- the distance of the atmospheric layer (pixel) from the observer, and
- the distance of the pixel from the radiant and subsequently the expected angular velocity of shower meteors.

Among the parameters which are constant in the whole field of view we have:

- the limiting magnitude (so far, we have no procedure to determine a variable limiting magnitude in the field of view, since often only a few stars are visible),
- the height of the meteor shower radiant above the horizon (including zenith attraction),
- the altitude of the meteor layer at which shower meteors typically light up (the altitude depends on the meteor shower velocity and the radiant altitude), and
- the population index of the meteor shower.

How much impact does the radiant height have on the flux density? If the radiant is located at zenith, the meteoroids hit the atmosphere at right angles and the particle density peaks. The lower the radiant height, the shallower is the entry angle of the meteoroids into the atmosphere and the larger is the collection area they share. The number of meteoroids per unit atmosphere decreases approximately with the sine of the radiant height. However, in reality the entry angle is not constant, since meteoroids recorded by a camera that looks

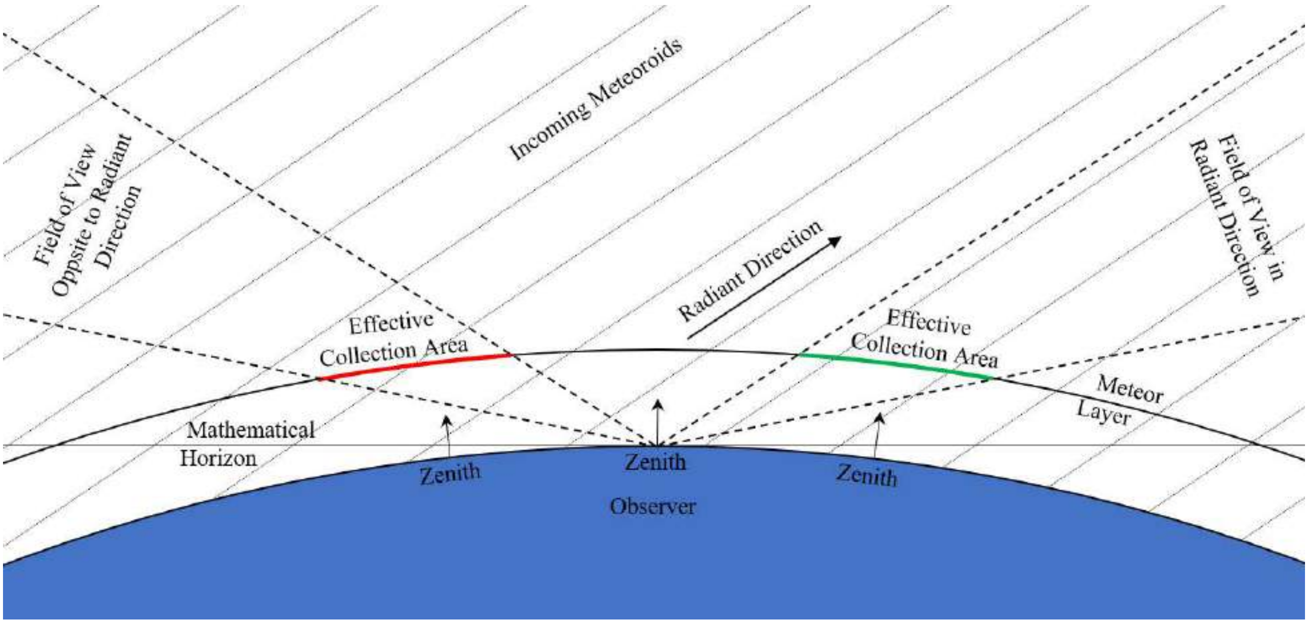

Figure 6 – Scale model to demonstrate the impact of the radiant altitude on the effective collection area. In case of a camera that observes in the radiant direction, the meteoroids hit the atmospheric layer (green segment, right) at a slightly larger angle than in case of a camera that observes in the opposite direction (red segment, left). The difference depends on the radiant altitude at the location that lies directly below the observed atmospheric layer.

towards the radiant (Figure 6, right) hit the atmosphere at a slightly larger angle than meteoroids recorded by a camera that looks into the opposite direction (Figure 6, left). To model the effect correctly, we need to determine the geographic coordinates of the location directly below the observed atmospheric layer, and determine the radiant height for this location. The deviation is larger when the radiant is lower (since the sine changes more rapidly for lower radiant heights) and when the field of view of the camera is lower (since the observed atmospheric layer is farther away from the observer). In practice, IMO Network cameras often observe atmospheric layers at a distance of a few hundred kilometers. Hence, the radiant altitude may deviate by a few degrees.

To evaluate the effect, we calculated the geographic position below the atmospheric layer pixel-wise and determined the radiant altitude at that site. Thereafter we analysed how the effective collection area and flux density changed by this new algorithm over all cameras and meteor showers in 2017 May. The deviation was typically less than 3% per night (Figure 7), such that the described effect has no significant impact on the flux density. We will still calculate the radiant altitude on a pixel-by-pixel basis in the future to eliminate all known inaccuracies.

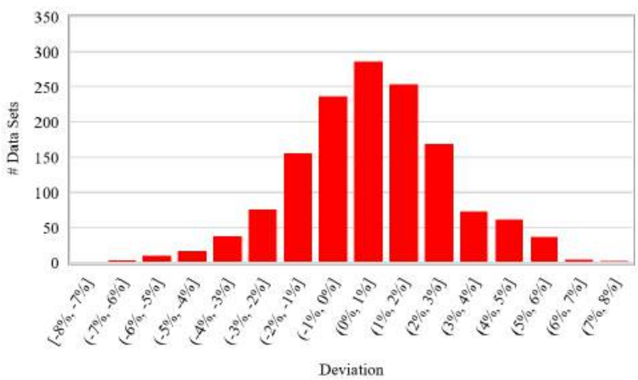

Figure 7 – Histogram over the deviations of the effective collection area between constant and pixel-wise computed radiant altitude.

References

Molau S., Kac J., Berko E., Crivello S., Stomeo E., Igaz A., Barentsen G., and Goncalves R. (2013). “Results of the IMO Video Meteor Network – May 2013”. *WGN, Journal of the IMO*, **41:4**, 133–138.

Handling Editor: Javor Kac

Table 1 – Observers contributing to 2017 May data of the IMO Video Meteor Network. Eff.CA designates the effective collection area; the overall number of nights is the number of nights with at least one camera operating, the overall observing time and number of meteors are sums over all cameras.

Code	Name	Location	Camera	FOV [°²]	Stellar LM [mag]	Eff.CA [km²]	Nights	Time [h]	Meteors
ARLRA	Arlt	Ludwigsfelde/DE	Ludwig2 (0.8/8)	1475	6.2	3779	23	86.2	324
BERER	Berkó	Ludányhalászi/HU	Hulud1 (0.8/3.8)	5542	4.8	3847	7	40.6	135
BOMMA	Bombardini	Faenza/IT	Mario (1.2/4.0)	5794	3.3	739	28	144.7	438
BREMA	Breukers	Hengelo/NL	Mbb3 (0.75/6)	2399	4.2	699	23	85.8	137
BRIBE	Klemt	Herne/DE	Hermine (0.8/6)	2374	4.2	678	23	93.1	163
		Bergisch Gladbach/DE	Klemoi (0.8/6)	2286	4.6	1080	23	94.6	158
CARMA	Carli	Monte Baldo/IT	Bmh2 (1.5/4.5)*	4243	3.0	371	22	96.0	383
CASFL	Castellani	Monte Baldo/IT	Bmh1 (0.8/6)	2350	5.0	1611	20	114.3	191
CINFR	Cineglosso	Faenza/IT	Jenni (1.2/4)	5886	3.9	1222	28	158.0	237
CRIST	Crivello	Valbrevenna/IT	Bilbo (0.8/3.8)	5458	4.2	1772	28	130.4	302
			C3P8 (0.8/3.8)	5455	4.2	1586	26	120.3	205
			Stg38 (0.8/3.8)	5614	4.4	2007	29	146.3	537
ELTMA	Eltri	Venezia/IT	Met38 (0.8/3.8)	5631	4.3	2151	20	92.9	184
FORKE	Förster	Carlsfeld/DE	Akm3 (0.75/6)	2375	5.1	2154	21	104.7	227
GONRU	Goncalves	Foz do Arelho/PT	Farelho1 (1.0/2.6)	6328	2.8	469	24	79.1	156
		Tomar/PT	Templar1 (0.8/6)	2179	5.3	1842	28	156.9	440
			Templar2 (0.8/6)	2080	5.0	1508	27	146.1	343
			Templar3 (0.8/8)	1438	4.3	571	21	122.7	113
			Templar4 (0.8/3.8)	4475	3.0	442	28	136.5	311
			Templar5 (0.75/6)	2312	5.0	2259	24	128.1	254
GOVMI	Govedič	Središče ob Dravi/SI	Orion2 (0.8/8)	1447	5.5	1841	23	89.3	177
			Orion4 (0.95/5)	2662	4.3	1043	19	75.6	86
HERCA	Hergenrother	Tucson/US	Salsa3 (0.8/3.8)	2336	4.1	544	29	226.0	476
HINWO	Hinz	Schwarzenberg/DE	Hinwo1 (0.75/6)	2291	5.1	1819	21	105.5	179
IGAAN	Igaz	Hódmezővásárhely/HU	Huhod (0.8/3.8)	5502	3.4	764	15	63.4	45
		Budapest/HU	Hupol (1.2/4)	3790	3.3	475	11	48.4	23
JONKA	Jonas	Budapest/HU	Husor (0.95/4)	2286	3.9	445	25	83.9	67
			Husor2 (0.95/3.5)	2465	3.9	715	23	100.6	108
KACJA	Kac	Ljubljana/SI	Orion1 (0.8/8)	1399	3.8	268	24	108.7	353
		Kamnik/SI	Cvetka (0.8/3.8)*	4914	4.3	1842	15	76.2	210
			Rezika (0.8/6)	2270	4.4	840	15	79.8	380
			Stefka (0.8/3.8)	5471	2.8	379	15	70.9	141
		Kostanjevec/SI	Metka (0.8/12)*	715	6.4	640	1	3.0	1
KOSDE	Koschny	Izana Obs./ES	Icc7 (0.85/25)*	714	5.9	1464	9	56.6	259
			Lic1 (2.8/50)*	2255	6.2	5670	10	64.7	364
		La Palma/ES	Icc9 (0.85/25)*	683	6.7	2951	4	11.4	70
LOJTO	Łojek	Grabniak/PL	Pav57 (1.0/5)	1631	3.5	269	9	46.3	99
LOPAL	Lopes	Lisbon/PT	Naso1 (0.75/6)	2377	3.8	506	21	92.0	104

Table 1 – Observers contributing to 2017 May data of the IMO Video Meteor Network – continued from previous page.

Code	Name	Location	Camera	FOV $[^{\circ 2}]$	Stellar LM [mag]	Eff.CA $[\mathrm{km}^2]$	Nights	Time [h]	Meteors
MACMA	Maciejewski	Chełm/PL	Pav35 (0.8/3.8)	5495	4.0	1584	23	80.1	104
			Pav36 (0.8/3.8)*	5668	4.0	1573	24	95.2	167
			Pav43 (0.75/4.5)*	3132	3.1	319	22	56.4	67
			Pav60 (0.75/4.5)	2250	3.1	281	27	101.6	223
MARRU	Marques	Lisbon/PT	Cab1 (0.75/6)	2362	4.8	1517	27	165.4	270
			Ran1 (1.4/4.5)	4405	4.0	1241	18	112.8	166
MASMI	Maslov	Novosibirsk/RU	Nowatec (0.8/3.8)	5574	3.6	773	22	51.6	98
MOLSI	Molau	Seysdorf/DE	Avis2 (1.4/50)*	1230	6.9	6152	24	105.3	682
			Escimo2 (0.85/25)	155	8.1	3415	22	111.5	224
			Mincam1 (0.8/8)	1477	4.9	1084	23	104.0	323
		Ketzür/DE	Remo1 (0.8/8)	1467	6.5	5491	26	81.6	271
			Remo2 (0.8/8)	1478	6.4	4778	25	78.2	319
			Remo3 (0.8/8)	1420	5.6	1967	27	106.2	313
			Remo4 (0.8/8)	1478	6.5	5358	24	98.9	414
MORJO	Morvai	Fülöpszállás/HU	Huful (1.4/5)	2522	3.5	532	25	135.3	96
MOSFA	Moschini	Rovereto/IT	Rover (1.4/4.5)	3896	4.2	1292	22	16.6	106
OCHPA	Ochner	Albiano/IT	Albiano (1.2/4.5)	2944	3.5	358	15	86.8	106
OTTMI	Otte	Pearl City/US	Orie1 (1.4/5.7)	3837	3.8	460	18	55.1	92
PERZS	Perkó	Becsehely/HU	Hubec (0.8/3.8)*	5498	2.9	460	23	102.7	185
ROTEC	Rothenberg	Berlin/DE	Armefa (0.8/6)	2366	4.5	911	16	70.7	113
SARAN	Saraiva	Carnaxide/PT	Ro1 (0.75/6)	2362	3.7	381	20	119.2	173
			Ro2 (0.75/6)	2381	3.8	459	22	116.5	197
			Ro3 (0.8/12)	710	5.2	619	24	125.3	272
			Ro4 (1.0/8)	1582	4.2	549	20	108.5	96
			Sofia (0.8/12)	738	5.3	907	19	97.6	120
SCHHA	Schremmer	Niederkrüchten/DE	Doraemon (0.8/3.8)	4900	3.0	409	23	88.1	146
SLAST	Slavec	Ljubljana/SI	Kayak1 (1.8/28)	563	6.2	1294	22	102.9	170
			Kayak2 (0.8/12)	741	5.5	920	22	108.2	87
STOEN	Stomeo	Scorze/IT	Min38 (0.8/3.8)	5566	4.8	3270	27	91.8	367
			Noa38 (0.8/3.8)	5609	4.2	1911	27	94.8	322
			Sco38 (0.8/3.8)	5598	4.8	3306	27	98.1	391
STRJO	Strunk	Herford/DE	Mincam2 (0.8/6)	2354	5.4	2751	17	74.0	207
			Mincam3 (0.8/6)	2338	5.5	3590	22	90.7	156
			Mincam5 (0.8/6)	2349	5.0	1896	24	98.5	176
			Mincam6 (0.8/6)	2395	5.1	2178	18	77.9	127
TEPIS	Tepliczky	Agostyán/HU	Huago (0.75/4.5)	2427	4.4	1036	30	120.9	142
			Humob (0.8/6)	2388	4.8	1607	28	125.0	190
WEGWA	Wegrzyk	Nieznaszyn/PL	Pav78 (0.8/6)	2286	4.0	778	21	57.2	73
YRJIL	Yrjölä	Kuusankoski/FI	Finexcam (0.8/6)	2337	5.5	3574	11	28.3	56
* active field of view smaller than video frame						Overall	31	7 319.1	16 187

Results of the IMO Video Meteor Network — June 2017, and effective collection area study

Sirko Molau[1], *Stefano Crivello*[2], *Rui Goncalves*[3], *Carlos Saraiva*[4], *Enrico Stomeo*[5], *and Javor Kac*[6]

Over 18 000 meteors were recorded by the IMO Video Meteor Network cameras during more than 7 100 hours of observing time during 2017 June. The June Bootids were not detectable this year. Nearly 50 Daytime Arietids were recorded in 2017, and a first flux density profile for this shower in the optical domain is calculated, using video data from the period 2011–2017. Effective collection area of video cameras is discussed in more detail.

Received 2018 January 2

1 Introduction

June lacks impressive meteor showers and the nights in the northern hemisphere are shorter at the start of summer than in any other month. Nevertheless, this month often provides nice observing conditions for observers, and 2017 was no exception in this respect. 57 out of 77 active video cameras managed to observe during twenty or more nights, Enrico Stomeo's SCO38 observed without any gaps at all. There were at least 30 cameras active during each June night, with up to 70 cameras active at the best times. In total we collected over 7 100 hours of effective observing time (Table 1 and Figure 1), which falls just 40 hours short of the all-time best result from June 2015. The 18 626 meteors which were observed in June are close to the average of the last few years.

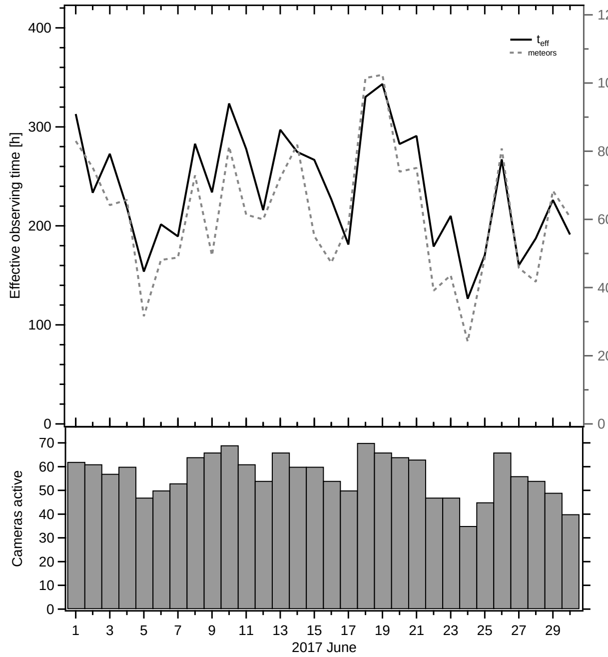

Figure 1 – Monthly summary for the effective observing time (solid black line), number of meteors (dashed gray line) and number of cameras active (bars) in 2017 June.

2 June meteor showers

The June Bootids in the last ten days of the month were not detectable, matching the findings of the last few years.

We recorded nearly 50 potential Daytime Arietids at the beginning of June. However, from experience we know that there will be a certain "sporadic contamination" among these. The mean activity profile of the Arietids from all data since 2011 (Figure 2) does not yet provide a clear picture.

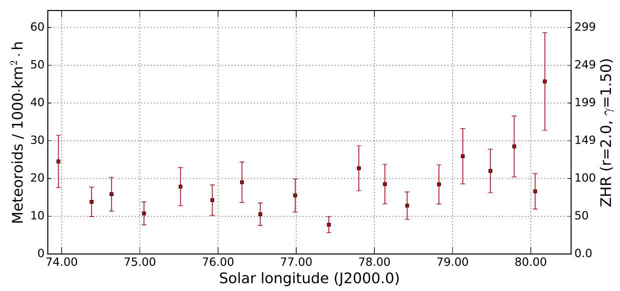

Figure 2 – Mean flux density profile of the Daytime Arietids 2011–2017, derived from video data of the IMO Network.

3 Effective collection area

Let us continue the analysis of the effective collection area of a meteor camera from the previous report (Molau et al., 2017b). We discussed which parameters affect the effective collection area in which way.

Pixel-dependent parameters are as follows:

- the atmospheric segment covered by a pixel (area),
- the distance of the atmospheric segment (pixel) from the observer,
- the distance of the pixel from the radiant and, thus, the expected angular velocity of shower meteors,

[1]Abenstalstr. 13b, 84072 Seysdorf, Germany. Email: sirko@molau.de
[2]Via Bobbio 9a/18, 16137 Genova, Italy. Email: stefano.crivello@libero.it
[3]Urbanizacao da Boavista, Lote 46, Linhaceira, 2305-114 Asseiceira, Tomar, Portugal. Email: rui.goncalves@ipt.pt
[4]Rua Aquilino Ribeiro, 23 - 1 Dto. 2790028 Carnaxide, Portugal. Email: carlos.saraiva@netcabo.pt
[5]via Umbria 21/d, 30037 Scorze (VE), Italy. Email: stom@iol.it
[6]Na Ajdov hrib 24, 2310 Slovenska Bistrica, Slovenia. Email: javor.kac@orion-drustvo.si

IMO bibcode WGN-456-molau-vidjun
NASA-ADS bibcode 2017JIMO...45..149M

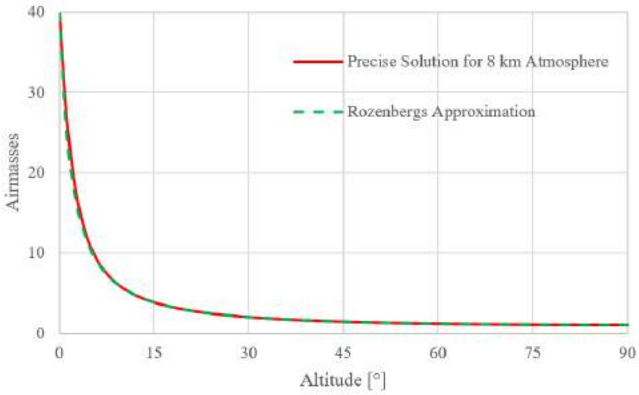

Figure 3 – Airmass depending on the altitude above the horizon. At zenith it is exactly one airmass.

- the altitude of the meteor shower radiant above the horizon (including zenith attraction).

Factors that are constant over the full field of view include:

- the limiting magnitude of the camera,
- the height of the "meteor layer" at which shower meteors become luminous on average,
- the population index of the meteor shower.

In the first implementation of the algorithm in 2010 the atmospheric extinction was also calculated. Later it was removed, because it is covered implicitly by the stellar limiting magnitude. The limiting magnitude of a camera is measured as an average value over the full field of view, because there are often too few stars to measure individual parts of the field of view independently. When there is low cloud, or the Moon is inside the field of view, or when observing in a direction that is close to the horizon with strong atmospheric extinction, the limiting magnitude may vary significantly. For this reason, we now introduce at least the differential extinction in the algorithm. Depending on the altitude, the extinction for each pixel is calculated with a constant of 0.35 mag per airmass (corresponding to the extinction at zenith). Thereafter, the average extinction is calculated over all pixels in the cameras field of view, and replaced by the measured average stellar limiting magnitude. Pixels closer to the horizon will get a somewhat smaller, and pixels closer to the zenith a somewhat higher stellar limiting magnitude than the measured average value. The effect of this correction is small, but it further improves the modelling of the effective collection area of the camera.

Short diversion: In the literature, the airmass which the star light has to travel depending on the zenith distance z is often given as $\cos(z + 0.025e^{-11\cos(z)})^{-1}$ The equation originates form the book "Twilight: A Study in Atmospheric Optics" from Rozenberg (1966). It should yield similar values to those from our geometrically derived equation to calculate the distance of the meteor layer from the observer, if the height of the meteor layer is replaced by the "height of the atmosphere". Indeed, both equations yield almost identical values if the height of the atmosphere is defined as 8 kilometers.

Closely linked to the effective collection area is the often-repeated question, in what direction a meteor camera would record most meteors. In the magazine *Sternschnuppe* of the "VdS Fachgruppe Meteore", Mirko Nitschke (1993) once derived that the best observing direction would be between the radiant and the zenith.

Meanwhile we have a more accurate model, supported by actual measurements. In the January report (Molau et al., 2017a) we calculated the effective collection area for individual meteor showers and cameras. We now want to analyze the effect of each parameter in detail. For this purpose, the corresponding procedure of MetRec was moved into an extra program that calculates the effective collection area per square degree under given boundary conditions. The result can be visualized statically and dynamically.

Let us first analyze with an example, the effect that the above-mentioned parameters have on the effective collection area in principle. For this we select a meteor layer altitude of 100 km and a field of view 10° above the horizon. At this altitude, the distance from the meteor layer to the camera is 480 km. Thus, the cameras observe a piece of atmosphere that is 4.8 times as distant as at the zenith. Whereas 1° at the zenith correspond to about 1.75 km at the meteor layer, it is 8 km in horizontal direction at the altitude of 10°. In vertical direction, the atmosphere is "squeezed", because we are looking at a tilted atmospheric layer, so one degree corresponds to as much as 34 km in vertical direction. The overall area of one square degree at the meteor layer increases by a factor of 95 from 3 km^2 at the zenith to 280 km^2 at 10° altitude. The collection area only depends on the height of the meteor layer, which is between 75 and 110 km, depending on the meteor shower velocity and the radiant height above the horizon. It is totally independent of the observing conditions at the ground.

On the other hand, the following effects reduce the limiting magnitude of the camera:

- Due to the 4.8 times distance, the light intensity reduces according to the inverse square distance law by a factor of 23, which corresponds to about 3.4 mag.
- The angular velocity of meteors low at the horizon is so small that the loss in limiting magnitude compared to stars for a normal video camera is less than 0.1 mag.
- The atmospheric extinction only 10° above the horizon is about 1.5 mag at a typical observing site at sea level.

In total we have a loss of 5 magnitudes, if we ignore the small effect of these factors at zenith. For a population index of 2.0 this corresponds to a reduction of the meteor number by a factor of $2^5 = 32$, i.e. only one third compared to the 95-times increase of the collection area towards the horizon. For a population index of 3.0, the number of meteors decreases by a factor of

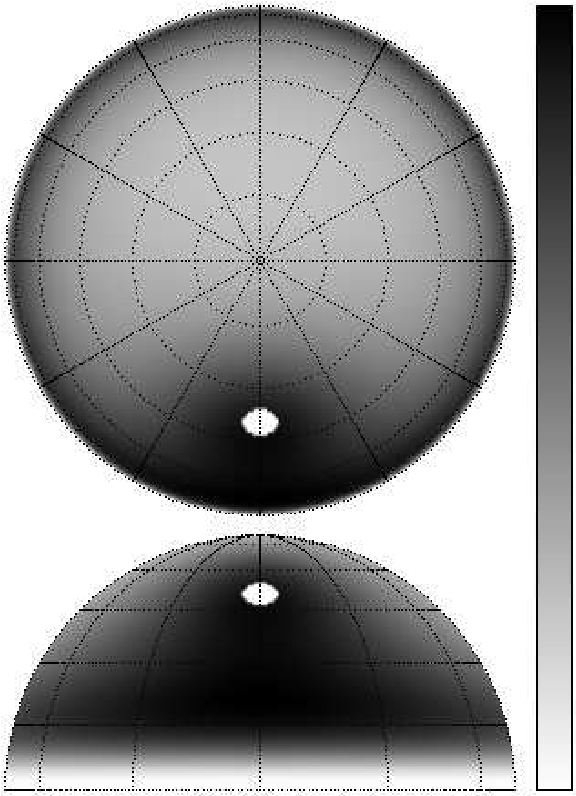

Figure 4 – Effective collection area of a meteor camera per square degree at the celestial sphere for an average meteor shower. Above is the total view of the sky with the zenith at the center, below is the horizontal view in radiant direction. White represents zero, black the biggest effective collection area.

$3^5 = 243$. In the case, the reduction is by a factor of 2.5 larger than the increase of the collection area towards the horizon.

In the case of large correction factors (i.e. in particular near the horizon), the population index is of critical importance. Also, the atmospheric extinction, i.e. the quality of the observing site, is of crucial importance near the horizon. The meteor shower velocity and the resolution of the meteor camera, on the other hand, become only important for observing fields closer to the zenith, because meteors near the horizon are generally quite slow due to the large distance. The absolute value of the limiting magnitude at zenith plays no role in this analysis, because it affects all areas in the sky in the same way.

We now want to calculate the effective collection area of the full visible hemisphere for an average meteor shower. Its radiant has a declination of 10° and it is located south in our example. The shower has a velocity of $v_{\text{inf}} = 50$ km/s and a population index of $r = 2.5$. The resolution of the meteor camera is 10 pixels per degree and the variance of stellar images 1.0 (corresponding to a Mintron camera with 8-mm 1/2" c-mount lens). Figure 4 depicts the effective collection area per square degree – the darker the value, the larger the collection area. The upper figure shows the full hemisphere with the zenith at the center (north is up, east to the right), the lower figure depicts the view to the horizon in the radiant direction. The grey levels reach linearly from 0 (white) to the corresponding maximum value (black). We do not give absolute values, since they are irrelevant for this comparison of different observing directions.

We recognize two areas with largest collection area and, thus, the highest probability to record a shower meteor: In the direct vicinity of the radiant and at about 15° altitude. There will be no meteors directly at the radiant, because their angular velocity is too slow and they are filtered out by the software as possible satellites. Close to the horizon, the collection area is nearly independent of the observing direction, because the meteor velocity is in principle quite small.

Let us now analyze the impact of each individual parameter in detail. Figure 5 compares a slow meteor shower with $v_{\text{inf}} = 30$ km/s (left) and a fast shower with $v_{\text{inf}} = 70$ km/s (right) under otherwise unchanged boundary conditions. Both figures are scaled independently for their maximum values (at the same scale, the right figure would be much brighter, because fast meteors have a lower limiting magnitude overall). In case of slower meteor showers, the "blind spot" at the radiant is larger and observing directions close to the horizon more effective. In case of larger velocities, regions close to the radiant and between the radiant and the horizon are preferred.

The impact of the population index and the extinction on the perfect observing direction is well-known from visual observations. In case of the Leonids storm in South Korea in 2001 with a low population index and extinction, for example, there were clearly more meteors visible close to the horizon than at higher altitudes. The effect was even more dramatic for the airborne missions operating at the same time, which observed with practically no atmospheric extinction at all.

That is reflected in Figures 6 and 7. For a population index of $r = 2.0$ (Figure 6, left) most meteors are visible close to the horizon – the radiant direction plays practically no role anymore. For a population index of $r = 3.0$ (Figure 6, right), however, areas close to the radiant are clearly preferred.

The effect is similar at observing sites with different sky quality. At favorable observing sites with an extinction of 0.20 mag per airmass, fields of view near the horizon are clearly preferred (Figure 7, left), whereas at poor observing sites with large extinction the areas near the radiant are preferred (Figure 7, right).

Note that all figures so far are valid for a particular point in time only. Our unguided cameras, however, observe a full night long whereby the observing geometry changes significantly. If we observe our average meteor shower over six hours, during which the radiant moves from east to south, we see that all positions close to the radiant smear out and in total the collection area close to the horizon improves (Figure 8).

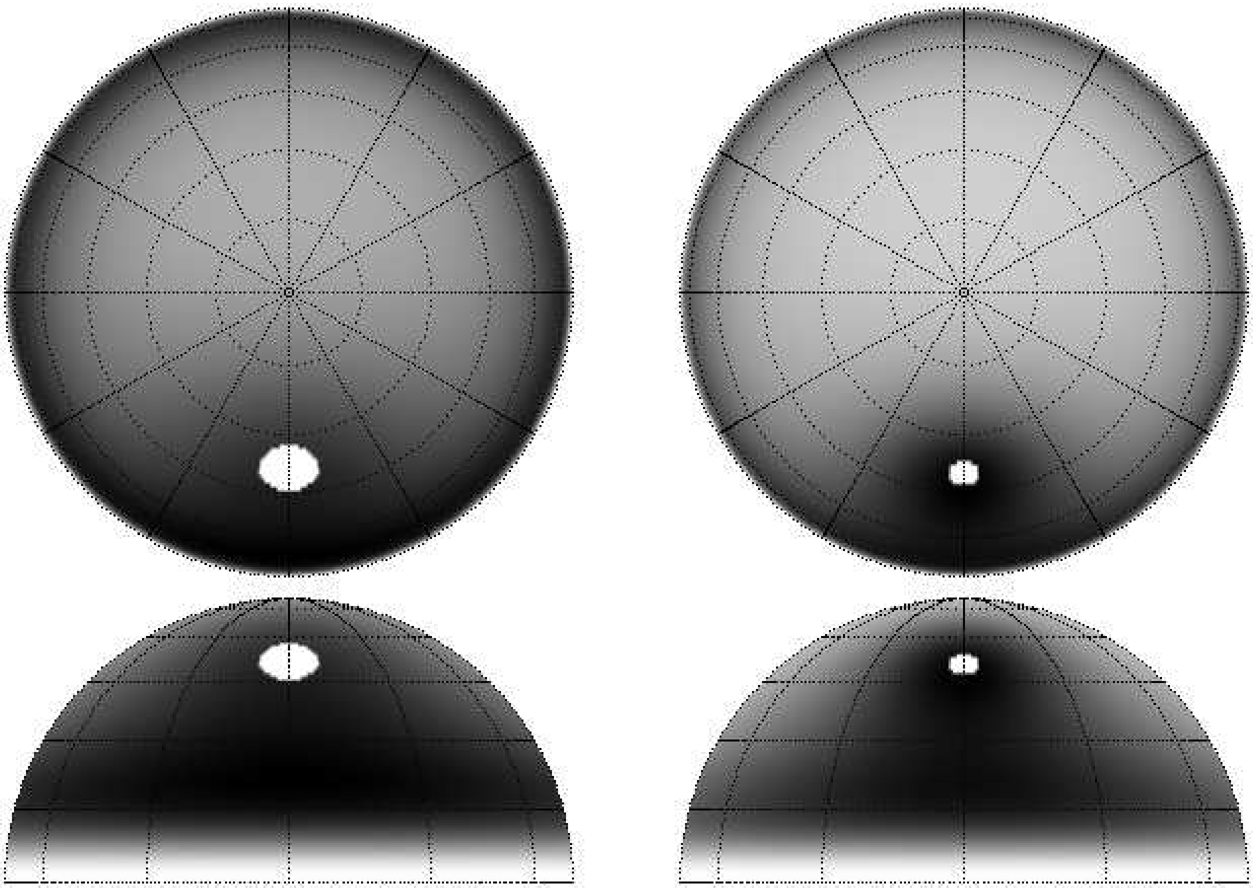

Figure 5 – Comparison of the effective collection area for a meteor shower with low (left) and high velocity (right). The grey levels of the two figures are scaled independently of each other.

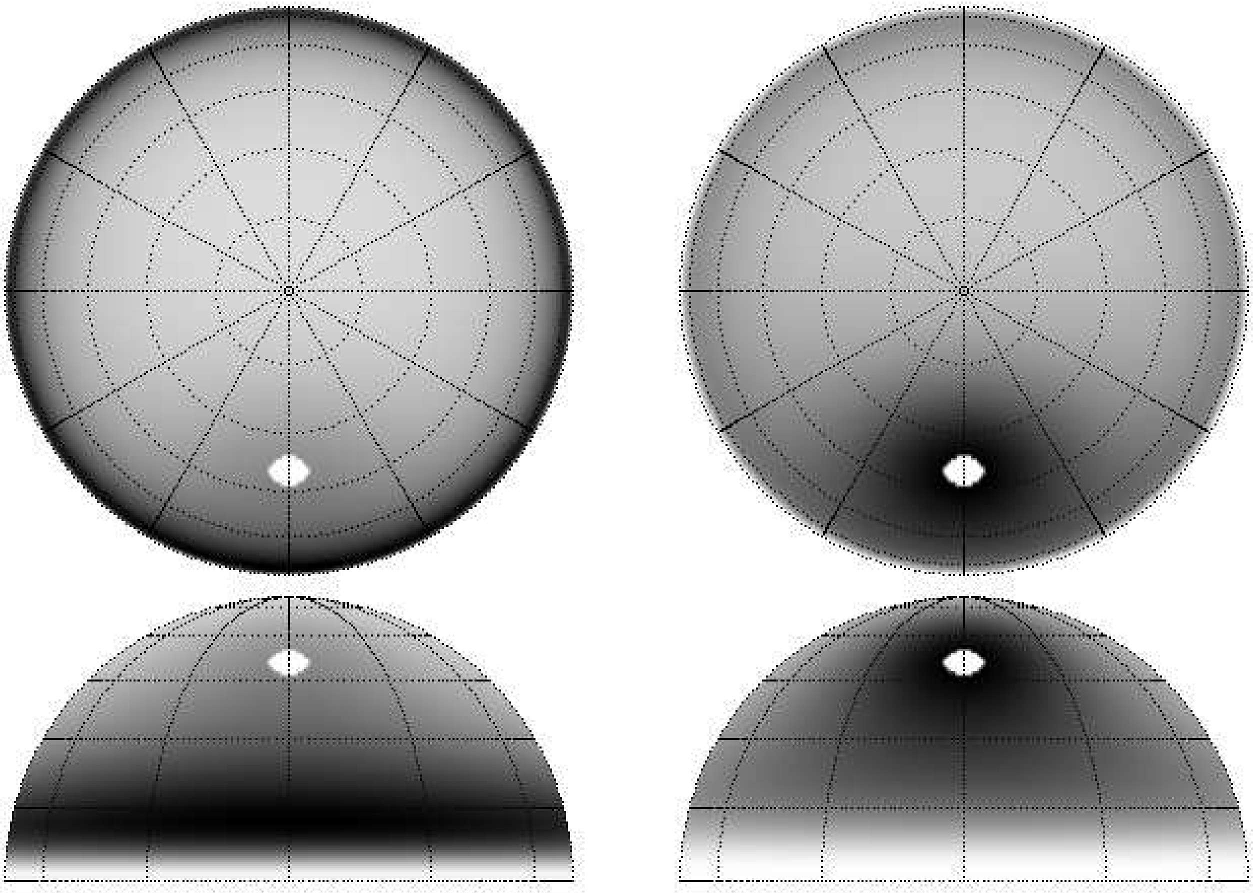

Figure 6 – Comparison of the effective collection area for a meteor shower with low (left) and high population index (right). The grey levels of the two figures are scaled independently of each other.

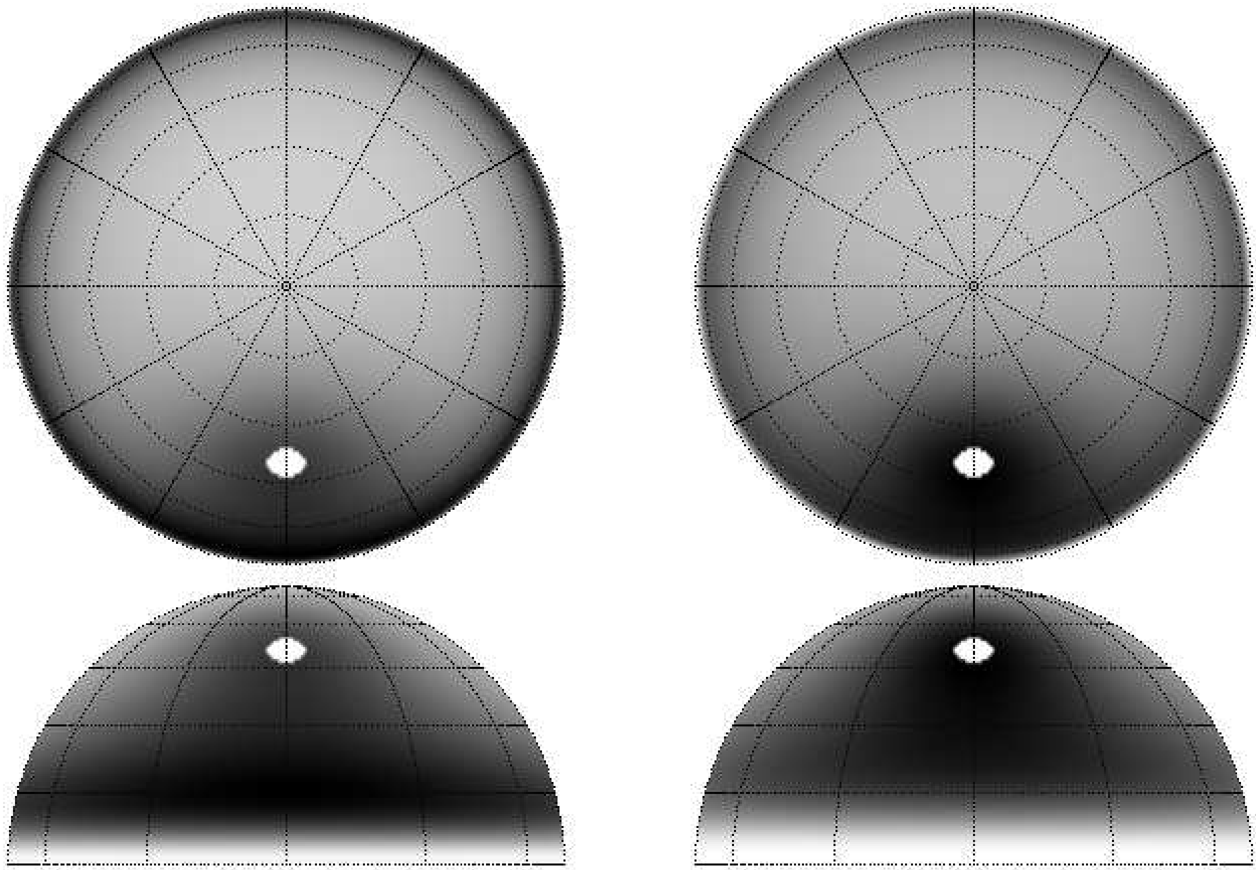

Figure 7 – Comparison of the effective collection area for observing sites with low (left) and high atmospheric extinction (right). The grey levels of the two figures are scaled independently of each other.

References

Molau S., Crivello S., Goncalves R., Saraiva C., Stomeo E., and Kac J. (2017a). "Results of the IMO Video Meteor Network – January 2017". *WGN, Journal of the IMO*, **45:3**, 63–66.

Molau S., Crivello S., Goncalves R., Saraiva C., Stomeo E., and Kac J. (2017b). "Results of the IMO Video Meteor Network – May 2017, and flux density calculation". *WGN, Journal of the IMO*, **45:6**, 144–148.

Nitschke M. (1993). "Videoaufzeichnung von Meteoren Teil 2: Ausrichtung der Kamera". *Sternschnuppe*, **5:2**, 38–41. (in German).

Rozenberg G. V. (1996). *Twilight: A Study in Atmospheric Optics*. Springer US.

Handling Editor: Javor Kac

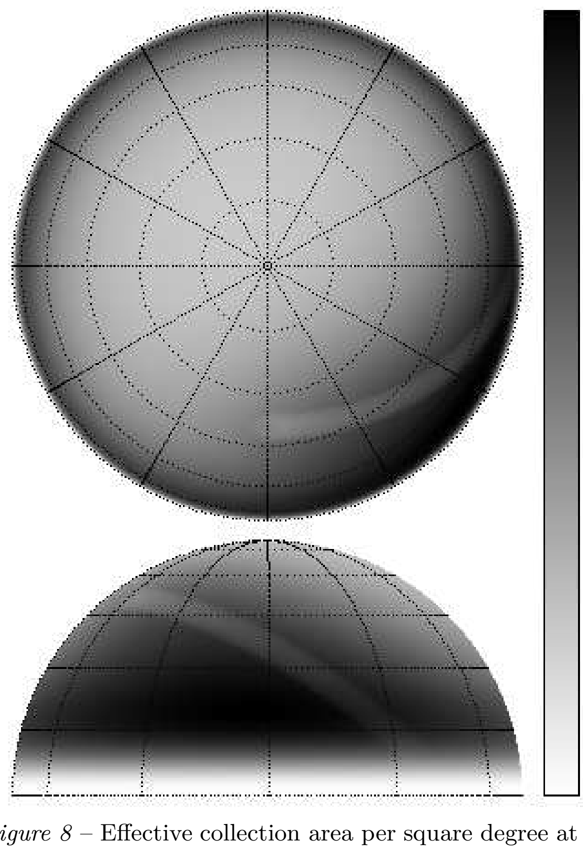

Figure 8 – Effective collection area per square degree at the celestial sphere for an average meteor shower, whose radiant is moving from east to south during six hours of observation.

Table 1 – Observers contributing to 2017 June data of the IMO Video Meteor Network. Eff.CA designates the effective collection area; the overall number of nights is the number of nights with at least one camera operating, the overall observing time and number of meteors are sums over all cameras.

Code	Name	Location	Camera	FOV [°²]	Stellar LM [mag]	Eff.CA [km²]	Nights	Time [h]	Meteors
ARLRA	Arlt	Ludwigsfelde/DE	Ludwig2 (0.8/8)	1475	6.2	3779	23	56.9	258
BERER	Berkó	Ludányhalászi/HU	Hulud1 (0.8/3.8)	5542	4.8	3847	10	52.3	207
BOMMA	Bombardini	Faenza/IT	Mario (1.2/4.0)	5794	3.3	739	29	153.1	524
BREMA	Breukers	Hengelo/NL	Mbb3 (0.75/6)	2399	4.2	699	20	75.1	163
BRIBE	Klemt	Herne/DE	Hermine (0.8/6)	2374	4.2	678	23	81.5	191
		Bergisch Gladbach/DE	Klemoi (0.8/6)	2286	4.6	1080	24	77.9	148
CARMA	Carli	Monte Baldo/IT	Bmh2 (1.5/4.5)*	4243	3.0	371	28	101.8	448
CASFL	Castellani	Monte Baldo/IT	Bmh1 (0.8/6)	2350	5.0	1611	25	120.4	214
CINFR	Cineglosso	Faenza/IT	Jenni (1.2/4)	5886	3.9	1222	29	173.6	336
CRIST	Crivello	Valbrevenna/IT	Bilbo (0.8/3.8)	5458	4.2	1772	27	133.4	346
			C3P8 (0.8/3.8)	5455	4.2	1586	25	107.7	216
			Stg38 (0.8/3.8)	5614	4.4	2007	28	141.7	624
ELTMA	Eltri	Venezia/IT	Met38 (0.8/3.8)	5631	4.3	2151	23	81.0	236
FORKE	Förster	Carlsfeld/DE	Akm3 (0.75/6)	2375	5.1	2154	19	71.8	234
GONRU	Goncalves	Foz do Arelho/PT	Farelho1 (1.0/2.6)	6328	2.8	469	17	32.8	66
		Tomar/PT	Templar1 (0.8/6)	2179	5.3	1842	29	164.4	464
			Templar2 (0.8/6)	2080	5.0	1508	26	160.3	420
			Templar3 (0.8/8)	1438	4.3	571	24	128.2	131
			Templar4 (0.8/3.8)	4475	3.0	442	29	155.5	378
			Templar5 (0.75/6)	2312	5.0	2259	26	134.1	316
GOVMI	Govedič	Središče ob Dravi/SI	Orion2 (0.8/8)	1447	5.5	1841	22	98.0	201
			Orion4 (0.95/5)	2662	4.3	1043	24	89.8	118
HERCA	Hergenrother	Tucson/US	Salsa3 (0.8/3.8)	2336	4.1	544	27	192.0	298
HINWO	Hinz	Schwarzenberg/DE	Hinwo1 (0.75/6)	2291	5.1	1819	26	93.3	236
IGAAN	Igaz	Budapest/HU	Hupol (1.2/4)	3790	3.3	475	22	84.8	64
JONKA	Jonas	Budapest/HU	Husor (0.95/4)	2286	3.9	445	25	106.0	116
			Husor2 (0.95/3.5)	2465	3.9	715	24	112.6	140
KACJA	Kac	Ljubljana/SI	Orion1 (0.8/8)	1399	3.8	268	25	115.2	348
		Kamnik/SI	Cvetka (0.8/3.8)*	4914	4.3	1842	20	82.5	293
			Rezika (0.8/6)	2270	4.4	840	20	90.1	434
			Stefka (0.8/3.8)	5471	2.8	379	21	83.1	190
		Kostanjevec/SI	Metka (0.8/12)*	715	6.4	640	25	109.8	148
KOSDE	Koschny	Izana Obs./ES	Icc7 (0.85/25)*	714	5.9	1464	3	16.2	74
			Lic1 (2.8/50)*	2255	6.2	5670	7	53.1	515
		La Palma/ES	Icc9 (0.85/25)*	683	6.7	2951	11	64.8	667
LOJTO	Łojek	Grabniak/PL	Pav57 (1.0/5)	1631	3.5	269	7	30.1	69
LOPAL	Lopes	Lisbon/PT	Naso1 (0.75/6)	2377	3.8	506	5	28.5	37

Table 1 – Observers contributing to 2017 June data of the IMO Video Meteor Network – continued from previous page.

Code	Name	Location	Camera	FOV [°²]	Stellar LM [mag]	Eff.CA [km²]	Nights	Time [h]	Meteors
MACMA	Maciejewski	Chełm/PL	Pav35 (0.8/3.8)	5495	4.0	1584	23	67.5	161
			Pav36 (0.8/3.8)*	5668	4.0	1573	24	95.8	269
			Pav43 (0.75/4.5)*	3132	3.1	319	19	59.1	87
			Pav60 (0.75/4.5)	2250	3.1	281	25	94.2	264
MARRU	Marques	Lisbon/PT	Cab1 (0.75/6)	2362	4.8	1517	28	176.9	314
			Ran1 (1.4/4.5)	4405	4.0	1241	23	130.9	141
MASMI	Maslov	Novosibirsk/RU	Nowatec (0.8/3.8)	5574	3.6	773	11	19.1	57
MOLSI	Molau	Seysdorf/DE	Avis2 (1.4/50)*	1230	6.9	6152	26	96.7	644
			Escimo2 (0.85/25)	155	8.1	3415	25	110.4	244
			Mincam1 (0.8/8)	1477	4.9	1084	28	103.8	392
		Ketzür/DE	Remo1 (0.8/8)	1467	6.5	5491	21	58.4	286
			Remo2 (0.8/8)	1478	6.4	4778	23	61.9	332
			Remo3 (0.8/8)	1420	5.6	1967	20	70.3	306
			Remo4 (0.8/8)	1478	6.5	5358	21	69.0	404
MORJO	Morvai	Fülöpszállás/HU	Huful (1.4/5)	2522	3.5	532	27	141.6	160
MOSFA	Moschini	Rovereto/IT	Rover (1.4/4.5)	3896	4.2	1292	26	21.1	125
OCHPA	Ochner	Albiano/IT	Albiano (1.2/4.5)	2944	3.5	358	18	72.7	106
OTTMI	Otte	Pearl City/US	Orie1 (1.4/5.7)	3837	3.8	460	22	77.6	114
PERZS	Perkó	Becsehely/HU	Hubec (0.8/3.8)*	5498	2.9	460	23	103.9	232
ROTEC	Rothenberg	Berlin/DE	Armefa (0.8/6)	2366	4.5	911	14	52.6	126
SARAN	Saraiva	Carnaxide/PT	Ro1 (0.75/6)	2362	3.7	381	23	126.3	177
			Ro2 (0.75/6)	2381	3.8	459	26	146.0	224
			Ro3 (0.8/12)	710	5.2	619	24	139.8	310
			Ro4 (1.0/8)	1582	4.2	549	25	118.4	108
			Sofia (0.8/12)	738	5.3	907	16	71.2	94
SCALE	Scarpa	Alberoni/IT	Leo (1.2/4.5)*	4152	4.5	2052	26	92.7	88
SCHHA	Schremmer	Niederkrüchten/DE	Doraemon (0.8/3.8)	4900	3.0	409	24	82.9	152
SLAST	Slavec	Ljubljana/SI	Kayak1 (1.8/28)	563	6.2	1294	20	70.5	143
			Kayak2 (0.8/12)	741	5.5	920	22	87.4	69
STOEN	Stomeo	Scorze/IT	Min38 (0.8/3.8)	5566	4.8	3270	29	96.7	413
			Noa38 (0.8/3.8)	5609	4.2	1911	29	99.4	330
			Sco38 (0.8/3.8)	5598	4.8	3306	30	106.7	492
STRJO	Strunk	Herford/DE	Mincam2 (0.8/6)	2354	5.4	2751	22	76.6	287
			Mincam3 (0.8/6)	2338	5.5	3590	22	75.3	184
			Mincam5 (0.8/6)	2349	5.0	1896	2	8.9	21
			Mincam6 (0.8/6)	2395	5.1	2178	22	75.9	212
TEPIS	Tepliczky	Agostyán/HU	Huago (0.75/4.5)	2427	4.4	1036	20	73.9	168
			Humob (0.8/6)	2388	4.8	1607	23	97.7	161
WEGWA	Wegrzyk	Nieznaszyn/PL	Pav78 (0.8/6)	2286	4.0	778	25	79.1	230
YRJIL	Yrjölä	Kuusankoski/FI	Finexcam (0.8/6)	2337	5.5	3574	21	66.2	131
* active field of view smaller than video frame						Overall	30	7 128.5	18 626

CAMS BeNeLux network: results October 2017

Carl Johannink[1]

October 2017 was a very successful month for CAMS BeNeLux. 4163 orbits were determined from the collected data. We could confirm enhanced activity for the October Camelopardalids on October 5 (Johannink, 2017). The October Ursa Majorids showed a nice display in the period October 14–16. Finally, we recorded on October 14 activity from a radiant in the constellation Lynx. In the IAU database we found a shower (not established) that could be responsible for this activity: #228 OLY.

Received 2017 November 22

1 Introduction

Despite the unstable weather in October 2017, CAMS (Jenniskens et al., 2011) BeNeLux was able to collect data for 4163 simultaneous meteors. Especially during the period October 12 to 21, 80% to 100% of all 88 cameras could operate successfully. In this article, we describe some particular activity during this month.

2 The October Camelopardalids

During the evening hours of October 5 we have noticed activity of the October Camelopardalids. In a separate article we will discuss the results of these observations (Johannink, 2017).

3 The October Ursa Majorids

Since the start of our network in March 2012, we have collected data for the October Ursa Majorids (#333 OCU) around October 15 every year. But in none of these years' rates were as high as this year. Figure 1 shows the plot of all radiants found with CAMS on October 14/15. There is a cluster of radiants near RA = 145° and Dec = 65°, very close to the theoretical radiant of the October Ursa Majorids. 24 hours earlier there was no sign of activity from this stream. Activity was still visible at October 15/16.

Uehara et al. (2006), were the first to mention this stream in 2006. They found a radiant in the northwestern part of UMa at RA = 144.°8 and Dec = 64.°5 with orbital elements $q = 0.979$ AU; $e = 0.875$; $\omega = 163.°7$; $i = 99.°7$ and $\Omega = 202.°1$. As mentioned earlier, activity in 2017 was good, but from the data of CAMS California / UAE it is clear that there was no outburst (Figure 2).

The activity profile gives a short visibility for this stream, with a steep increase of rates before maximum and a slower decrease afterwards. This is in good agreement with our results this year: no, or nearly no activity on October 13/14 ($\lambda_\odot \sim 200°$), and clear activity 24 hours later ($\lambda_\odot \sim 201°$). Uehara et al. (2006) also noticed that the lightcurves of the October Ursa Majorids showed a peak intensity in the first part of the complete trail. In our data in 2017 we see this in ~ 70% of the captured OCUs. Figure 3a–d show some examples.

[1]Email: c.johannink@t-online.de

IMO bibcode WGN-456-johannink-camsoct
NASA-ADS bibcode 2017JIMO...45..156J

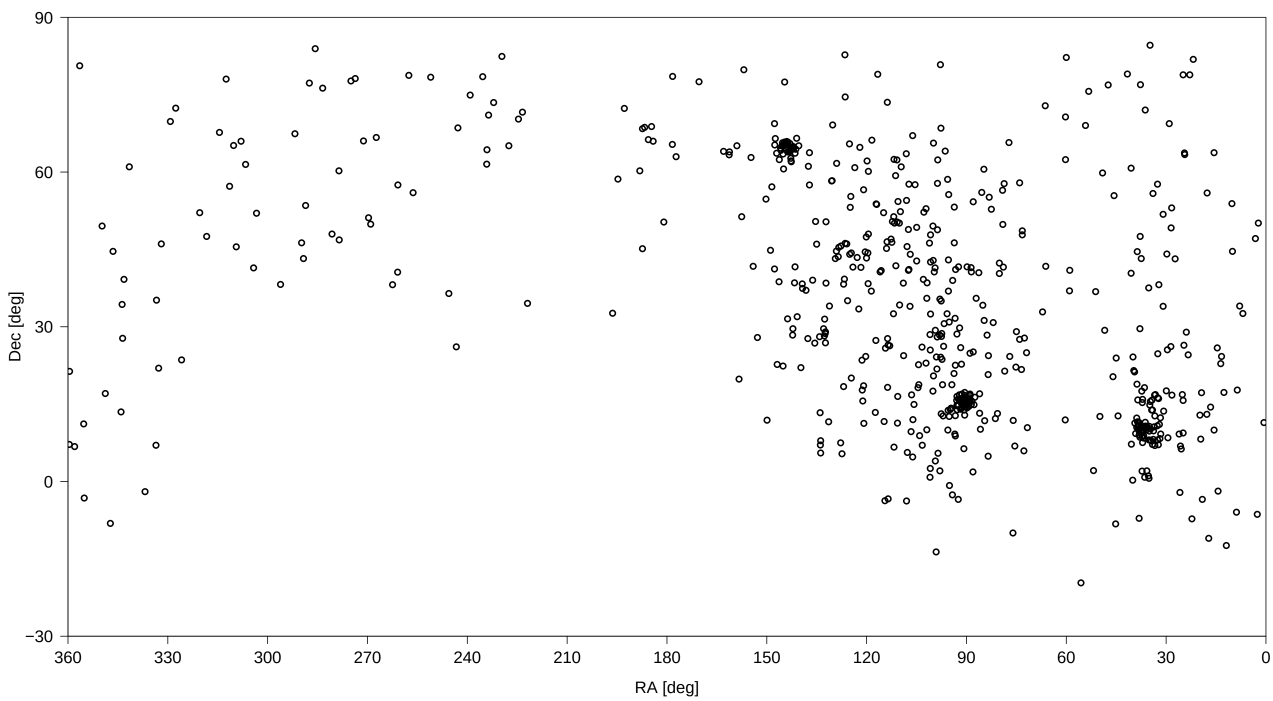

Figure 1 – Radiant plot for 2017 October 14/15 (651 simultaneous meteors).

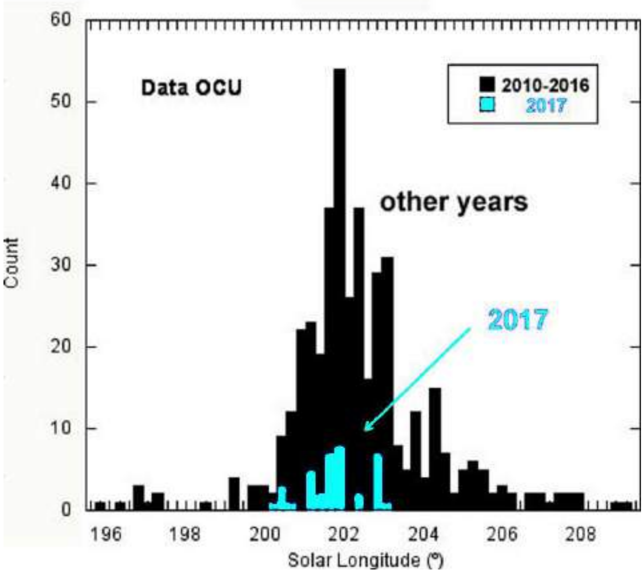

Figure 2 – Histogram with the number of OCU meteors plotted against solar longitude. Rates for 2017 in relation to results in the period 2010–2016 (based upon results of CAMS California / CAMS UAE).

The orbits of 40 OCUs were collected during the nights October 14/15, 15/16 and the evening hours of October 16/17. From these results we found a mean radiant at RA = 144.°9 and Dec = 64.°6. This is in good agreement with results from Uehara et al. (2006). Finally, Figure 4 gives a plot of the longitude of the perihelion versus inclination for these 40 October Ursa Majorids.

4 The October Lyncids

Looking at Figure 1 we noticed a separate cluster of radiants near RA = 110° and Dec = 50° (see also Figure 5).

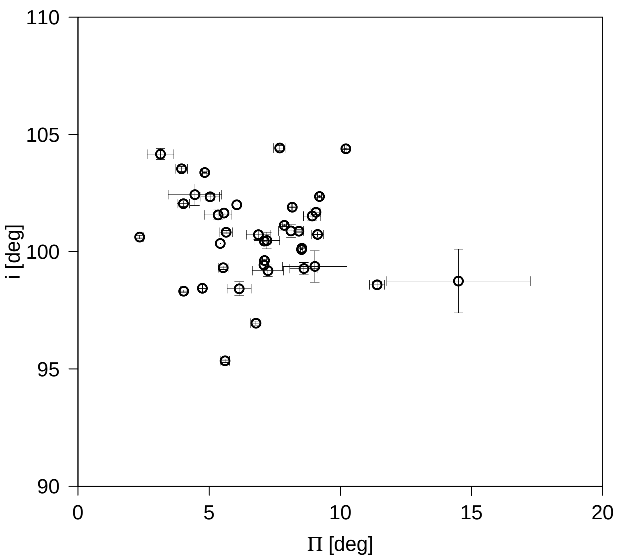

Figure 4 – Plot of the longitude of the perihelion (Π) versus inclination (i), based on 40 OCUs.

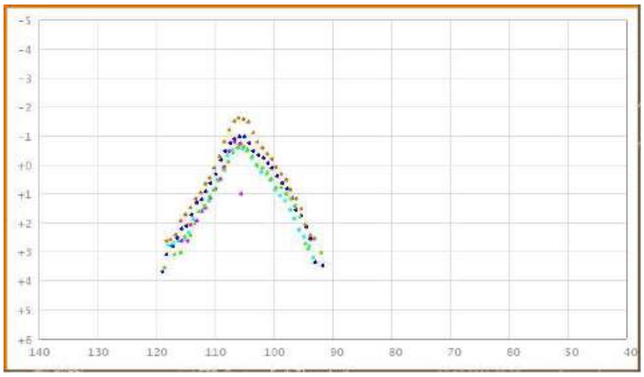

(a) OCU on 2017 October 15, $01^h57^m23^s$ UT.

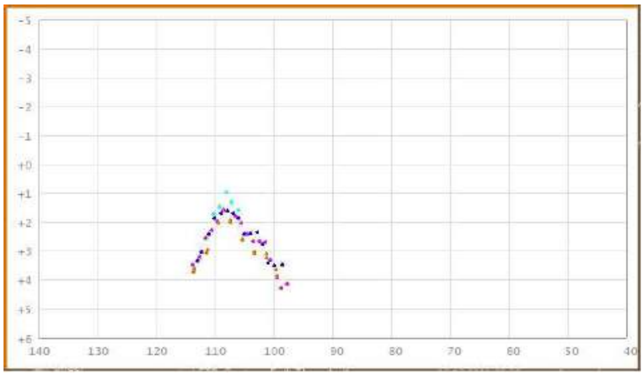

(b) OCU on 2017 October 15, $04^h47^m31^s$ UT.

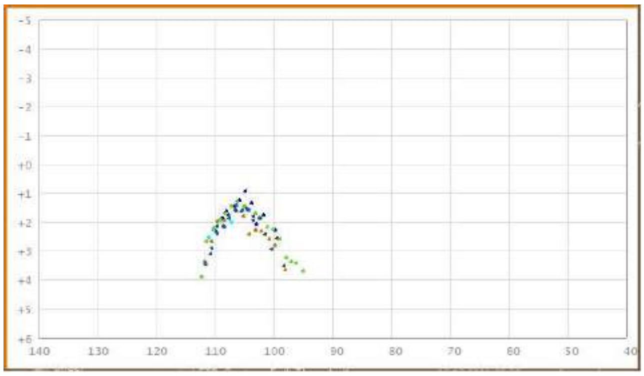

(c) OCU on 2017 October 15, $04^h52^m26^s$ UT.

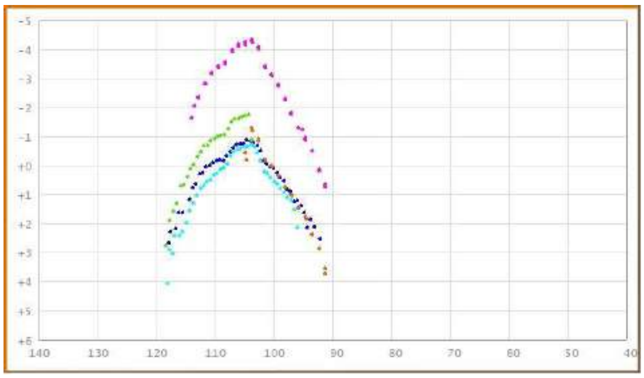

(d) OCU on 2017 October 15, $22^h37^m22^s$ UT.

Figure 3 – Examples of the October Ursa Majorid lightcurves.

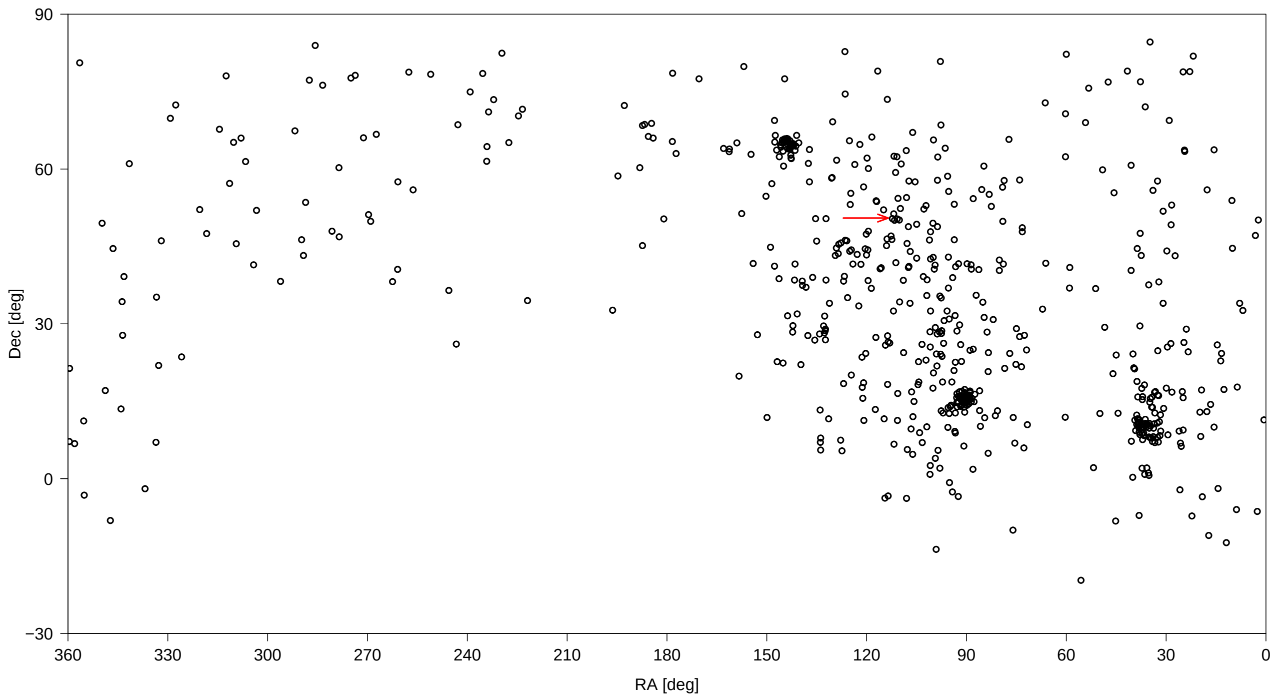

Figure 5 – All radiant positions from the night 2017 October 14/15; the red arrow points to a separate cluster of radiants mentioned in Section 4.

From the data obtained, we looked at the orbital elements of these five specific meteors. In Tables 1, 2 and 3 radiant positions, geocentric speed, orbital elements, and all stations that captured one or more of these five meteors are shown. In the IAU database (Jopek & Kaňuchová, 2017; Jopek & Kanuchova, 2014; Jopek & Jenniskens, 2011) we found at approximately the same solar longitude, a stream close to this radiant, that is not yet established: #228 OLY (October Lyncids). Until now, Jenniskens et al. (2016) found six meteors belonging to #228 in the period between October 10 and October 23. Table 1a gives the values for right ascension, declination and geocentric speed for #228 next to the values for our dataset. Most orbital elements are in good agreement with the orbital elements given for #228 in the IAU database. The deviation in argument of the perihelion (ω), and longitude of the perihelion (Π), could be explained by the deviation for perihelion distance (q) and the fact that the data in Jenniskens et al. (2016) is spread out over a larger period.

5 Conclusion

We found three streams with particular activity in the great amount of orbits collected in October 2017. Like in 2016, we found activity of the October Camelopardalids. The October Ursa Majorids showed good activity this year. Finally, we found in the October data an indication for the existence of the stream #228, October Lyncids.

Acknowledgements

Thanks to Reinder Bouma for his valuable comments, and to all participants in the CAMS BeNeLux Project.

References

Jenniskens P., Gural P. S., Dynneson L., Grigsby B. J., Newmane K. E., Borden M., Koop M., and Holman D. (2011). “CAMS: Cameras for Allsky Meteor Surveillance to establish minor meteor showers”. *Icarus*, **216**, 40–61.

Jenniskens P., Nénon Q., Albers J., Gural P. S., Haberman B., Holman D., Morales R., Grigsby B. J., Samuels D., and Johannink C. (2016). “The established meteor showers as observed by CAMS”. *Icarus*, **266**, 331–354.

Johannink C. (2017). “October Camelopardalids activity recorded by CAMS”. *WGN, Journal of the IMO*, **45:6**, 125–126.

Jopek T. J. and Jenniskens P. M. (2011). “The Working Group on Meteor Showers Nomenclature: A History, Current Status and a Call for Contributions”. In Cooke W., Moser D., Hardin B., and Janches D., editors, *Meteoroids: The Smallest Solar System Bodies, Proceedings of the Meteroids Conference held in Breckenridge, Colorado, USA, May 24-28, 2010.*, NASA/CP-2011-216469. pages 7–13.

Jopek T. J. and Kanuchova Z. (2014). “Current status of the IAU MDC Meteor Showers Database”. In Jopek T., Rietmeijer F., Watanabe J., and Williams I., editors, *The Meteoroids 2013, Proceedings of the Astronomical Conference held at A.M. University, Poznan, Poland, Aug. 26-30, 2013.* A.M. University Press, pages 353–364.

Table 1 – Radiant positions and geocentric speed plus their mean values of five possible #228 October Lyncids, captured by CAMS BeNeLux. Further data on the values from the IAU database for shower #228 (Jopek & Kaňuchová, 2017; Jopek & Kanuchova, 2014; Jopek & Jenniskens, 2011).

Nr.	Date	Time (UT)	RA [°]	Dec [°]	V_g [km/s]
83	2017 October 14	$21^h22^m49\overset{s}{.}42$	110.154 ± 0.074	50.119 ± 0.037	65.508 ± 0.083
99	2017 October 14	$22^h05^m54\overset{s}{.}86$	110.851 ± 0.075	50.314 ± 0.051	64.517 ± 0.063
254	2017 October 15	$00^h50^m43\overset{s}{.}40$	111.628 ± 0.47	50.094 ± 0.464	63.414 ± 0.202
434	2017 October 15	$02^h49^m33\overset{s}{.}55$	112.274 ± 0.199	50.393 ± 0.209	67.381 ± 0.356
639	2017 October 15	$04^h59^m55\overset{s}{.}05$	111.826 ± 0.7	50.332 ± 0.671	67.038 ± 0.512
mean			111.3	50.5	65.6
IAU #228			111.3	48.8	64.8

Table 2 – Orbital elements, and the mean values, of five possible #228 October Lyncids captured by CAMS BeNeLux and the values from the IAU database for #228 (Jopek & Kaňuchová, 2017; Jopek & Kanuchova, 2014; Jopek & Jenniskens, 2011).

Nr.	q [AU]	e	i [°]	ω [°]	Π [°]
83	0.96404 ± 0.00048	0.9699 ± 0.0074	132.304 ± 0.063	201.201 ± 0.17	42.678 ± 0.17
99	0.96613 ± 0.00048	0.8912 ± 0.0053	131.489 ± 0.087	200.974 ± 0.171	42.481 ± 0.171
254	0.96761 ± 0.00304	0.7915 ± 0.023	131.192 ± 0.706	201.135 ± 1.157	42.756 ± 1.157
434	0.97666 ± 0.00101	1.1421 ± 0.0346	132.561 ± 0.324	195.984 ± 0.455	37.688 ± 0.455
639	0.9733 ± 0.00346	1.1475 ± 0.05	131.061 ± 1.032	197.214 ± 1.271	39.008 ± 1.271
mean	0.9695	0.9884	131.7	199.3	40.9
IAU #228	0.926	—	133.3	211.7	57.5

Table 3 – The stations in the Netherlands / Belgium that captured these five meteors (314/315/318 C. Johannink, Gronau; 321 M. Breukers, Hengelo; 332 K. Jobse, Oostkapelle; 340/342/344 P. Neels, Ooltgensplaat; 347 E. Ballegooij, Heesch; 354 K. Miskotte, Ermelo; 362/364 R. Haas, Alphen ad Rijn; 372 H. Betlem, Leiden; 381 J.M. Biets, Wilderen; 384 P. Roggemans, Mechelen; 390 L. Gobin, Mechelen; 398 B. Dessoy, Zoersel).

Nr.	stations
83	_000318_000354_000362_000314
99	_000321_000384_000364_000372_000315_000347_000344
254	_000340_000390_000398
434	_000332_000342
639	_000381_000384_000364

Jopek T. J. and Kaňuchová Z. (2017). "IAU Meteor Data Center-the shower database: A status report". *Planetary and Space Science*, **143**, 3–6.

Uehara S., SonotaCo, Fujiwara Y., Furukawa T., Inoue H., Kageyama K., Maeda K., Muroishi H., Okamoto S., Masuzawa T., Sekiguchi T., Shimizu M., and Yamakawa H. (2006). "Detection of October Ursa Majorids in 2006". *WGN, Journal of the IMO*, **34:6**, 157–162.

Handling Editor: Javor Kac

History

On an 1850 report of a fireball from the Scorpiid-Sagittariid Complex

Anne van Weerden[1]

In the night of 13-14 May 1850 both Sir William Rowan Hamilton and his son William Edwin saw a meteor which was "many degrees more brilliant than Jupiter." This meteor has now been recognized as a member of the so-called Scorpiid-Sagittariid Complex. It makes Hamilton's report the earliest one of this complex, the hitherto earliest one stemming from 1878.

Received 2017 November 19

1 Introduction

On the 14th of May 1850 the Astronomer Royal of Ireland, Sir William Rowan Hamilton (1805–1865), sent a short report to *Saunders's Newsletter*, a Dublin daily newspaper, in which he described the observation of a "splendid" meteor (Hamilton, 1850). The report is not available open access and therefore given hereafter in its entirety.

Before giving Hamilton's report it is useful to know that as Ireland's Astronomer Royal he lived at Dunsink Observatory, which was built in 1785 at an elevated place about eight kilometers northwest of Dublin. Regularly attending the meetings of the Royal Irish Academy, Hamilton had the habit of walking to and from Dublin along the Royal Canal, which runs just over a kilometer south of the observatory. His usual route has been described by the organizers of the annual *Hamilton Walk*[a] and the *Quaternions by the Royal Canal: podcast tour*.[b]

Having taken this route means that on his way home Hamilton walked along the canal in a westward direction towards the Ashtown crossing, which must have been there already in 1850, both Maynooth and Clonsilla train station having been opened in 1848. At the Ashtown crossing he turned to the north, walked past Dunsinea, the house of family members, and then ascended the sloping fields towards the observatory. From Hamilton's 1880s biography it is known that he entered the observatory grounds through an iron wicket gate at the south side of the demesne,[c] and also in his days the hall-door was facing south.

Hamilton passed Dunsinea at its east side as can be seen in Figures 1 and 2, and as he wrote in the report given hereafter, he could see Jupiter and Spica, Alpha Virginis. At the time of the observation Jupiter was in the southwest at an altitude of about 23° and Spica in the south-southwest at about 22°, and also having needed only a few minutes to reach the observatory, Hamilton will have seen the meteor when he had already passed Dunsinea and was crossing the sloping fields.

2 The report

On the Meteor of the Night of May 13th 1850

To the Editor of Saunders's News Letter.
Observatory of Trinity College, near Dublin, May 14, 1850.

Sir – Although I do not see your valuable paper regularly, yet, as most of my fellow-citizens of Dublin do so, it occurs to me that they may like to have, through you, some particulars respecting the appearance of a splendid Meteor which was seen last night by two persons here, and will probably be found to have been noticed in other places also.

As I was walking out from Dublin, after attending the meeting of the Royal Irish Academy, which was held on the evening of yesterday, and when I had almost arrived at the Observatory under my charge, I was startled by a sudden light in the heavens on my left hand, and not much to the west of the south. Instantly turning to that side I saw what to me, who have not hitherto happened to witness many meteors (except the ordinary shooting stars), appeared to be by far the most beautiful celestial phenomenon that had ever been presented to my eyes. An orb of blueish light and of a planetary appearance, but by many degrees more brilliant than Jupiter – to which planet I had been looking the moment before – was seen to sail steadily, and, as it seemed, somewhat slowly, along over an arch of at least ten (or possibly fifteen) degrees, kindling at first till it attained a dazzling lustre, and then subsiding from a sort of incandescent brightness; yet not so gradually but that it might appear at last to have been suddenly extinguished: the whole progress of the phenomenon having not occupied, as I suppose, more than two or three seconds of time.

It was impossible, during the sudden apparition of so much beauty, to be cool enough to do more than gaze; but scarcely half a minute had elapsed, from its withdrawal, when I endeavoured to recall with care any particulars which it seemed possible to fix from recollection. As well as I could judge in the starlight, it was then about five minutes after mean midnight, Dublin time. I formed the estimates, already mentioned, of the duration and extent of the phenomenon. I remem-

[1]Email: a.vanweerden@uu.nl

IMO bibcode WGN-456-weerden-hamilton
NASA-ADS bibcode 2017JIMO...45..160W

[a]http://archive.maths.nuim.ie/hamiltonwalk. On one of these walks Hamilton found the quaternions, from which vector analysis emerged. This discovery is commemorated annually.

[b]http://ingeniousireland.ie/product/dublin-eureka-by-the-royal-canal-app-audio-guide

[c]Graves (1882; 1885; 1889)

Figure 1 – In this Google Maps screen print north is up, west is to the left. Dunsink Observatory can be seen at the top, Dublin is located in the southeast but outside this map, the Royal Canal can be seen at the bottom. Walking north from the Ashtown Crossing on what is now Scribblestown Avenue, along what then was Dunsinea and now the Teagasc Ashtown Food Research Center, Hamilton entered the observatory grounds from the south.

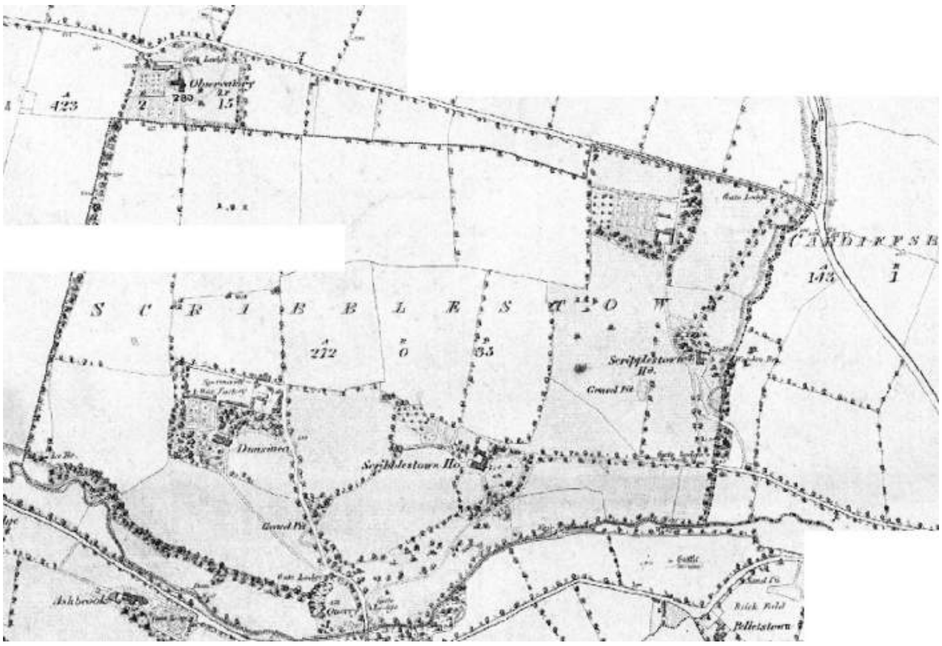

Figure 2 – This is a combination of four map sheets from the first Edition of the 1-inch *Ordnance Survey*, made between 1829 and 1842. In the map of Figure 1 the north, east and west borders are chosen to be equal to those in this map, but here the Royal Canal is not visible. Comparing the maps it can clearly be seen how many features of the grounds south of the observatory in Hamilton's days are still recognizable today. And how amazingly accurate the surveyors were. Dunsinea still seems to exist; if it is the same building indeed, the house now contains the Teagasc Ashtown National Food Centre Library.

See for these historical maps http://www.buildingsofireland.ie/cgi-bin/viewcounty.cgi?county=6 and http://maps.osi.ie/publicviewer/#V2,711016,738210,9,7.

bered also that the course of the meteor had seemed to be nearly parallel to the horizon and towards the west, but with a somewhat downward direction; and I fixed on the star Spica Virginis as one which would enable me to recover, at least approximately, the point of the heavens towards which the object had been moving. But, as an instance of the difficulty of recording, or rather of observing, without previous practice, the precise particulars of a sight so evanescent, I ought to add that I felt myself unable to declare, even from a recollection so very recent, whether the course of the meteor had been higher or lower than one which should have passed the above-mentioned star.

After not many minutes I reached the hall-door of the Observatory, which was opened for me by my son, William Edwin Hamilton. It would be trifling, and therefore inexcusable, to mention that circumstance here were it not that he had happened to be the second of the two observers, to whom allusion was made above. He met me, full of the beauty of the spectacle, of which he had been another witness, described the colour of the meteor as blue, and compared its appearance to that of the electric spark in the discharge of a highly charged jar; and entered into several particulars respecting the precise time and place of the phenomenon, which I verified and recorded, so far as was possible, on the instant, and of which the results may perhaps be of some utility or at least of some interest to those persons who are engaged in the study of meteoric astronomy. It appears that while he was sitting in the transit chair and was watching the gradual passage of the star Alpha of the Northern Crown, out of the field of the transit telescope, at the moment when that star had passed the last of the wires, by about an interval from one wire to another, he was startled by a sudden light shining through the southern window of the observing room – this window, although facing the south, being distant by several feet towards the west from the large slit in the roof to which the transit instrument was directed. The meteor seemed to occupy about a second in crossing the window; and immediately after its disappearance he traced on one of the transit pillars, before my return, a rude representation of its course. And on my requesting him to point out on the window itself the exact track which the meteor had taken, he drew at the time a line which agreed well with my own recollection.

I have to-day, along with my assistant, Mr. Charles Thompson – who took the transit last night of the star last referred to – made some measurements and calculations, founded on the foregoing particulars, and suppose that the following deductions from what was noticed by my son are not erroneous by more than a few seconds of time, and perhaps by a few degrees of space. It may then be stated that the beautiful meteor of last night (or rather of this morning), as seen from the transit chair of this Observatory, in latitude 53° 23' $13\frac{1}{2}$" North, and in longitude 25 minutes 21 seconds of time West of Greenwich, attained its greatest brightness, which was of a blue colour, at about four minutes and seven seconds after the mean midnight (local time) of Monday, the 13th of May, 1850; having then an azimuth of about thirty degrees to the West of the South, and an altitude of about sixteen degrees, which would answer, in round numbers, to a right ascension of thirteen hours, thirty minutes, and a north polar distance of one hundred and six degrees.

I am, sir, your obedient servant,
William Rowan Hamilton.

3 The observation data of the meteor

Remarkably much can be inferred from Hamilton's report. The only thing not immediately clear however is the date of the appearance of the meteor. Hamilton calls it "the Meteor of the Night of May 13th," and since he observed the meteor after midnight that seems to indicate that it appeared in the night of the 12–13th of May, but that cannot be the case. The meetings of the Royal Irish Academy were held on Mondays,[d] the meteor therefore appeared on what we would now would call the first minutes of the 14th of May 1850, which is indeed corroborated by Hamilton's remark that it was "rather of this morning."

The almost exact time of the appearance of the meteor, up to only a few seconds, is known by the fact that Thompson had taken the transit of Alphekka, the star Alpha of the Northern Crown.[e] Apparently directly after Thompson finished the observations William Edwin had taken Thompson's place in the transit chair; he recorded that Alphekka had just "passed the last of the wires, by about an interval from one wire to another." Alphekka just having crossed the meridian can clearly be seen in Figure 3.

A quite precise determination of the latitude of the path of the meteor was given by William Edwin, who saw it through the window facing south; the position of the chair and the window having been fixed allowed for such precision. That window was several feet west of the opening in the roof through which the transit of Alphekka had been observed; William Edwin therefore saw the meteor somewhat west of south, as also Hamilton reported. But William Edwin will not have seen the begin and end points of the path since he saw it only for about one second through the window; the determination of the longitude came from Hamilton's observation that it was travelling over "at least ten or possibly fifteen degrees" in the direction of Spica, and extinguished before reaching it. The combination of these two observations made it possible for Hamilton to provide such precise data.

[d]The meetings having taken place on Mondays can be read in Hamilton's biography, see Graves (1882; 1885; 1889). Also the day that he found the quaternions was a Monday; he then was walking with his wife towards Dublin to preside a meeting of the Royal Irish Academy, (Van Weerden, 2015, p. 12).

[e]Thompson measured the crossing of Alphekka over the meridian, the local north-south line, by observing the crossings over the wires of the transit instrument. In those days star transits were routinely measured in order to gain a better knowledge of their locations, as well as for regulating the observatory's central clock. See for instance (Lang, 1826) for an example of transit measurements.

According to the website of Dunsink Observatory,[f] its precise location is 53°23'12.30", −06°20'10.40"; its altitude as given by the *Astronomical Almanac for the Year 2016* is 85 m above sea level. In his report Hamilton gave Dublin mean time, which was measured at Dunsink Observatory, as 25 minutes and 21 seconds behind Greenwich mean time, which indeed exactly corresponds to the longitude given by Dunsink Observatory.

As regards the path of the meteor, Hamilton mentioned an error of a few seconds in time, and "perhaps" a few degrees of space. Therefore, in order to visualize the path of the meteor using STELLARIUM,[g] hereafter seconds will be neglected, and the time difference with Greenwich time will be rounded off to $-00^{\rm h}25^{\rm m}$.

Summarizing what is known about the meteor, Hamilton and Thompson calculated that the meteor attained its greatest brightness when at an altitude of about 16°, and an azimuth of about 30° west of south, or 210°. The brightness was "by many degrees more brilliant than Jupiter," its duration was 2–3 seconds, its colour blue, and it moved over 10–15 degrees. Its velocity was "somewhat slowly." It moved in a direction "nearly parallel to the horizon and towards the west" but somewhat downward. It headed towards Spica, but did not go past it.

4 Visualizing the path and a possible radiant

Using STELLARIUM to visualize the path of the meteor, three stars have been chosen as representing the point of greatest brightness, of which the ephemerides were given by Hamilton, a theoretical starting point, and a possible radiant.

For the point of greatest brightness the star HIP 66423A was chosen;[h] it was as close as possible to this point and is represented in Figure 4 by the rightmost circle. Its azimuth and altitude at the time of the appearance of the meteor were, rounded off, 210°10' and 16°15', respectively.

The starting point has been chosen as having had a distance to the point of greatest brightness of 15 degrees. Hamilton's largest estimation of the path of the meteor has been chosen because he did not see the real starting point; he reacted to the light of the meteor when he turned around to look at it. Hamilton also reported that the path had been nearly horizontal, therefore a difference in altitude has been chosen of 1.5 degrees. Although slightly influenced by the curvature of the coordinate system due to the chosen field of view, it can be seen in the screenshot that such a difference between the two points indeed seems to show a path as Hamilton described; almost horizontal but somewhat downwards. For this starting point the star HIP 71850 has been chosen, represented by the circle in the middle. Its azimuth and altitude were 194°0' and 17°30', respectively.

As regards a possible radiant, the considerations to choose the star HIP 81686, with azimuth and altitude 163°40' and 20°25', respectively, were that Hamilton mentioned that the speed of the meteor was somewhat slowly, and that its path was about ten to fifteen degrees, which is not very long for such a bright meteor; it seems to indicate that the meteor stayed rather close to the radiant. The radiant has therefore been assumed to have been at a distance from the starting point of two times the length of the visible path: about 2×15 degrees from the starting point, and consequently 2×1.5 degrees higher in altitude. That corresponds to an azimuth and altitude of 165° and 20°30', respectively, or a right ascension $\alpha = 16^{\rm h}28^{\rm m} = 248°$ and a declination $\delta = -15°$.

5 The Scorpiid-Sagittariid Complex: Anthelion

The estimated radiant of Hamilton's meteor thus had as its celestial coordinates $\alpha = 248°$ and $\delta = -15°$. That fits in well with the values in the table given by Gary Kronk in his 2014 book *Meteor Showers : An Annotated Catalog*[i] for possible radiants of the Scorpiid-Sagittariid Complex (Kronk, 2014, p. 131), which gives values for α between 232° and 350°, and for δ between $= -28°$ and +3°. In the chapter 'June showers' Kronk writes about the Scorpiid-Sagittariid Complex:

> This is the largest region of activity during the year, completely spanning the months of May through July and the constellations of Libra, Ophiuchus, Sagittarius, Scorpius, and Capricornus. Several individual radiants seem to be active each year, but research shows that few of these radiants produce annual displays. [...] None of these radiants produce more than 1–2 meteors per hour. [...] C. Hoffmeister (Hoffmeister, 1948) called this region the "Scorpius-Sagittarius System" [...] and said [the meteors] generally appear 165° west of the Sun [...].
>
> The earliest account of meteors coming from this region appeared in the 1878 July issue of The Observatory. W.F. Denning discussed three fireballs that were seen on 1878 June 7 (Denning, 1878). The first appeared in daylight, while the other two appeared in the early evening. In his conclusion, Denning said these last two appeared to diverge from a radiant near the star Antares. He gave the position as $\alpha = 246°$, $\delta = -20°$ and added that this was "not far from that of the detonating fireball of June 17, 1873."

[f] Dunsink Observatory: `https://www.dunsink.dias.ie`.

[g] Stellarium Night Sky Viewer, `http://www.stellarium.org`.

[h] The star designation HIP comes from the Hipparcos star catalogue, Hipparcos having been the astrometric satellite which measured star positions between 1989 and 1993.

[i] In this book Kronk describes over a 100 meteor showers, together with the history of their discovery and historical observations. (Kronk, 2014).

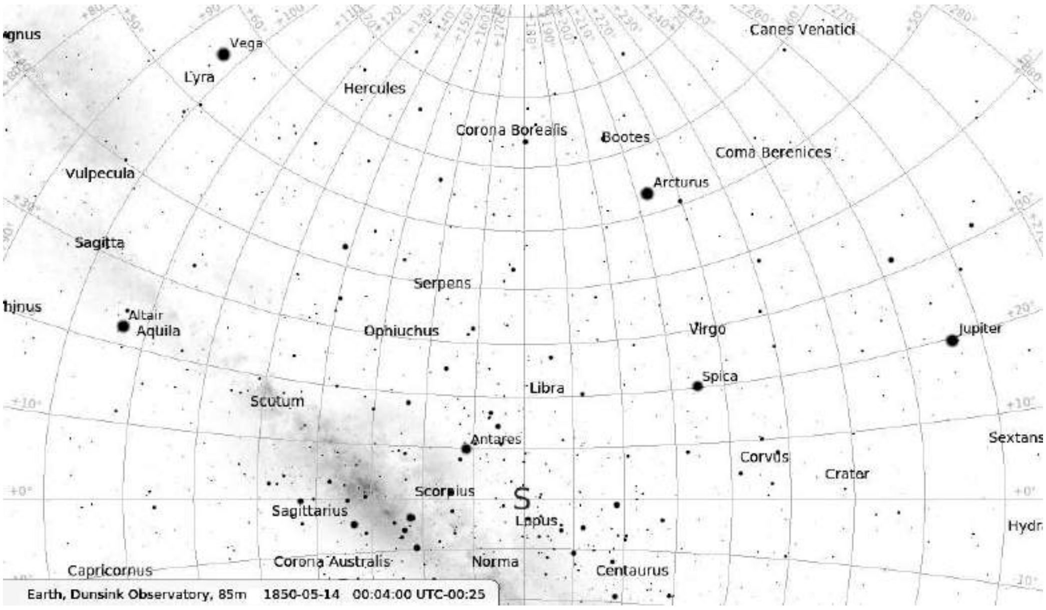

Figure 3 – In this Stellarium screen print west is to the right, the coordinates shown are azimuth and altitude. Alphekka, the brightest star of Corona Borealis, can be seen at the top; in accordance with Hamilton's report it just crossed the meridian. Jupiter is on the right side, in the south-west. The location settings in Stellarium have been set to the geographical coordinates as given by Dunsink Observatory; the time has been set to 25 minutes behind Greenwich Mean time, or for practical purposes UTC. For clarity, information other than time and place on the bar at the bottom of the screen has been removed and the bar itself has been moved, but no further modifications were made.

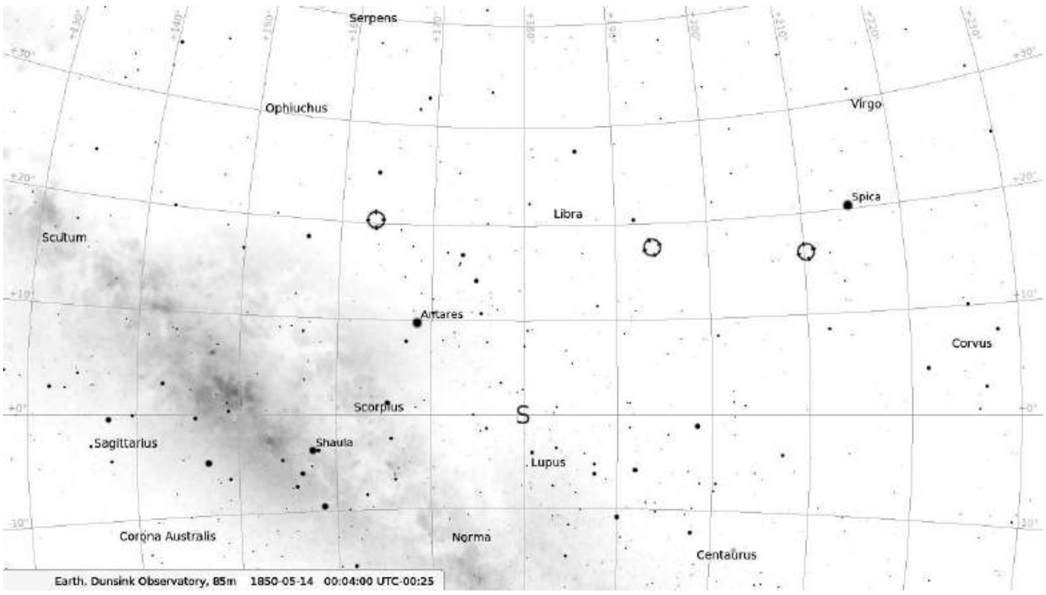

Figure 4 – Again west is to the right, the coordinates are azimuth and altitude, and the same time and location settings have been used as in Figure 3. While modifying the bar and adding the circles, for which each time a new screenshot was made, much care has been taken not to alter anything else. The circles indicate, from right to left, the point of greatest brightness, the starting point, and a possible radiant, each represented by a star as close as possible to the respective locations. The curvature of the coordinate system can be recognized in the apparent curvature of the theoretically derived and extended path.

Kronk further adds that "today, these "Ecliptical Currents" are known as "antihelion" radiants. [...] According to R. Lunsford (2004), "this material orbits the sun in low-inclination, direct orbits, and encounters the Earth on its inbound or pre-perihelion portion of its orbit." The meteors encounter Earth perpendicular to our planet's direction of motion." (Kronk, 2014, p. 127).

Lunsford gives radiants for Anthelion meteors (Lunsford, 2004, p. 82); for May 15 he gives as the celestial coordinates of the radiant $\alpha = 248°$, $\delta = -22°$, to which again the data given by Hamilton correspond very well, even if these points have shifted somewhat since Hamilton's time. It must be admitted that the declination of the estimated radiant of the 1850 meteor, $-15°$, is quite some degrees higher than $-22°$; yet the measure of what was "somewhat downward" of the meteor's path has been guessed, Hamilton mentioned an possible error of "a few degrees," and Lunsford does not give widths of these radiants. Again fitting very well with the Anthelion meteors is the "somewhat slowly" velocity of the 1850 meteor as mentioned by Hamilton; Lunsford records that the Anthelion meteors "appear to be of average velocity, lacking both very fast and very slow meteors." (Lunsford, 2004, p. 81).

6 Conclusion

It has been shown that Hamilton's meteor can be recognized as having come from one of the Anthelion radiants, the Scorpiid-Sagittariid Complex. Kronk mentioned that the earliest account of meteors coming from this region was from W.F. Denning in 1878, and Denning did mention a "detonating fireball" in 1873. The meteor seen by Hamilton and his son in 1850 therefore appeared and was reported 23 years before the observation of this earliest fireball.

7 Acknowledgements

I would like to thank my colleague Rob van Gent for his quick insight into the conditions of this meteor; I had not thought of searching for a radiant. Many thanks are due to the people of the Boston College Libraries for providing a very fine scan of the pages of *Saunders's News-letter*. And of course to my library colleagues Memet Ozberk and Wiebe Boumans for helping me with the request.

References

Denning W. F. (1878). "The Meteors of June 7". *The Observatory : a Monthly Review of Astronomy*, **II:15**, 90–93. (`https://archive.org/stream/observatory28unkngoog#page/n103/mode/2up`).

Graves R. P. (1882, 1885, 1889). *Life of Sir William Rowan Hamilton Knt., LL.D., D.C.L., M.R.I.A., Andrews Professor of Astronomy in the University of Dublin and Royal Astronomer of Ireland, Etc. Etc.: including Selections from his Poems, Correspondence, and Miscellaneous Writings*, volume 1, 2, 3. Dublin: Hodges, Figgis, & Co. (`https://archive.org/details/lifeofsirwilliam01gravuoft`, `https://archive.org/details/lifeofsirwilliam02gravuoft`, `https://archive.org/details/lifeofsirwilliam03gravuoft`).

Hamilton, Sir W. R. (1850). "On the meteor of the night of may 13th 1850". *Saunders's News-letter, and Daily Advertiser*, **33,726**. Thursday, May 16, 1850.

Hoffmeister C. (1948). *Meteorströme*. Leipzig: Johann Ambrosius Barth Verlag.

Kronk G. W. (2014). *Meteor Showers: An Annotated Catalog, second edition*. New York: Springer.

Lang A. (1826). "Observations of the meridian transit of the moons enlightened limb, and some stars preceding and following her, made at St. Croix, with an altitude, azimuth and transit-circle". *Astronomische Nachrichten*, **5**, 113–120. (`http://articles.adsabs.harvard.edu/full/1826AN......5..113L`).

Lunsford R. (2004). "The anthelion radiant". *WGN, Journal of the IMO*, **32:3**, 81–83. (`http://articles.adsabs.harvard.edu/full/2004JIMO...32...81L`).

Weerden, A. van (2015). *A Victorian marriage : Sir William Rowan Hamilton, First edition with corrections 2017.* Stedum: J. Fransje van Weerden. (`https://books.google.com/books?id=6Ow9DwAAQBAJ`).

Handling Editors: Robert Lunsford and Javor Kac
This paper has been typeset from a LaTeX file prepared by the author.

The International Meteor Organization

www.imo.net

Follow us on Facebook
InternationalMeteorOrganization

Follow us on Twitter
@IMOMeteors

Council

President: Cis Verbeeck,
Bogaertsheide 5, 2560 Kessel, Belgium.
e-mail: cis.verbeeck@scarlet.be

Vice-President: Jürgen Rendtel,
Eschenweg 16, D-14476 Marquardt, Germany.
tel. +49 33208 50753
e-mail: jrendtel@aip.de

Secretary-General: Robert Lunsford,
14884 Quail Valley Way, El Cajon,
CA 92021-2227, USA. tel. +1 619 755 7791
e-mail: lunro.imo.usa@cox.net

Treasurer: Marc Gyssens, Heerbaan 74,
B-2530 Boechout, Belgium.
e-mail: marc.gyssens@uhasselt.be
BIC: GEBABEBB
IBAN: BE30 0014 7327 5911
Bank transfer costs are always at your expense.

Other Council members:

Megan Argo, Jodrell Bank Centre for Astrophysics, Alan Turing building, University of Manchester, Oxford Road, Manchester, M13 9PL, UK.
e-mail: megan.argo@gmail.com

Geert Barentsen, NASA Ames Research Center, M/S 244-30, Moffett Field CA 94035, USA.
e-mail: hello@geert.io

Javor Kac (see details under WGN)

Detlef Koschny, Zeestraat 46, NL-2211 XH Noordwijkerhout, Netherlands.
e-mail: detlef.koschny@esa.int

Masahiro Koseki, 4-3-5 Annaka, Annaka-shi, Gunma-ken 379-0116, Japan.
e-mail: geh04301@nifty.ne.jp

Sirko Molau, Abenstalstraße 13b, D-84072 Seysdorf, Germany. e-mail: sirko@molau.de

Jean-Louis Rault, Société Astronomique de France, 16, rue de la Vallée, 91360 Epinay sur Orge, France. e-mail: f6agr@orange.fr

Paul Roggemans, Pijnboomstraat 25, 2800 Mechelen, Belgium, e-mail: paul.roggemans@gmail.com

Galina Ryabova, Res. Inst. of Appl. Math. & Mech., Tomsk State University, Lenin pr. 36, build. 27, 634050 Tomsk, Russian Federation.
e-mail: ryabova@niipmm.tsu.ru

Damir Šegon, J. Rakovca 3, 52100 Pula, Croatia. e-mail: damir.segon@pu.t-com.hr

Juraj Tóth, Fac. Math., Phys. & Inf., Comenius Univ., Mlynska dolina, 84248 Bratislava, Slovakia.
e-mail: toth@fmph.uniba.sk

Commission Directors

Visual Commission: Rainer Arlt (rarlt@aip.de)
Generic e-mail address: visual@imo.net
Electronic visual report form:
http://www.imo.net/visual/report/electronic

Video Commission: Sirko Molau (video@imo.net)

Photographic Commission: Bill Ward (William.Ward@glasgow.ac.uk)
Generic e-mail address: photo@imo.net

Radio Commission: Jean-Louis Rault (radio@imo.net)

Fireballs: Online fireball reports:
http://fireballs.imo.net

Outreach Officer

Jure Atanackov, e-mail: jureatanackov@gmail.com

Press Officer

Megan Argo, e-mail: megan.argo@gmail.com

Webmaster

Karl Antier, e-mail: webmaster@imo.net

WGN

Editor-in-chief: Javor Kac
Na Ajdov hrib 24, SI-2310 Slovenska Bistrica, Slovenia. e-mail: wgn@imo.net;
include METEOR in the e-mail subject line

IMO Sales

Available from the Treasurer or the Electronic Shop on the IMO Website	€	$
IMO membership, including subscription to WGN Vol. 45 (2017)		
Surface mail	26	35
Air Mail (outside Europe only)	49	65
Electronic subscription only	21	25
Proceedings of the International Meteor Conference on paper		
1990, 1991, 1993, 1995, 1996, 1999, 2000, 2002, 2003, per year	9	12
2007, 2010, 2011, per year	15	20
2012, 2013, 2014, 2015 per year	25	34
2016	30	40
Proceedings of the Meteor Orbit Determination Workshop 2006	15	20
Radio Meteor School Proceedings 2005	15	20
Handbook for Meteor Observers	15	20
Meteor Shower Workbook	12	16
Electronic media		
Meteor Beliefs Project ZIP archive	6	8

St. Patrick's Day fireball of 2016

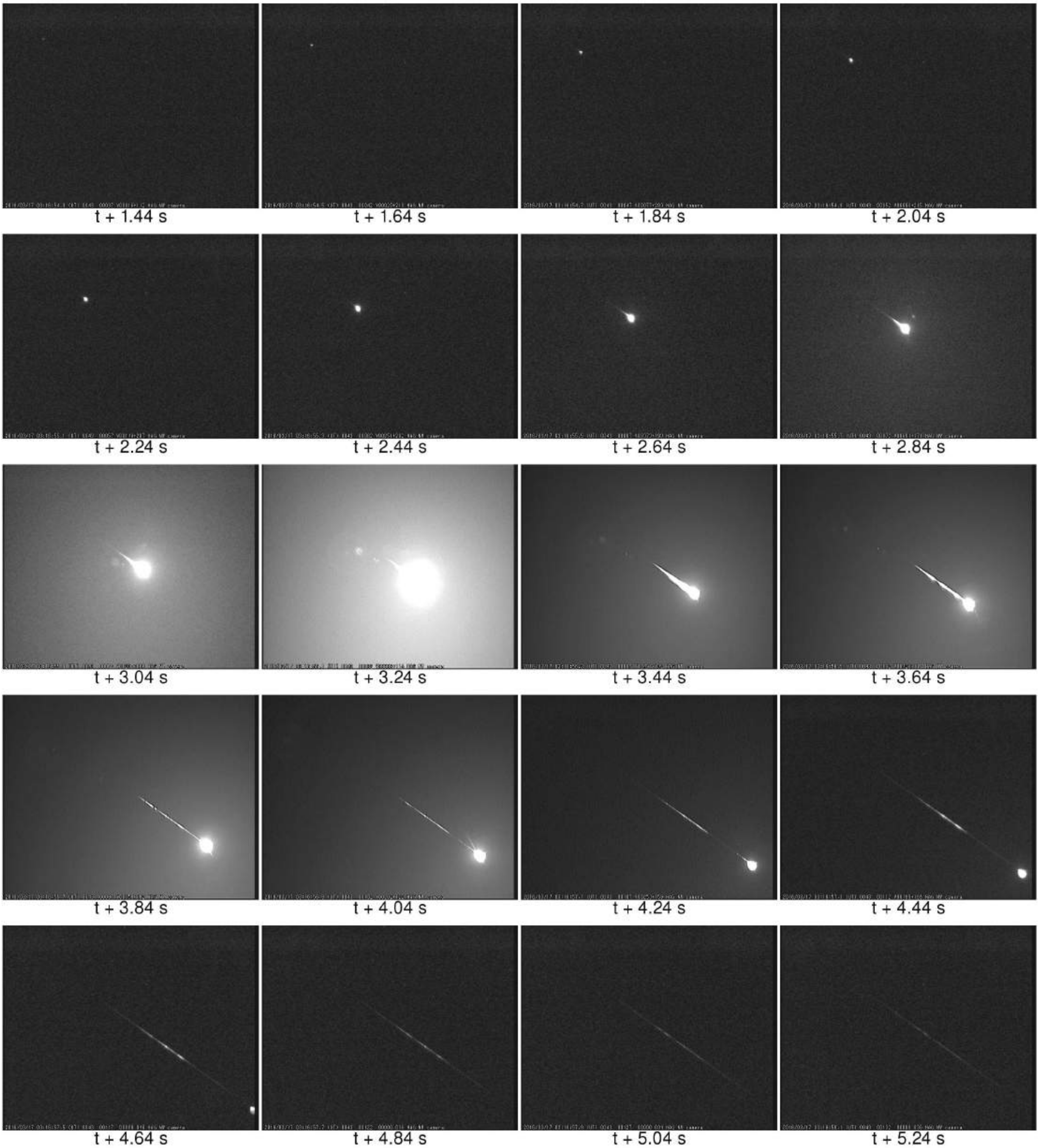

This spectacular fireball occurred in the early morning of 2016 March 17 at $03^{\mathrm{h}}16^{\mathrm{m}}54^{\mathrm{s}}$ UT. Selected individual frames of the Clanfield station meteor camera video record are shown, which are separated by 0.2 s. Labels below each frame mark the time elapsed since the start of the detection. UKMON analysis shows this was a sporadic meteor, with a $v_{\mathrm{G}} = 43.5$ km/s and perihelion distance at only $q = 0.048$ AU. The meteoroid entered the atmosphere with a fairly low angle of 32.1° and was first detected at a height of 112.7 km. The terminal height was 38.3 km when the velocity was 26.6 km/s. Video credit: Steve Bosley / Hampshire Astronomy Group (members of the UKMON and the NEMETODE networks).